STRATUS CONSULTING

Climate Change in Park City: An Assessment of Climate, Snowpack, and Economic Impacts

Prepared for:

The Park City Foundation
PO Box 681499
Park City, UT 84068

Climate Change in Park City:
An Assessment of Climate,
Snowpack, and Economic Impacts

Prepared for:

The Park City Foundation
PO Box 681499
Park City, UT 84068

Prepared by:

Stratus Consulting Inc.
PO Box 4059
Boulder, CO 80306-4059
303-381-8000

1920 L St. NW, Ste. 420
Washington, DC 20036

Contact:

Brian Lazar

September 29, 2009
SC11855

Contents

Appendices

Figures

Tables

Acronyms and Abbreviations

AOGCM	Atmosphere/Ocean General Circulation Model
AR4	Fourth Assessment Report (Intergovernmental Panel on Climate Change)
BCCR	Bjerknes Centre for Climate Research
BEA	Bureau of Economic Analysis
CNRM	Centre National de Recherches Météorologiques
CO_2	carbon dioxide
CSIRO	Commonwealth Scientific and Industrial Research Organisation
DEM	digital elevation model
ETM+	Enhanced Thematic Mapper
ft	feet
GCM	general circulation model
GDP	gross domestic product
GFDL	Geophysical Fluid Dynamics Laboratory
GHG	greenhouse gas
GMT	Global Mean Temperature
Gt	gigaton
I/O	input-output
IPCC	Intergovernmental Panel on Climate Change
km	kilometer
km^2	square kilometer
m	meter
MAGICC	Model for the Assessment of Greenhouse-gas Induced Climate Change
mm	millimeters
MRI	Meteorological Research Institute
NDSI	Normalized Difference Snow Index
NDVI	Normalized Difference Vegetation Index
NED	National Elevation Dataset
NOAA	National Oceanic and Atmospheric Administration

PCM   Parallel Climate Model
PCMDI   Program for Climate Model Diagnosis and Intercomparison
PCMR   Park City Mountain Resort
ppm   parts per million

RCM   regional climate model
RIMS II   Regional Input-Output Modeling system

SCA   snow-covered area
SCENGEN   Global and Regional Climate SCENario GENerator
SDSM   statistical downscaling model
SNOTEL   SNOpack TELemetry
SRES   *Special Report on Emission Scenarios*
SRM   Snowmelt Runoff Model
SWE   snow-water equivalent
SWIR   short wave infrared

TM   Thematic Mapper

UKMO   United Kingdom Meteorological Office
USGS   U.S. Geological Survey

1.   Introduction and Summary

Climate change caused by greenhouse gases (GHGs) has long been a concern of snow-dependent industries, as changes in snow and ice are predicted to be some of the first effects of a warming climate (Barry et al., 2007; Lemke et al., 2007; Armstrong and Brun, 2008). Changes to snowpack can impact a range of commercial activities from water resource management to ski area operations (Tegart et al., 1990; Watson et al., 1996; National Assessment Synthesis Team, 2000; McCarthy et al., 2001; Barry et al., 2007; Lemke et al., 2007). For example, several studies have analyzed the effects of potential climate change on ski areas and winter tourism, and all of the studies have projected negative consequences for the industry (Galloway, 1988; König, 1998; Hennessy et al., 2003; Scott et al., 2003, 2007, 2008; Scott and Jones, 2005; AGCI, 2006; Climate Impacts Group, 2006; Nolin and Daly, 2006; Agrawala, 2007).

The ski tourism industry in Utah is an important part of the regional economy, generating an estimated 19,323 jobs and $416,936,054 in total earnings of Utah's workers in the 2005–2006 ski season (Isaacson, 2006). Given the importance of the Utah ski industry and the dependence of that industry on snow, climate change impacts to snowpack at Utah ski resorts can have a significant impact on the regional economy in the future. Moreover, understanding how climate change may affect snow conditions, such as snow coverage and depth, can help Utah ski area managers plan for the changes to mitigate their adverse effects.

In this study, we used climate, snowpack, and economic models to estimate how the duration and quality of the snowpack at the Park City ski area, in the Wasatch Mountains of north central Utah, may change in the near and more distant future under climate changes caused by GHG emissions, and how the regional economy could subsequently be impacted because of changes in winter tourism. Climate in the Park City area in the years 2030, 2050, and 2075 is predicted under several different scenarios of GHG emissions using several different global climate models coupled with regional and statistical climate models. The predicted Park City climate is then used to predict the length of the ski season, the timing of snowpack buildup and melt, and daily values of snow depth and coverage from the bottom to the top of the mountain.

We estimated skier days in 2030 and 2050 using an observed statistical relationship between snowpack characteristics and skier days in the near past. We then estimated the relationship between skier days and total economic output, earnings, and jobs in the Park City region using economic models. Lastly, we estimated the total economic impact of climate change on the ski industry as the change in skier days times the economic impact per skier day.

Our study predicts that Park City's climate will change substantially as a result of increased atmospheric GHG concentrations. Temperatures are predicted to rise and precipitation amount, timing, intensity are predicted to change. As a result, total snowpack and snow coverage will be

reduced, the ski season will be shorter, and less of Park City Mountain Resort (PCMR) will be skiable. The impacts to snowpack are more severe further in the future, and under scenarios with higher GHG emissions.

Our economic modeling results indicate that projected decreases in snowpack will have severe economic consequences for the region. By 2030, the estimated decrease in snowpack is estimated to result in $120.0 million in lost output. This lost output is estimated to result in an estimated 1,137 lost jobs and $20.4 million in the form of lost earnings (or labor income). By 2050, the potential impacts range from $160.4 million in lost output, $27.2 million in lost earnings, and 1,520 lost jobs (low emissions scenarios) to $392.3 million in lost output, $66.6 million in lost earnings, and 3,717 lost jobs (high emissions scenario).

The remainder of this report will discuss the methods and results of the climate, snowpack, and economic modeling and is organized as follows:

▶   Chapter 2: Climate change overview, modeling methods, and projections

▶   Chapter 3: Snowpack modeling methods and projections

▶   Chapter 4: Economic modeling methods and projections

▶   Chapter 5: Uncertainty

▶   Chapter 6: Summary and conclusions

▶   Appendix A: Description of emissions scenarios and storylines

▶   Appendix B: Methods for spatial averaging of climate model projections

▶   Appendix C: General circulation models and their simulations of observed current climate

▶   Appendix D: Statistical downscaling model calibrations to local weather station

▶   Appendix E: Geographic information systems/remote sensing methods for processing satellite images into snow-covered area

▶   Appendix F: Economic skier day model and regression analysis

▶   Appendix G: Description of economic input-output multipliers.

2.   Overview of Climate Change

2.1   Background

The term "climate change" refers broadly to changes in climate that are caused by the increasing atmospheric concentrations of GHGs.[1] These GHGs include carbon dioxide (CO_2) from fossil fuel combustion and land use change, methane from waste disposal and energy resource development, nitrous oxide from agriculture and industrial operations, and halocarbons used mainly by industry and for refrigeration.

The IPCC has concluded that climate is changing [Fourth Assessment Report (AR4); Solomon et al., 2007]. Averaged around the world, annual mean temperatures rose by 0.74 +/- 0.18°C (1.3 +/- 0.32°F) since 1900, and 11 of the 12 warmest years during the instrumental record of global surface temperature (since 1850) have occurred since 1995. Other aspects of climate such as precipitation patterns and the frequency and intensity of extreme weather events have also changed (AR4; Solomon et al., 2007). The panel concluded that human activities, including fossil fuel burning and land use changes, are very likely[2] responsible for at least half of the increase in the global average temperature in the last half century.

The IPCC AR4 (Solomon et al., 2007) projected that, averaged around the world, the annual mean temperature from 1990 to 2100 is likely to rise by between 1.1 and 6.4°C (2.0 to 11.5°F). The change in regional temperatures will vary considerably from place to place. The AR4 (Christensen et al., 2007, p. 850) concluded the following:

> The annual mean warming in North America is *likely* to exceed the global mean warming in most areas. Seasonally, warming is *likely* to be largest in winter in northern regions and in summer in the southwest. Minimum winter temperatures are *likely* to increase more than the average in northern North America. Maximum summer temperatures are *likely* to increase more than the average in the southwest. [Italics in original.]

---

1. For a more detailed discussion of climate change science, such as descriptions of the greenhouse effect, readers are encouraged to go to the report by the Intergovernmental Panel on Climate Change (IPCC; Solomon et al., 2007). The IPCC was created by the United Nations and World Meteorological Organization to provide advice on the state of the science to policymakers. Every five to seven years, the IPCC issues a comprehensive summary on the latest consensus views about climate change science, environmental and socioeconomic impacts and the potential for adaptation, and options for lessening future change through various strategies for emissions reduction (i.e., mitigation). All of their assessment reports on how climate will change can be found at http://www.ipcc.ch/.

2. IPCC defines "virtually certain" as having at least a 99% probability, "very likely" as having a 90 to 99% probability, and "likely" as having a 66 to 90% probability.

An increase in temperature will lead to many other impacts on climate and our environment. An example that is directly relevant to this study is that snow-covered area (SCA) will contract. Higher temperatures are likely to cause more precipitation to come as rain rather than snow during the year. Snow season length and snow depth are very likely to decrease in most of North America, including Park City. Snowmelt peak runoff is highly likely to be earlier in the year, with more snowmelt contributing to streamflow during winter and early spring and much less snowmelt contribution to streamflow during late spring and summer.

The increase in global temperature will also cause an increase in evaporation, which in turn will cause global average precipitation to increase. However, precipitation will not increase everywhere or in all seasons. The IPCC (Meehl et al., 2007, p. 750) states the following about regional precipitation patterns:

> For a future warmer climate, the current generation of models indicates that precipitation generally increases in the areas of regional tropical precipitation maxima (such as the monsoon regimes) and over the tropical Pacific in particular, with general decreases in the subtropics, and increases at high latitudes as a consequence of a general intensification of the global hydrological cycle. Globally averaged mean water vapour, evaporation and precipitation are projected to increase.

In North America, climate models also tend to project that annual mean precipitation is *very likely* to increase in Canada and the Northeast United States, and *likely* to decrease in the Southwest. In southern Canada, precipitation is *likely* to increase in winter and spring but decrease in summer (Christensen et al., 2007) [Italics in original.]

2.2   Recent Climate Trends

To help put predicted climate changes in the Park City region in perspective, we investigated trends in observed historical climate data for the region. The climate in the Park City region has been changing in recent decades, and here we review the historical temperature records of weather stations with reliable long-term records. We performed a linear regression using a 90% confidence interval to evaluate trends in the average annual maximum and minimum temperatures, since changes in minimum temperatures have important implications for ski area operations such as snowmaking. In each of the following plots, the regression lines indicate the point slope estimate of temperature rate of change, which can express how rapidly temperatures have been changing in the recent past in the region. The slope (or rate of change) is expressed as a number, with a possible range. Using a 90% confidence means that there is a 90% chance that the true slope falls within the range we are showing, but the point slope estimate is the most likely rate of change.

Temperature records for the region are relatively short compared to the global record, and any observed changes in temperature in any one region cannot be tied specifically to GHG effects on global climate, which demonstrate that global temperatures have increased over the last century. The analysis of the regional temperature history is to evaluate whether a similar increase is apparent in the data local to the Park City region.

2.2.1   Salt Lake City airport

Figure 2.1 illustrates the historical maximum and minimum annual average temperatures recorded from 1948 through 2008, at the weather station located at the Salt Lake City airport (data available at http://www.wrcc.dri.edu/cgi-bin/cliMAIN.pl?ut7598; WRCC, 2008d).
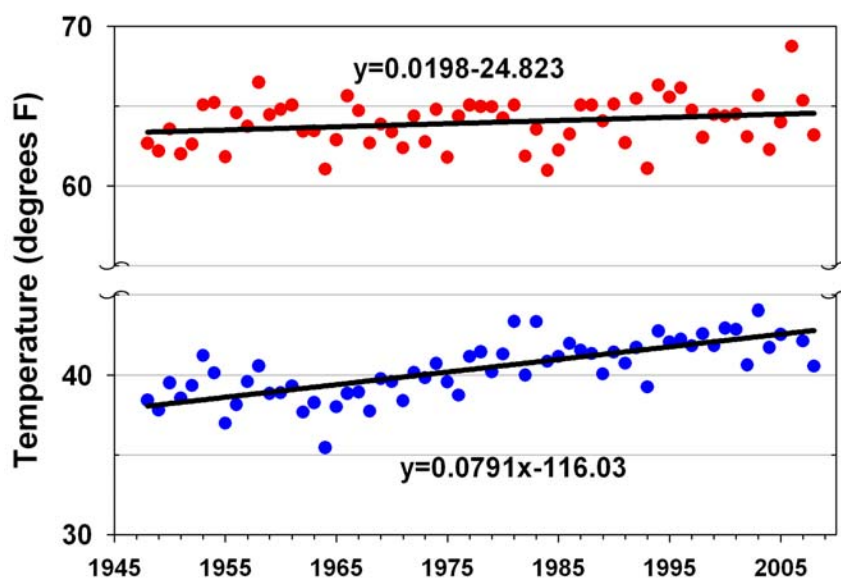
Figure 2.1. Maximum (top) and minimum (bottom) average annual temperatures (in °F) at the Salt Lake City airport from 1948 through 2008.

Using the 90% confidence interval, trends indicate that:

▸   Maximum temperatures are increasing at a rate of 0.11 +/- 0.10°C/decade (0.2 +/- 0.18°F/decade). This means that there is a 90% probability, based on available data, that yearly maximum temperatures at the Salt Lake City airport have increased at a rate between 0.01°C/decade and 0.21°C/decade (0.02°F/decade to 0.38°F/decade) since 1948.

▶   Minimum temperatures are increasing more rapidly at a rate of 0.44°C/decade
        +/-0.09°C/decade (0.79°F/decade +/- 0.16°F/decade). This means that there is a 90%
        probability, based on available data, that yearly minimum temperatures at the Salt Lake
        City airport have increased at a rate between 0.35°C/decade and 0.53°C/decade
        (0.63°F/decade to 0.95°F/decade).

2.2.2   Solitude Brighton weather station

Figure 2.2 illustrates the historical maximum and minimum annual average temperatures
recorded from 1949 through 2008, at the weather station located at Solitude Brighton (data
available at http://www.wrcc.dri.edu/cgi-bin/cliMAIN.pl?ut7846; WRCC, 2008e).
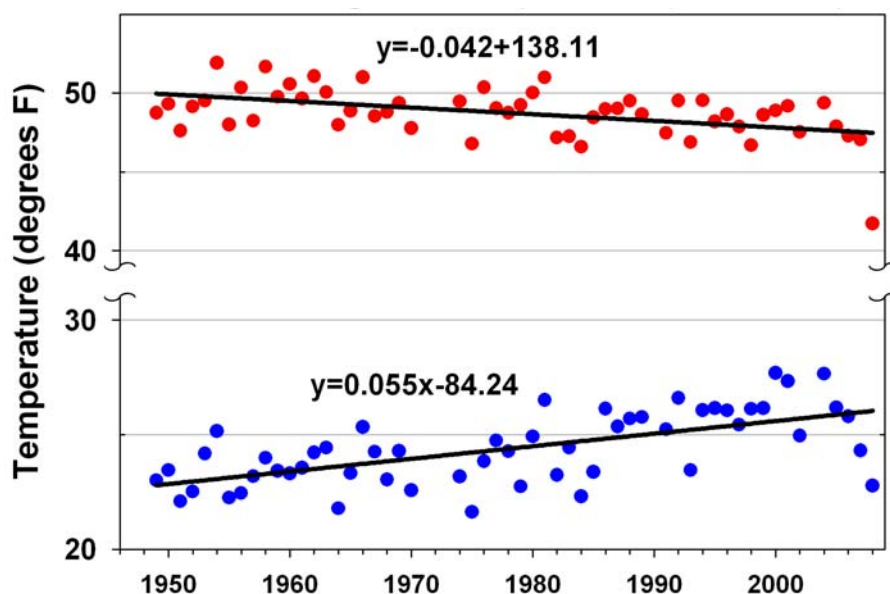
**Figure 2.2. Maximum (top) and minimum (bottom) average annual temperatures (in °F)
at the Solitude Brighton weather station from 1949 through 2008.**

Using the 90% confidence interval, trends indicate that:

▶   Maximum temperatures are *decreasing* at a rate of -0.23°C/decade +/- 0.10°C/decade
        (-0.42°F/decade +/- 0.18°F/decade). This means that there is a 90% probability, based on
        available data, that yearly maximum temperatures at the Solitude Brighton station have

decreased at a rate between -0.33°C/decade and -0.13°C/decade (-0.60°F/decade to -0.24°F/decade).

▸ Minimum temperatures are warming at a rate of 0.31°C/decade +/- 0.09°C/decade (0.55°F/decade +/- 0.16°F/decade). This means that there is a 90% probability, based on available data, that yearly maximum temperatures at the Solitude Brighton station have increased at a rate between 0.22°C/decade and 0.40°C/decade (0.39°F/decade to 0.71°F/decade).

2.2.3 Logan

Figure 2.3 illustrates the historical maximum and minimum annual average temperatures recorded from 1896 through 2008, at the weather station located at Utah State University in Logan (data available at http://www.wrcc.dri.edu/cgi-bin/cliMAIN.pl?ut5186; WRCC, 2008b).
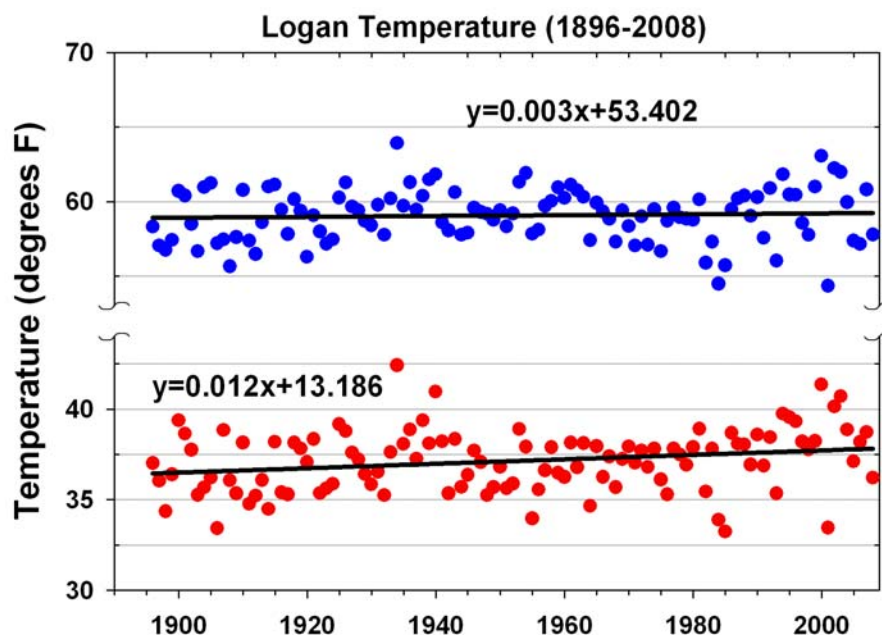
Figure 2.3. Maximum (top) and minimum (bottom) annual temperatures (in °F) at the Utah State University weather station in Logan from 1896 through 2008.

Using the 90% confidence interval, trends indicate that:

▶ Maximum temperatures are increasing at a rate of 0.02°C/decade +/- 0.04°C/decade (0.03°F/decade +/- 0.08°F/decade). We interpret this to mean that it is more likely than not that maximum temperatures are warming.

▶ Minimum temperatures are warming at a rate of 0.07°C/decade +/- 0.04°C/decade (0.12°F/decade +/- 0.08°F/decade). This means that there is a 90% probability, based on available data, that yearly minimum temperatures at the Logan station have increased at a rate between 0.04°C/decade and 0.11°C/decade (0.04°F/decade to 0.20°F/decade).

2.2.4   Mountain Dell Dam

Figure 2.4 illustrates the historical maximum and minimum annual average temperatures recorded from 1949 through 2008, at the weather station located at the Mountain Dell Dam (data available at http://www.wrcc.dri.edu/cgi-bin/cliMAIN.pl?ut5892; WRCC, 2008c).
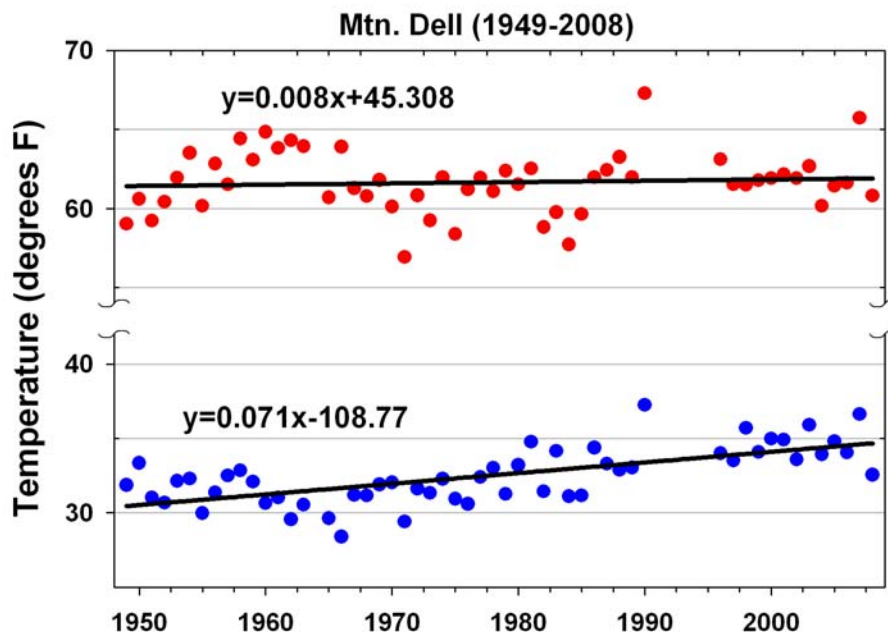
Figure 2.4. Maximum (top) and minimum (bottom) annual temperatures (in °F) at the Mountain Dell Dam weather station from 1949 through 2008.

Using the 90% confidence interval, trends indicate that:

▸ Maximum temperatures are increasing at a rate of 0.04°C/decade +/- 0.14°C/decade (0.08°F/decade +/- 0.25°F/decade). We interpret this to mean that it is more likely than not that maximum temperatures are warming.

▸ Minimum temperatures are warming at a rate of 0.39°C/decade +/- 0.10°C/decade (0.71°F/decade +/- 0.18°F/decade). This means that there is a 90% probability, based on available data, that yearly minimum temperatures at the Mountain Dell station have increased at a rate between 0.29°C/decade and 0.49°C/decade (0.53°F/decade to 0.89°F/decade).

2.2.5 Summary of temperature trends

Table 2.1 summarizes the trend analysis results, using the 90% confidence interval. The temperature ranges indicate the lower and upper bounds of changes per decade in yearly minimum and maximum temperatures.

Table 2.1. Summary of temperature rate of change per decade using the entire available temperature record (full records)

Weather station	90% confidence interval for the max. temp change (°F)/decade	90% confidence interval for the min. temp change (°F)/decade	Period of record
Salt Lake City airport	0.02 to 0.38	0.63 to 0.95	1948 to 2008
Solitude Brighton	-0.60 to -0.24	0.39 to 0.71	1949 to 2008
Logan	-0.06 to 0.11	0.04 to 0.20	1896 to 2008
Mountain Dell	-0.17 to 0.33	0.53 to 0.89	1949 to 2008

From the above temperature trends, we can draw the following conclusions:

1. Daily minimum average temperatures are warming at all locations while maximum temperatures display no consistent trend.

2. Minimum temperatures are warming between 0.04 and 0.95°F per decade. This implies that a 5°F warming could be reached by mid-century. This finding is consistent with the climate model predictions we discuss in Section 2.6.

3.   It is uncertain whether or not maximum daily temperatures are warming, cooling, or staying the same. The temperature *change* ranges from -0.60 to 0.38°F per decade. This is consistent with IPCC predictions that minimum temperatures are likely to be more affected than maximum temperatures.

2.3   Future Climate Change Scenarios

In modeling future climate change at the regional level, such as Park City, there are several areas where it makes sense to model a range of possible conditions. For example, we do not know exactly how GHG emissions will change in the future, so we can model several different possible future paths of GHG emissions. These different possibilities are called scenarios, and we developed several scenarios that represent a range of possible future situations. Scenarios are often used to assess the consequences of possible future conditions, and to assist organizations or individuals in preparing and responding to them. For example, businesses might use scenarios of future economic conditions to decide whether certain strategies or investments make sense now.

The scenarios that we used bracket a plausible range of potential changes in climate. By evaluating a range of plausible conditions, we were able to improve our understanding of how the climate at Park City will respond to different scenarios of global climate change.

We developed scenarios and climate model predictions for three periods: the 2030s, 2050s, and the 2070s. We project out to 2075 because it is likely that the current path of GHG emissions will lead to substantial changes in climate that will still be apparent at least that far into the future (although reduction of emissions could substantially reduce climate change over this century). For the remainder of the report we will refer to these time periods as the years 2030, 2050, and 2075.

2.4   Selecting Park City Climate Change Scenarios

Three factors are critical for modeling how Park City's climate might change:

1.   Future global GHG emissions
2.   How global climate will respond to increases in GHG concentrations
3.   How global climate change will affect the regional climate around Park City.

Estimates of GHG emissions and the sensitivity of Global Mean Temperature (GMT) to increases in GHG concentrations are inputs to the models we used to predict changes in climate variables. We then examined the predictions of seven climate models for a single region to

explore predicted patterns of climate change in the Park City region. We describe GHG emissions scenarios and the issue of a climate sensitivity parameter in the sections that follow.

2.4.1 GHG emissions

Future changes in GHG emissions depend on many factors, including population growth, technology, economic growth, environmental stewardship, and government. The IPCC tried to capture a wide range of potential changes in GHG emissions in its *Special Report on Emission Scenarios* (SRES; Nakićenović and Swart, 2000). The SRES scenarios are grouped into four scenario families (A1, A2, B1, and B2), which are described in more detail in Appendix A. The four scenario families capture six individual emissions scenarios that the IPCC developed to reflect different future conditions regarding population growth, economic growth, variability in growth across the world, the level of economic integration, the strength of environmentalism, and improvements in technology.[3] For this study, we used IPCC scenarios that represent a range of potential future GHG emissions and concentrations. For most of our evaluations, we used B1 as the low-end projection, A1FI as the high-end projection, and A1B as a mid-range projection. For one of our modeling approaches, we used B2 as a moderate projection, and A2 as a high projection.

Figure 2.5a shows CO_2 emissions for six of the SRES scenarios and the IPCC IS92a scenario (a scenario corresponding to an increase of CO_2 at a rate of 1% per year until year 2100) (Leggett et al., 1992). CO_2 is one of the GHGs that contributes to climate change, and we show it here as an illustration of the total GHG emissions modeled in each of the scenarios. Compared to current CO_2 emissions of 7 gigatons (Gt)/year, in scenario A1B CO_2 emissions reach 15 Gt/year by 2030, peak at about 17 Gt/year by 2050, and slightly decline to about 13 Gt/year by 2100. The A1FI scenario has slightly higher CO_2 emissions than A1B by 2030, but by 2050 is at 24 Gt/year, and by 2080 reaches 29 Gt/year. From there, the emissions slightly decrease. In contrast, the B1 scenario emits 9 Gt/year by 2030, peaks at 10 Gt/year in 2040, and then declines to 6 Gt/year in 2100.

Figure 2.5b shows atmospheric CO_2 concentrations predicted under the different emissions scenarios. For thousands of years before the Industrial Revolution, atmospheric CO_2 concentrations were no more than 280 parts per million (ppm). Today, concentrations have increased to over 380 ppm. For the 2030s, CO_2 concentrations across all SRES scenarios are similar, even though there are predicted to be substantial differences in CO_2 emissions (Figure 2.5a). By 2050, the CO_2 concentrations predicted by the seven scenarios begin to diverge, and by 2075, there is a wide spread in estimated concentrations. Scenario A1B is

---

3. IPCC is looking into developing new emissions scenarios and these may capture a wider range of potential future GHG emissions.
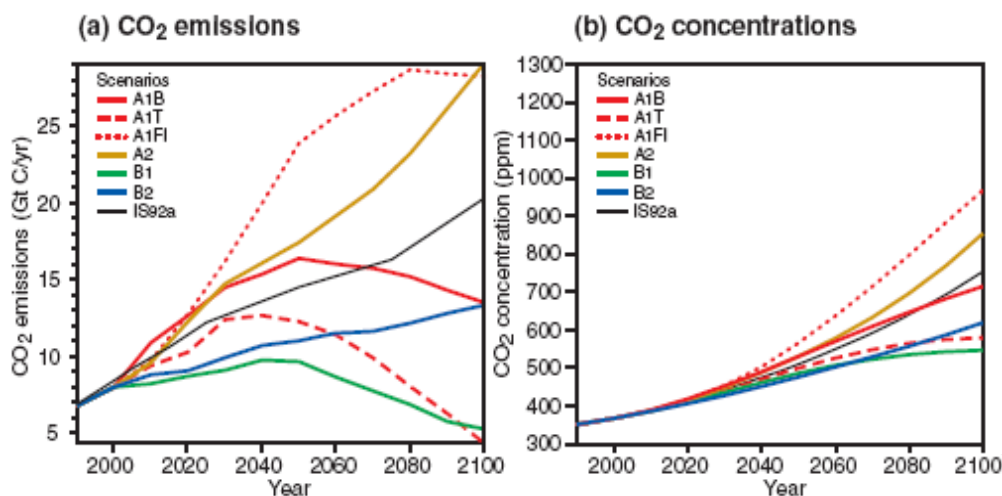
Figure 2.5. SRES projections of CO$_2$ emissions and concentrations.

Source: Houghton et al., 2001.

approximately in the middle of the range of predicted future concentrations, reaching close to 600 ppm by 2075. A1FI has the highest concentrations, reaching close to 800 ppm by 2075, and B1 has the lowest, reaching about 500 ppm by 2075. The A2 scenario produces CO$_2$ concentrations of about 700 ppm by 2075, which is between the A1B and A1FI scenarios. The B2 scenario produces CO$_2$ concentrations of just over 500 ppm by 2075, which is between the CO$_2$ concentrations in the A1B and B1 scenarios.

In addition to representing low, middle, and high projections for GHG emissions and concentrations, scenarios B1, A1B, and A1FI represent the low, middle, and high predictions for GMT. For the year 2030, we only used the A1B scenario since the three scenarios are so similar at that time, but for 2050 and 2075 predictions, we used all three scenarios.

2.4.2   Sensitivity

The second critical factor affecting predictions of the effect of increasing concentrations of GHGs on climate in Park City is how much the Earth's climate as a whole will change for a given increase in CO$_2$ concentration in the atmosphere. This rate of global temperature increase relative to the rate of atmospheric CO$_2$ concentration increase is called the sensitivity. Typically, sensitivity is expressed as the rise in GMT as a result of a doubling of the atmospheric CO$_2$ concentration from historic levels ($2 \times CO_2$). The IPCC AR4 (Solomon et al., 2007, p. 65) states:

Analysis of models together with constraints from observations suggest that the equilibrium climate sensitivity is *likely* to be in the range 2°C to 4.5°C, with a best estimate value of about 3°C. It is *very unlikely* to be less than 1.5°C. [Italics in original.]

Based on this recent review and consultations with several atmospheric scientists, we decided to use 3°C as the estimate of sensitivity in our modeling for this project. In other words, our models use the estimate that a doubling of atmospheric CO_2 concentrations will cause a 3°C increase in GMT.

2.4.3   Patterns of regional climate change

The third critical factor for predicting future climate at Park City is how global climate change will be manifested at the regional and local scales of Park City. We used dynamical and statistical downscaling approaches to predict climate changes in the Park City region from seven global general circulation model (GCM) projections, as discussed in Section 2.5.

2.5   Climate Models

We used the developed climate scenarios, described in Section 2.4, as inputs to climate models to project future climate in the Park City region. There are various methods available for modeling future climate, all of which to some degree depend on the output from global GCMs. We used three types of modeling approaches, using global GCMs, regional climate models (RCMs), and a statistical downscaling model (SDSM) to examine potential future climate in the Park City region. All three modeling approaches provide projections of changes in temperature and precipitation on a monthly and annual basis:

▸ The first modeling approach directly relies on output from the global GCMs. We used the tool MAGICC/SCENGEN to process GCM projections. MAGICC/SCENGEN is a coupling of two models that allow users to investigate future climate change and its uncertainties at regional scales (Wigley, 2008). It scales output from multiple GCMs to a common grid scale [240 kilometers (km) (150 miles) on a side], and allows users to run a range of emissions scenarios for a particular area of interest. MAGICC stands for Model for the Assessment of Greenhouse-gas Induced Climate Change. SCENGEN stands for Global and Regional Climate SCENario GENerator.

▸ The second modeling approach uses a regional climate model. RCMs are high-resolution models built for a region, such as the United States, that is "nested" within a GCM. This means that the output from the GCMs provide the boundary conditions for the smaller-

scale RCMs. We used an RCM called MM5 (Leung et al., 2003a, 2003b, 2004; Leung and Qian, 2005) that is nested in the Parallel Climate Model (PCM; Dai et al., 2004). We refer to this as the PCM-RCM model.

▸ The statistical downscaling model is the third modeling approach in which we use the statistical relationship between variables at a large scale and at a local scale to estimate how climate at a specific location, such as a weather station, may change in response to changes in GHG concentrations. The SDSM develops a statistical relationship between GCM output for current climate for a particular grid cell and observed climate at a weather station within that grid cell. It then uses this relationship to predict future climate at that weather station based on projected output for the GCM gird cell.

2.5.1   MAGICC/SCENGEN

MAGICC uses GHG emissions scenarios to predict GMT and precipitation. SCENGEN constructs climate change scenarios using results from MAGICC, and scales the results to predict regional climate changes in 2.5° latitude by 2.5° longitude cells [approximately 240 km (150 miles) on a side]. Output from SCENGEN includes changes from historic averages in temperature and precipitation and changes in temperature and precipitation variation.

The SCENGEN grid boxes around Park City are shown in Figure 2.6. In reality, climate within a grid box can vary substantially because of topographic relief, but SCENGEN does not capture climatic differences at this scale. The values for the grid cell containing Park City are calculated as the average of the cell and the eight surrounding cells. The nine-cell (7.5° × 7.5°) area average is generally considered a more stable estimate of site changes since results for an individual grid cell are subject to more noise than a larger area surrounding the site. A discussion of the smoothing process for the SCENGEN output, and its advantages, is provided in Appendix B.

To run MAGICC/SCENGEN, the user must define which GCMs to include as climate drivers. GCMs are sophisticated, complex models that form the basis for many climate change models. GCMs attempt to mimic the Earth's climate drivers, including the oceans, land, ice, atmosphere, and biosphere, by integrating equations of fluid dynamics, chemistry, and biology. There are numerous GCMs, and we were most interested in the models that best simulate the current climate at the global, continental, and regional scales. In an evaluation of the ability of 20 existing GCMs to simulate current climate globally, over the contiguous United States and in the Park City region, Wigley (2008) concluded that the following seven models performed best.[4]

---

4. For more information on model selection, see the MAGICC/SCENGEN user manual; available at http://www.cgd.ucar.edu/cas/wigley/magicc/UserMan5.3.v2.pdf.
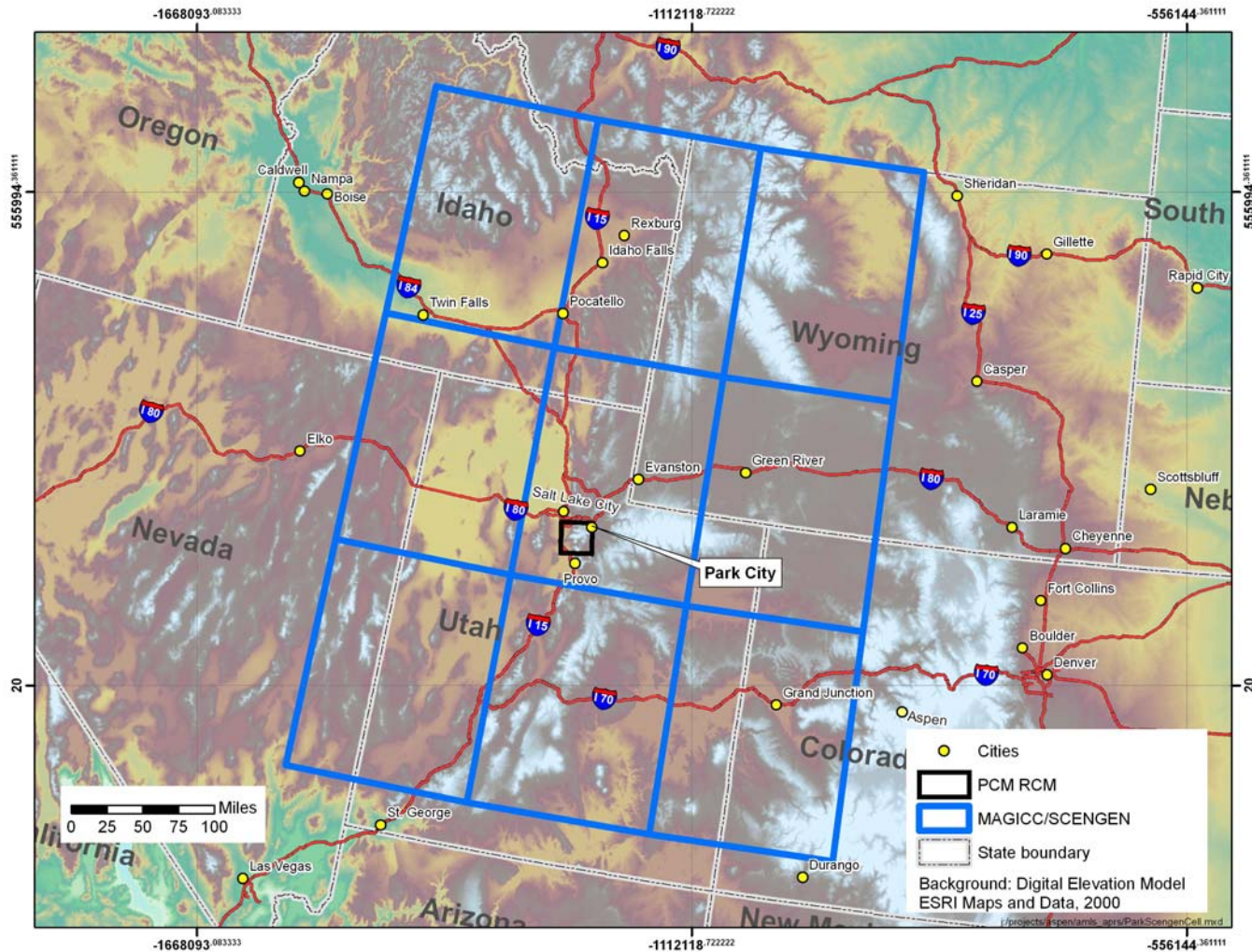
Figure 2.6. 2009 SCENGEN grid boxes and the PCM-RCM domain containing Park City. The coordinates of the SCENGEN boxes are 37.5° to 45°N latitude and 107.5° to 115°W longitude. The coordinates of the PCM-RCM boxes are 37.5° to 45°N latitude and 107.5° to 115°W longitude 40.33° to 40.71°N to 111.50° to 111.87°W.

▸   CSIRO-Mk3.0 – Commonwealth Scientific and Industrial Research Organisation, Atmospheric Research, Australia

▸   UKMO-HadCM3 –Hadley Centre for Climate Prediction and Research/Met Office, United Kingdom Meteorological Office

▸   UKMO-HadGEM1 –Hadley Centre for Climate Prediction and Research/Met Office, United Kingdom Meteorological Office

▸   BCCR-BCM2.0 – Bjerknes Centre for Climate Research, Norway

▸   CNRM-CM3 – Météo-France/Centre National de Recherches Météorologiques, France

▸   GFDL-CM2.1 – U.S. Department of Commerce/National Oceanic and Atmospheric Administration (NOAA)/Geophysical Fluid Dynamics Laboratory, United States

▸   MRI-CGCM2.3.2 – Meteorological Research Institute, Japan.

Therefore, we used these seven GCMs in our analysis.

These models are described on the website for the Program for Climate Model Diagnosis and Intercomparison (PCMDI, 2008).We examined climate predictions from MAGICC/SCENGEN using each of the seven GCMs independently, and used an average of output from the seven GCMs to project climate change in the Park City region. Appendix C presents an analysis of the seven models' simulation of current climate in the nine SCENGEN grid boxes centered on Park City.

2.5.2   PCM-RCM

For a higher resolution estimate of changes in climate in the Park City area, we used the model PCM-RCM "MM5" (Leung et al., 2003a, 2003b, 2004; Leung and Qian, 2005). PCM-RCM "MM5" has grid boxes approximately 36 km (20 miles) on a side (Figure 2.6), approximately an order of magnitude less in area than the GCM grids. The model is nested in the PCM GCM (Dai et al., 2004). It is currently not possible to run this model past 2075.

The approximate boundaries of the PCM-RCM grid box are 40.33° to 40.71°N to 111.50° to 111.87°W. The average elevation of the grid box is 2,086 meters (m) [6,844 feet (ft)]. The PCM-RCM results for the selected years are averages of time periods centered on the specific years. The time periods are defined as follows: 2030 is the average of model simulations for 2020 to 2040, 2050 is the average of model simulations for 2040 to 2060, and 2070 is the average of model simulations for 2065 to 2075. The predicted changes in precipitation and temperature are

reported as changes relative to the base period of 1990 (the average of model simulations for 1981 to 2000). We used the temperature and precipitation outputs from PCM-RCM for the snowpack analysis.

2.5.3   SDSM

The statistical relationship between climate variables at a large scale and at a local scale can be used to estimate how climate at a specific location may change as a result of future climate change at the global scale. This approach necessarily assumes that the current relationship between climate variables at a large-scale and at a specific location do not vary with climate change.

The only emissions scenarios that can currently be downscaled with the SDSM are A2 and B2. We used these emissions scenarios and output from the UKMO-HadCM3 GCM for the grid cell containing Park City. The output was downscaled using the SDSM to the Thaynes Canyon SNOpack TELemetry (SNOTEL) (NRCS, 2009) at the mid-mountain station at the Park City ski area (see Appendix D authored by Dr. Rob Wilby). The statistical relationship developed using the SDSM was then used to project future climate at Thaynes Canyon from the projected GCM output.

2.6   Predictions of Climate Change

2.6.1   MAGICC/SCENGEN

We first report temperature and precipitation predictions for the central A1B emissions scenario for each of the seven individual GCMs and for the average of the seven GCMs in 2030, 2050, and 2075. We then examine the differences between temperature and precipitation predicted for each of the three emissions scenarios (A1FI, A1B, and B1) using the average of the seven GCMs.

Figure 2.7(A) presents estimated change in average annual temperature (in °C) for Park City in 2030 (relative to 1990) using the A1B scenario. The first seven bars are results for individual models; the last bar is the model average. Under this scenario, the average model prediction for the increase in global temperature is 1.6°C (about 3°F), with a range of 1.1 to 1.9°C (2 to 3.5°F) across the seven models, which is a relatively small variability.

Figure 2.7(B) presents the estimated changes in annual precipitation in 2030 relative to 1990 for A1B. Six of the seven GCMs predict a decrease in precipitation for Park City (up to a 9.3% decrease), and the average across the models is a 3.5% decrease. MRI-CGCM2.3.2 predicts a
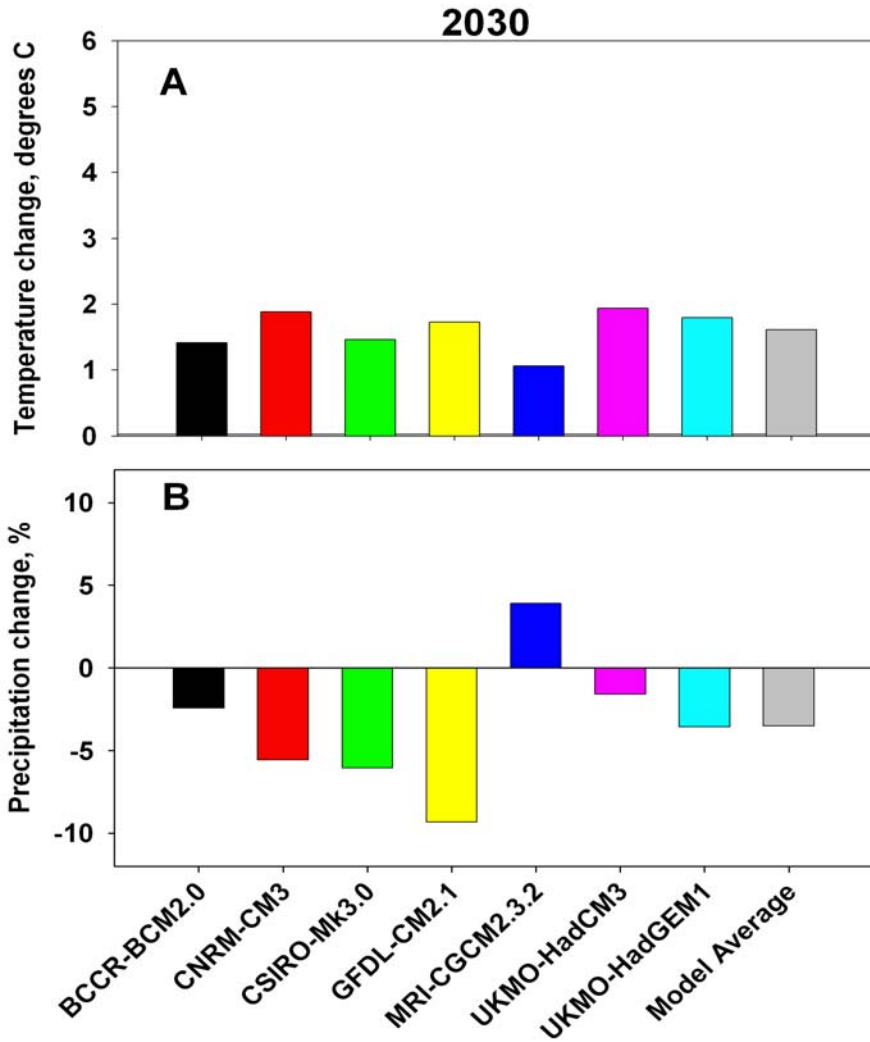
Figure 2.7. Estimated average annual temperature (A) and total annual precipitation (B) changes in Park City, predicted by seven GCMs, for the A1B emissions scenario in 2030.

slight increase in precipitation (3.9%). Estimated decreases are partially a result of the assumed increase in GHGs and partially the result of aerosols (e.g., sulfur dioxide). Aerosols are a GHG and thus are projected as part of the emissions scenarios, along with CO_2 and other GHG emissions. If aerosol increases are not as large as in the A1B scenario, estimated decreases in precipitation would not be as large.

By 2050, average warming near Park City for the A1B scenario is 2.3°C (4.1°F) with a range of 1.5 to 2.9°C (2.7 to 5.2°F) across the seven models. All seven models predict similar results (Figure 2.8A). Predictions for precipitation are much more variable: the predicted changes in precipitation range from -10.4% to +10.8% (Figure 2.8B). Based on the average of seven models, the total annual precipitation is predicted to decrease by -1.3%.
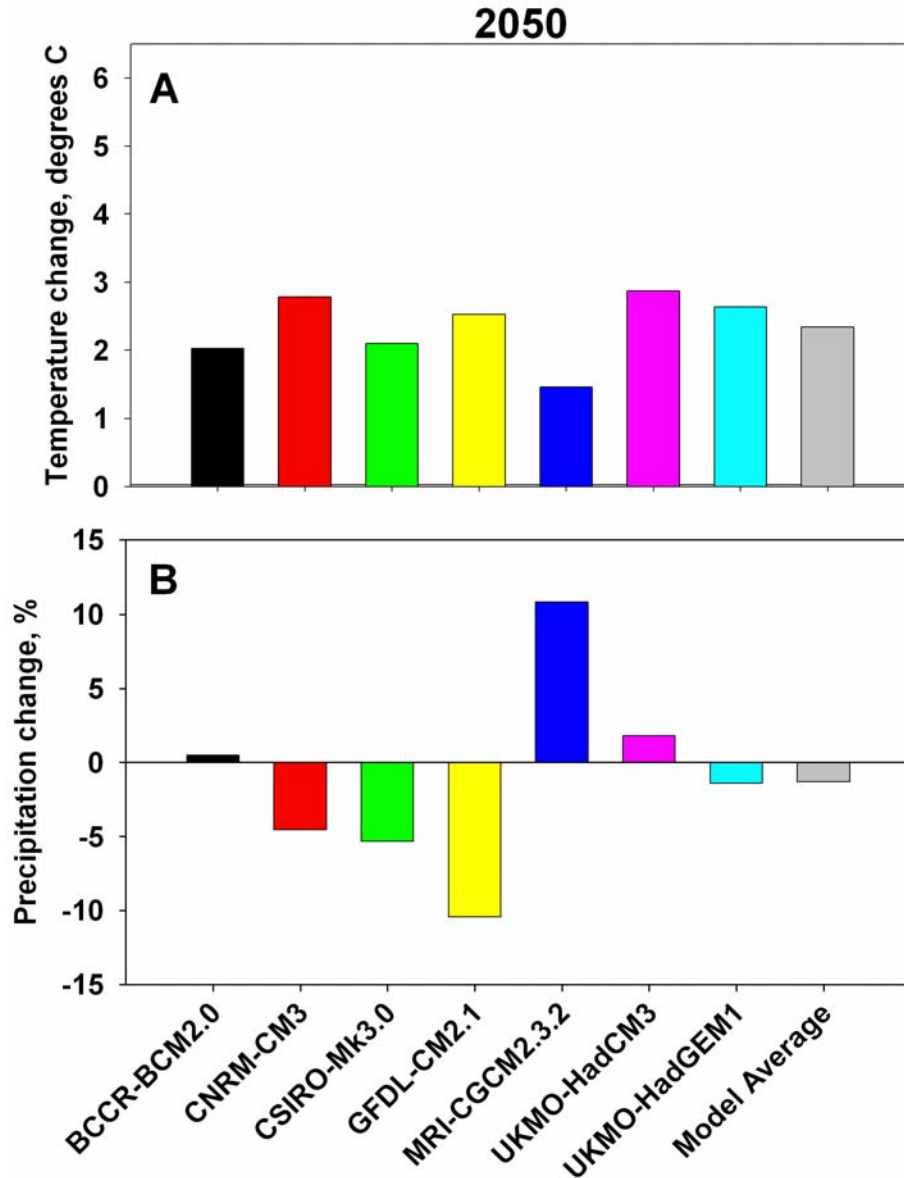
Figure 2.8. Estimated average annual temperature (A) and total annual precipitation (B) changes in Park City, predicted by seven GCMs, for the A1B emissions scenario in 2050.

By 2075, the seven GCMs predict an average warming near Park City of 3.8°C (6.8°F), with a range of 2.6 to 4.6°C (4.7 to 8.3°F) (Figure 2.9A). The average of the seven GCMs predicts a precipitation decrease of 4.3% compared to 1990 (Figure 2.9B). The wettest model, MRI-CGCM2.3.2, predicts a 13.1% increase in precipitation, while the driest, GFDL-CM2.1, predicts a 16.8% decrease.
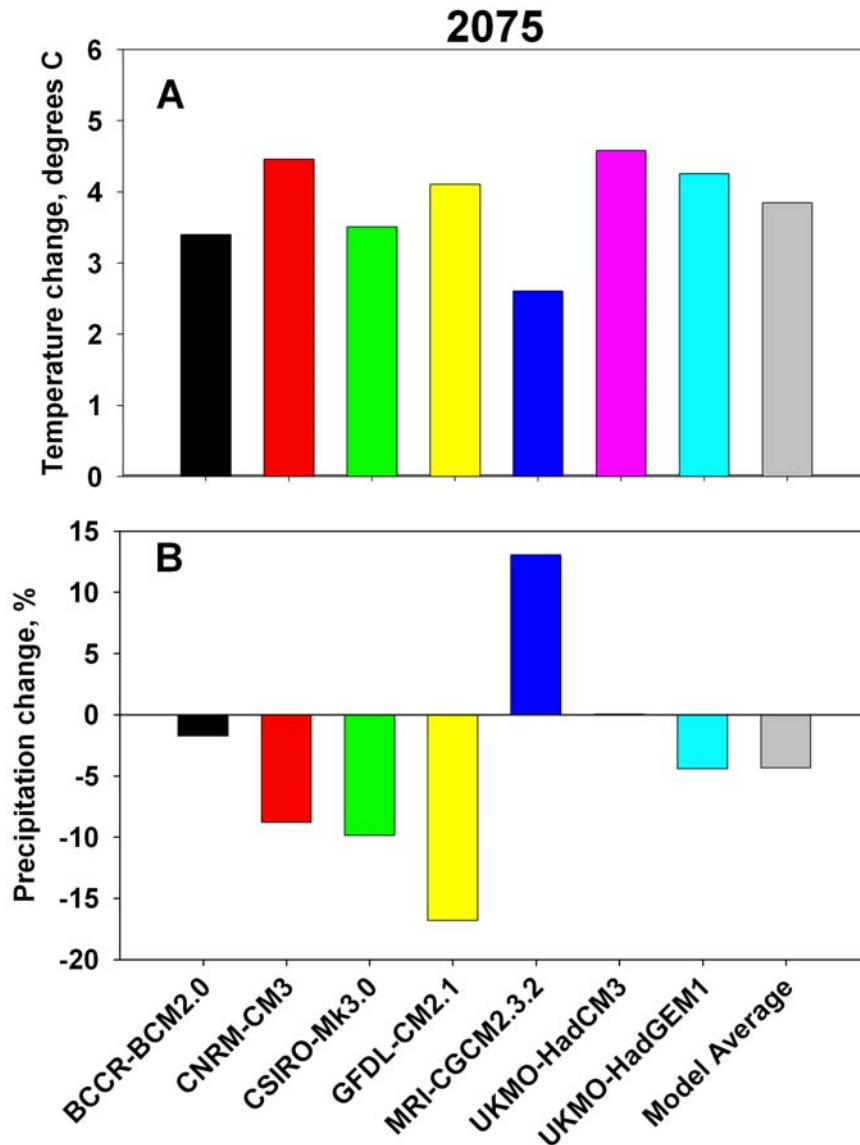
Figure 2.9. Estimated annual temperature (A) and precipitation (B) changes in Park City, predicted by seven GCMs, for the A1B emissions scenario in 2075.

Even though a majority of the models predict a decrease in precipitation, we do not interpret this as a consensus. There is too much variability across the models to be confident about whether precipitation will increase or decrease.

Next, we examined differences between temperature and precipitation predicted for each of the three emissions scenarios (B1 – low, A1B – middle, and A1FI – high) in 2030, 2050, and 2075, using the average of the seven GCMs (Tables 2.2 and 2.3). The temperatures are predicted to increase with increasing GHG emissions, and with time. Under the high GHG emissions scenario (A1FI), the average temperature increase in 2050 is 3.1°C (5.6°F), and in 2075 is 5.0°C (9.0°F). Under the low GHG emissions scenario (B1), the average temperature increase is 1.8°C (3.2°F) in 2050 and 2.8°C (4.9°F) in 2075. The largest temperature increases are predicted for the summer months, while the smallest increases are predicted for the winter months. This is the case for all three emissions scenarios (Figure 2.10).

Table 2.2. MAGICC/SCENGEN predictions of mean annual temperature change (°C) **relative to 1990 for low, middle, and high emissions scenarios.** "Average" = averaged input from seven GCMs. "Range" = range of results from each of the seven individual GCMs.

| | Emissions scenario | | | | | |
| | **B1 – low** | | **A1B – middle** | | **A1FI – high** | |
Year	**Average**	**Range**	**Average**	**Range**	**Average**	**Range**
2030	1.7°	1.5 to 2.1	1.6°	1.1 to 1.9	1.6°	1.0 to 1.9
2050	1.8°	1.4 to 2.1	2.3°	1.5 to 2.9	3.1°	2.0 to 3.7
2075	2.8°	1.9 to 3.3	3.8°	2.6 to 4.6	5.0°	3.2 to 6.1

Table 2.3. MAGICC/SCENGEN predictions of mean annual precipitation change (%) **relative to 1990 for low, middle, and high emissions scenarios, using averaged input from five GCMs.** "Average" = averaged input from seven GCMs. "Range" = range of results from each of the seven individual GCMs.

| | Scenarios | | | | | |
| | **B1 – low** | | **A1B – middle** | | **A1FI – high** | |
Year	**Average**	**Range**	**Average**	**Range**	**Average**	**Range**
2030	-5.4	-10.1 to 0.5	-3.5	-9.3 to 3.9	-3.4	-9.4 to 4.3
2050	-0.7	-7.6 to 8.2	-1.3	-10.4 to 10.8	-4.5	-15.6 to 10.6
2075	-4.0	-12.6 to 7.4	-4.3	-16.8 to 13.1	-4.5	-21.8 to 21.3
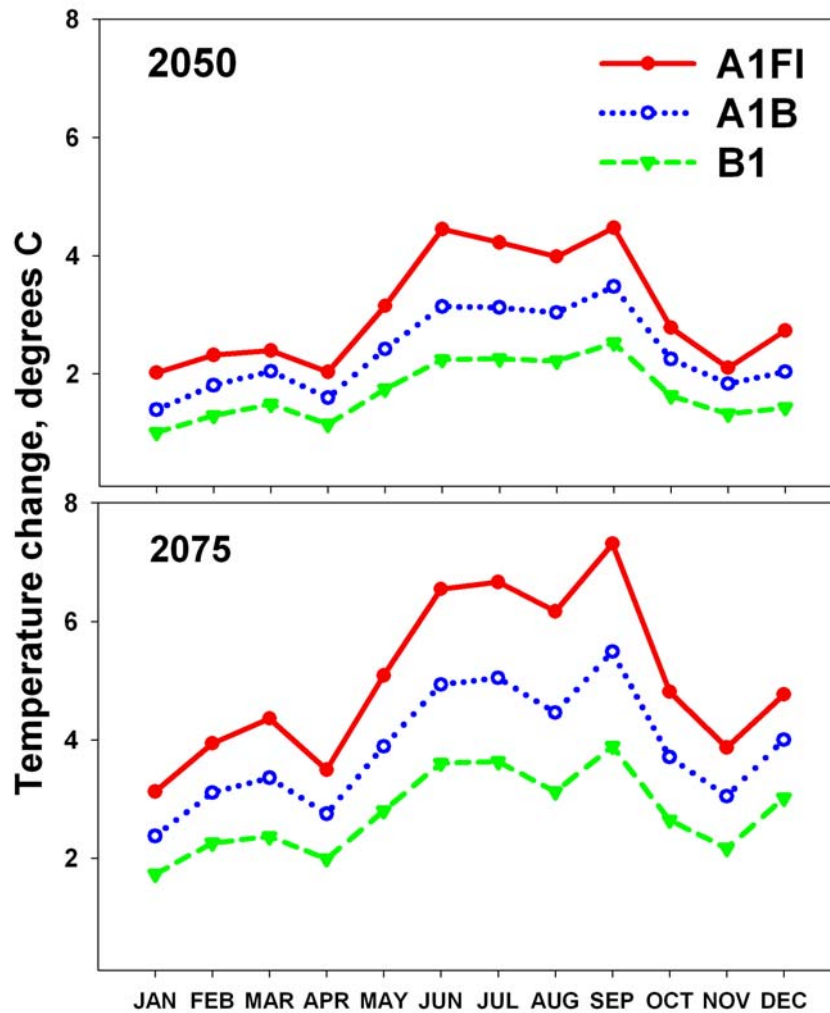
Figure 2.10. MAGICC/SCENGEN projections of monthly average temperature changes (compared to 1990) for the A1FI – high, A1B – middle, and B1 – low emissions scenarios for 2050 and 2075, using averaged projections from seven GCMs as input.

The change in precipitation appears to be more sensitive to the choice of GCM than to emissions scenario (Table 2.3), meaning that predictions of the change in precipitation are more uncertain across the different models than predictions of the change in temperature.

2.6.2   PCM-RCM

For the Park City area in 2030, PCM-RCM predicts an increase in temperature relative to the base year 1990 for each month except November (Figure 2.11A). Averaged over the year, precipitation is predicted to change by less than 10%. However, PCM-RCM predicts a decrease in precipitation from October through March, and an increase in April, July, and August (Figure 2.11B).
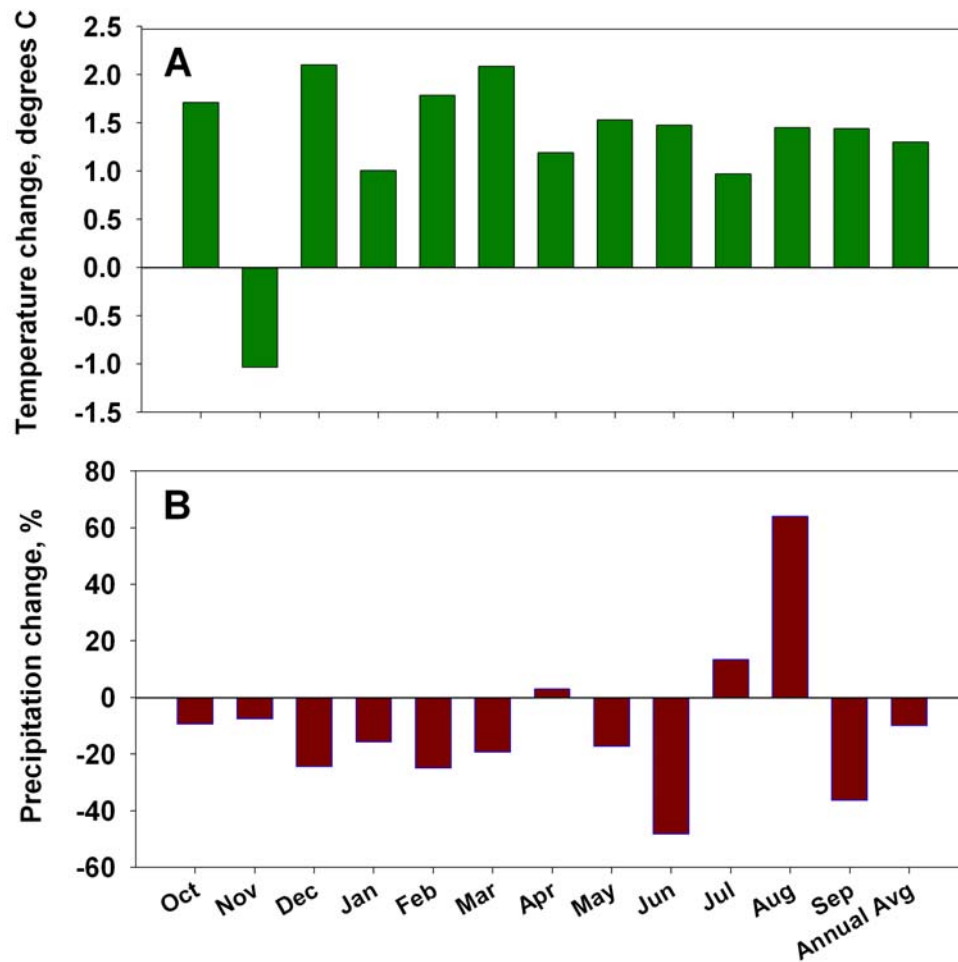
Figure 2.11. Predicted changes in monthly average temperature (A) and total monthly precipitation (B) from PCM-RCM in 2030.

By 2050, the average annual temperature increase is greater than that predicted for 2030, and most monthly average temperature increases are greater than in 2030 (Figure 2.12A). Average annual precipitation is predicted to decrease by approximately 10% (Figure 2.12B). Precipitation in October through April is predicted to decrease by 9%.
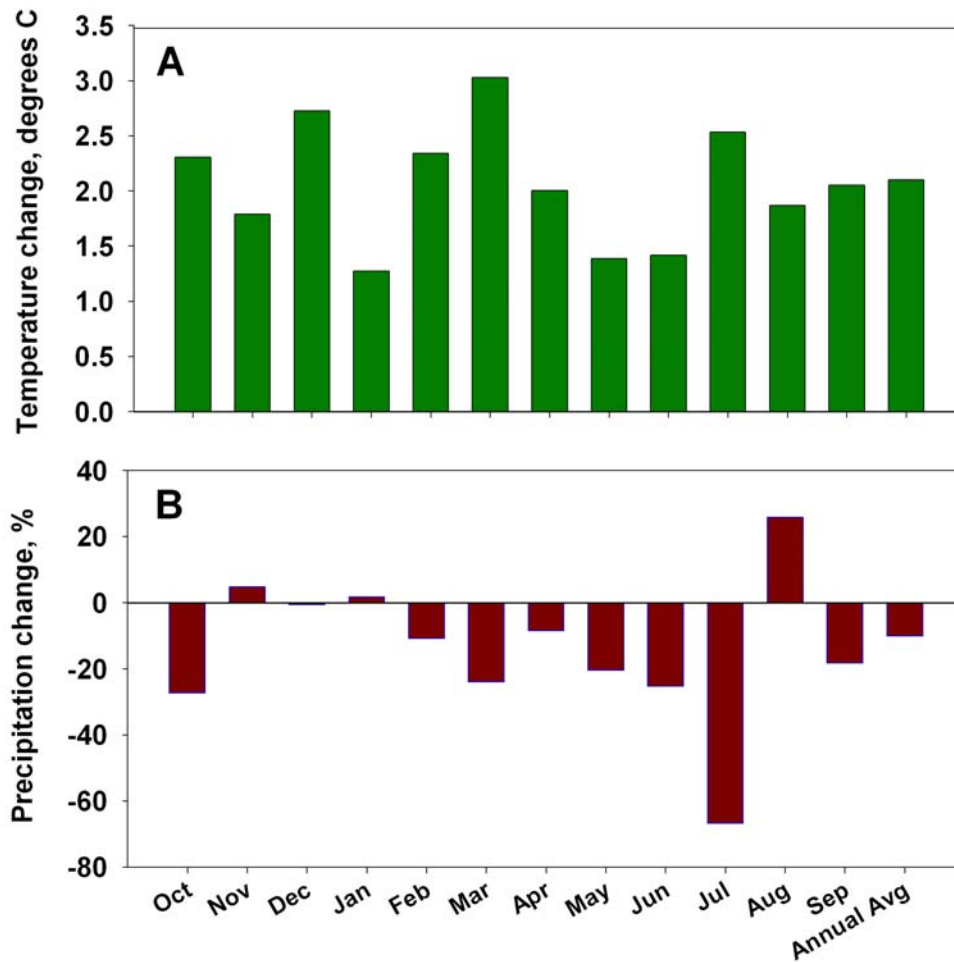
Figure 2.12. Projected changes in monthly average temperature (A) and precipitation (B) from PCM-RCM in 2050.

By 2070,[5] the average annual temperature increase is slightly greater than that predicted for 2050 (Figure 2.13A). In January, temperature is predicted to decrease relative to 1990. Average annual precipitation is predicted to decrease by approximately 10%. This annual decrease is driven by a predicted 40% decrease for May through September (Figure 2.13B). Precipitation in October through April is predicted to increase by 6% despite February being predicted to be 40% drier.
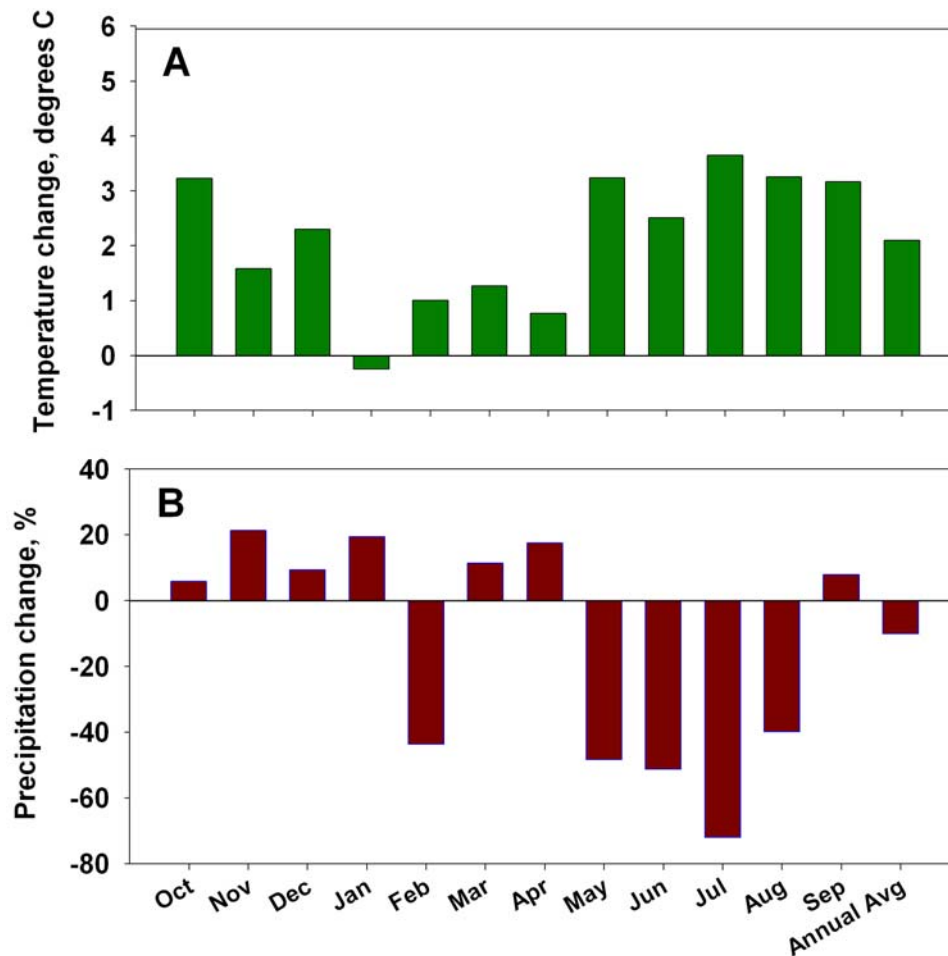
Figure 2.13. Projected changes in monthly average temperature (A) and precipitation (B) from PCM-RCM in 2070.

---

5. PCM-RCM projections are for 2070 (rather than 2075) because PCM-RCM analysis requires that we take an average of multiple years, centered on the time period of interest. Since PCM-RCM projections are only available to 2075, we centered our average on 2070.

PCM-RCM generally predicts smaller temperature increases than MAGICC/SCENGEN and the seven GCMs. Consistent with the MAGICC/SCENGEN and GCM predictions, PCM-RCM predicts a small decrease in total annual precipitation, even though precipitation may increase in some months.

2.6.3   SDSM

Dr. Rob Wilby ran the SDSM for Park City under the A2 and B2 emission scenarios (Appendix A), and the UKMO-HadCM3 GCM (Appendix D). The predictions of temperature and precipitation changes using statistical downscaling of the UKMO-HadCM3 are shown in Table 2.4. The results are downscaled to the mid-mountain station at the Park City ski area, which is located at 2,813 m (9,230 ft). The temperature increases predicted using this downscaling approach are generally smaller than those predicted by MAGICC/SCENGEN and the GCMs. The direction of precipitation change is similar, but the predicted reduction in total annual precipitation is more severe.

Table 2.4. Predicted changes in temperature and precipitation using statistical downscaling from UKMO-HadCM3 to the mid-mountain station at Park City ski area, 2,813 m (9,230 ft)

Year	Scenario	Average annual temperature increase (°C)	Total annual precipitation change (%)
2030	B2 – Moderate	1.45°	-12.0
	A2 – High	1.05°	-2.0
2050	B2 – Moderate	2.09°	-11.1
	A2 – High	2.16°	-12.0
2075	B2 – Moderate	2.72°	-16.5
	A2 – High	3.63°	-13.5

2.7   Summary

Under all of the emissions scenarios, all of the models predict a substantial increase in temperature for the Park City area over the next 70 years. The predicted average annual increase in temperature for Park City ranges from about 1.0 to 2.1°C (1.8 to 3.8°F) by 2030 under all scenarios. By 2050, all scenarios predict an average annual increase in temperature ranging from about 1.4 to 3.7°C (2.5 to 6.7°F). The predicted average annual increase in temperature for Park

City ranges from about 2.7 to 3.6°C (4.9 to 6.5°F) by 2075 by the SDSM modeling approach to about 2.8 to 5.0°C (5.0 to 9.0°F) by 2075 by the MAGICC/SCENGEN model. The GCMs simulate observed temperatures well, and generally agree on the direction and magnitude of warming. This gives us a high degree of confidence in the temperature projections for the Park City region.

On average, the MAGICC/SCENGEN, PCM-RCM, and SDSM models predict a decrease in precipitation regardless of the emissions scenario and modeling approach, with the largest reductions in precipitation predicted for the summer months. Given the variability in the results among the GCMs, we cannot be certain about the direction or magnitude of change in precipitation.

3.   Park City Mountain Resort Snowpack Modeling

3.1   Introduction

We parameterized and ran a snowpack model to evaluate how snow at the PCMR could be affected by the climate change predictions described in Chapter 2. Our objectives were to estimate the length of the ski season, the timing of snowpack buildup and melt, and the snow depth and coverage at specific times and elevations under future climate change.

3.2   Snowmelt Runoff Model

We used the Snowmelt Runoff Model (SRM; Martinec, 1975; Martinec et al., 1994; SRM, 2002) to examine snowpack characteristics at PCMR. The SRM is designed to predict snow coverage and snowmelt runoff patterns and is based on the fundamental concept that changes in air temperature provide an index of snowmelt. The SRM calculates the maximum snow in storage on a defined winter end date, beyond which the SRM predicts the melting process and the subsequent reduction in SCA. We then develop a relationship between SCA and snow depth to predict snow depth from modeled SCA. We use projected snow depth to determine if skiable snow will be present at different elevations at different time during the ski season. Skiable snow is defined by mountain managers as a snowpack with a minimum depth of approximately 6 inches.

To model the rate and spatial distribution of snowpack buildup during the fall and early winter months, we developed an additional model component for use with the SRM. The start of snowpack buildup is defined as the date when precipitation falls as snow rather than as rain and remains as snow on the ground. Since snowpack buildup is dictated by temperature and precipitation, we used changes in temperature to determine the change in when snow begins to accumulate by applying the predicted changes in Park City area temperature from the climate models to average weekly observed historical records. We scaled the historic rates of change in SCA by changes in precipitation.

The spatial extent of this evaluation was the area within the current (2009) PCMR property boundary [17.5 square kilometers (km^2)]. The property boundary encompasses a vertical relief of approximately 1,067 m (3,500 ft), from the base area at 2,100 m (6,890 ft) to the highest elevation at 3,170 m (10,400 ft). We created four elevation zones with an average elevation span of 265 m (872 ft) and modeled snowpack coverage separately within each of the zones (Figure 3.1).
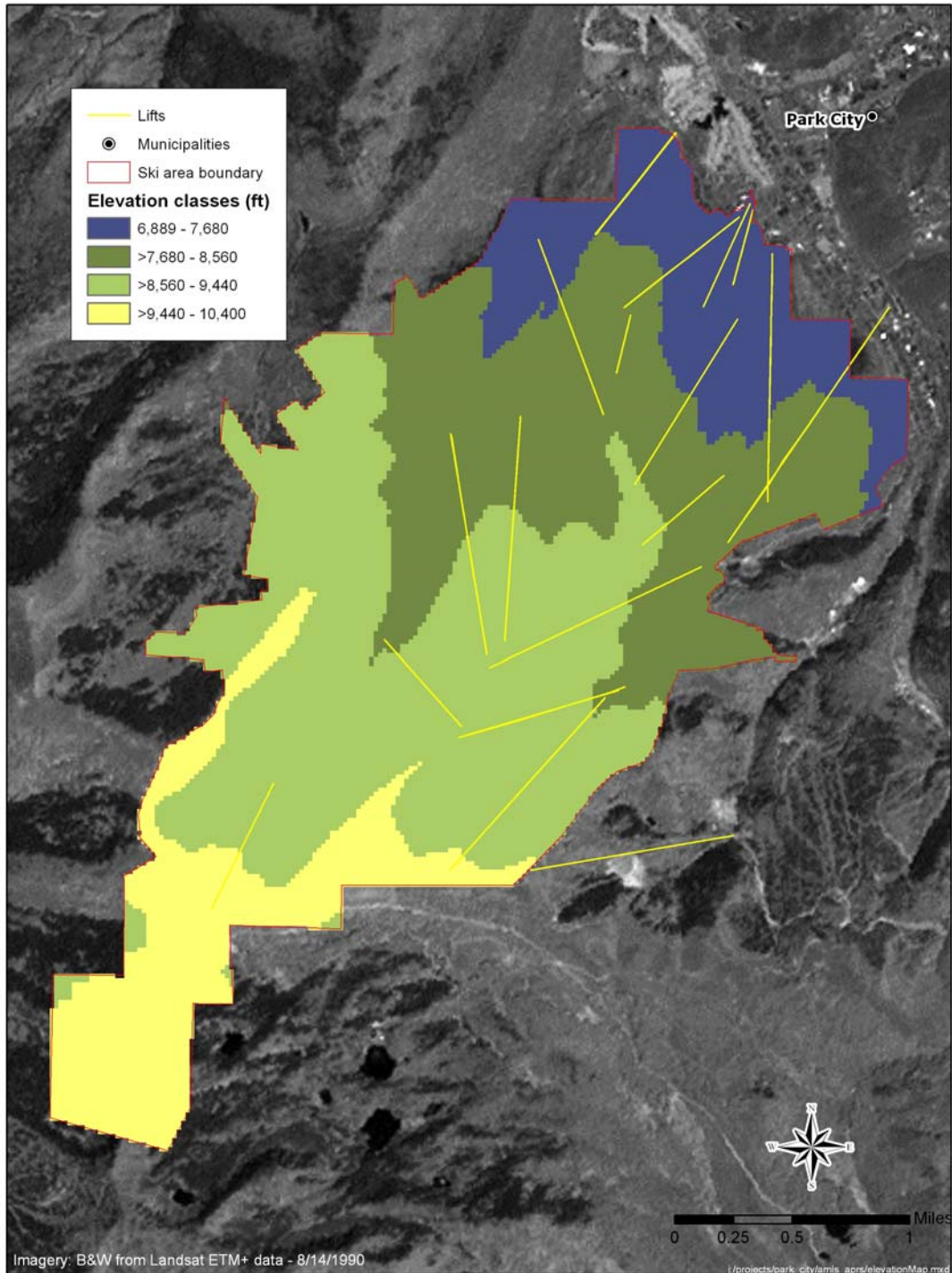
Figure 3.1. Spatial extent of the SRM evaluation. Colors identify the four elevation zones for which snowmelt is modeled. Blue is the base area and yellow is the top of the ski area.

The SRM requires current climate data and an estimate of daily SCA which are described in the following sections.

3.2.1   Current climate data

The SRM requires full-year temperature and precipitation datasets as model input, and we identified two sources of meteorological data for the PCMR area that meet this criteria. Full-year datasets were available from the weather station at the golf course in the town of Park City [elevation 2,080 m (6,824 ft)], and from the Thaynes Canyon U.S. Geological Survey (USGS) SNOTEL site located near the mid-mountain station in the ski area [elevation 2,813 m (9,230 ft)]. The golf course station is within 23 m (76 ft) of the base area elevation and is approximately a quarter mile away, and we used data from the golf course to estimate both temperature and precipitation conditions at the bottom of PCMR. For temperatures between the base area and Thaynes Canyon and above Thaynes Canyon, we used the observed rate of change in temperature with elevation, based on differences in concurrent temperatures at the two weather stations. The resulting average, which is called a lapse rate, is 0.40°C/100 m. For each 100-m increase in elevation, we expect temperature to decrease 0.4°C on average. For precipitation, we compared cumulative winter snowfall, measured in snow-water equivalent (SWE) at the Thaynes Canyon SNOTEL station and the adjacent ski area weather station (Summit station) and found that the totals matched very well (Figure 3.2). This allowed us to use precipitation data from Thaynes Canyon to represent precipitation from the mid to upper parts of PCMR.
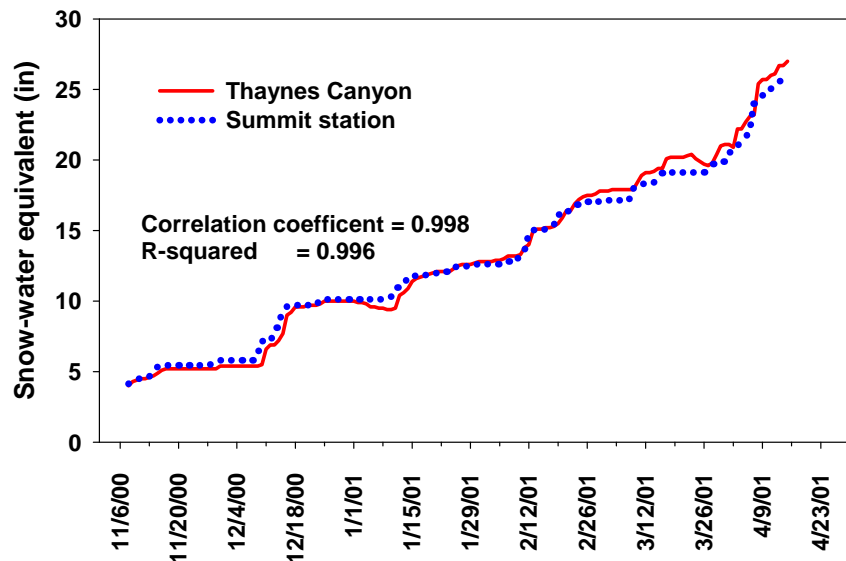
Figure 3.2. Comparison of cumulative SWE between Thaynes Canyon and the mid-mountain Summit station on Park City Mountain.

3.2.2   Snow-covered area

The SRM requires daily estimates of SCA. We estimated SCA using high resolution Landsat images. Since obtaining high-resolution images for every year would be prohibitively expensive, we selected 2000–2001 as the ski season that is reasonably representative of the historical average SCA. Figure 3.3 shows that precipitation and SWE at Thaynes Canyon from the October 2000 through September 2001 season were similar to average precipitation and SWE from 1971 to 2000. PCMR managers and snow safety directors agreed that the 2000–2001 season snowpack was representative of average conditions.

THAYNES CANYON SNOTEL for Water Year 2001

*** Provisional Data, Subject to Change ***
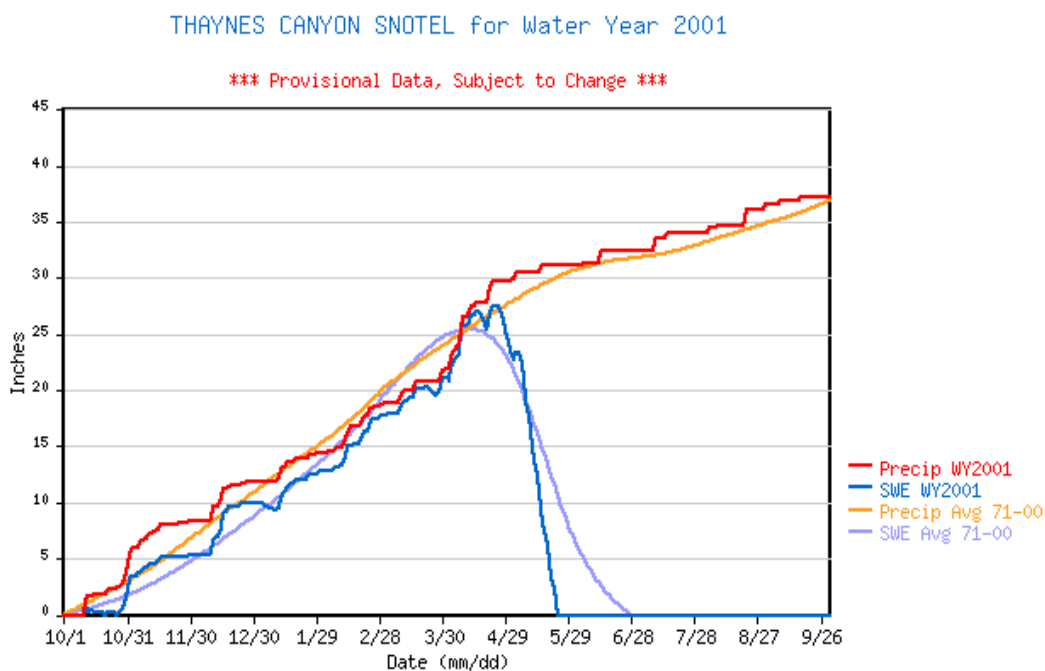
Figure 3.3. SWE and cumulative precipitation measured at the Thaynes Canyon USGS SNOTEL station on Park City Mountain. The historical average is taken from 1971 to 2000. The 2000–2001 season is representative of the historical average.

Source: NRCS, 2009.

We used six Landsat Enhanced Thematic Mapper (ETM+) scenes from 2000 and 2001 (October 19, December 30, January 31, March 4, April 5, and May 7) to estimate SCA for the ski season. The SCA for each date was combined with digital topography to derive estimates of SCA by elevation band. To estimate SCA on all other days, we interpolated linearly between the six scene dates (Figure 3.4). In Appendix E, we describe the SCA estimates in more detail.
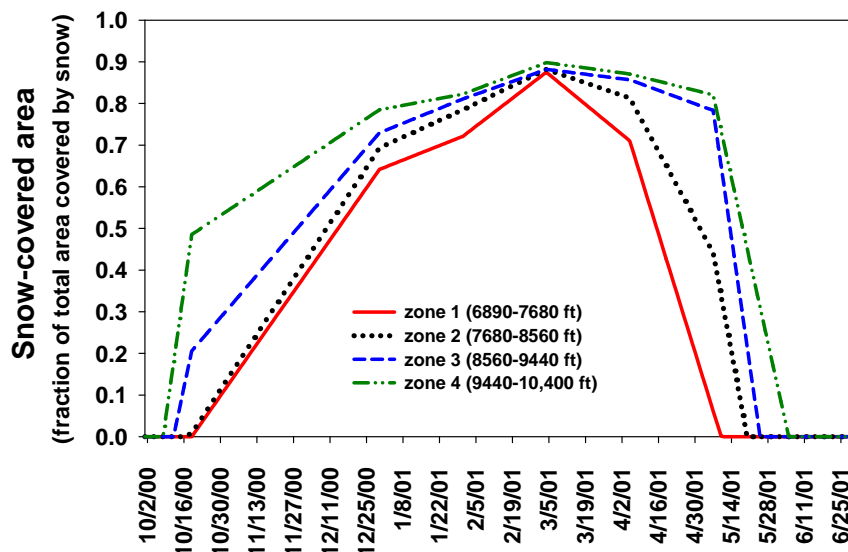
Figure 3.4. Daily time series of SCA by elevation zone for the 2000–2001 ski season.

3.3   SRM Runs

We ran the SRM to simulate melt patterns for the 2000–2001 ski season. SCA depletion due to melt is driven by climate variables and the snow-density-derived degree-day factor. A degree-day is the number of days multiplied by temperature, and the degree-day factor converts degree-days to melt. A degree-day over freezing temperature produces melt, and one below freezing temperature does not. The SRM does not require calibration for modeling SCA depletion since the degree day factor is derived directly from measured snow densities. Varying the snow density-derived degree day factor within reasonable limits (0.2 to 0.8) does not affect the SCA depletion results. We evaluated the ability of the SRM to simulate historical conditions by comparing modeled SCA depletion for elevation Zone 3 to SWE depletion measured at Thaynes Canyon, which is located within Zone 3, for the spring of 2001 (Figure 3.5). SWE is simply the snowpack depth multiplied by snowpack density, thus SWE and snow depth are indicators of one another. Although SCA and snow depth are not equal, they are related in a predictable way (Figure 3.6). Figure 3.5 illustrates that the model predictions of SCA in Zone 3 of PCMR match the actual data for the rate and timing of depletion of SWE at the Thaynes Canyon SNOTEL site, indicating that the model simulates historical observations of SWE in an average year reasonably well.
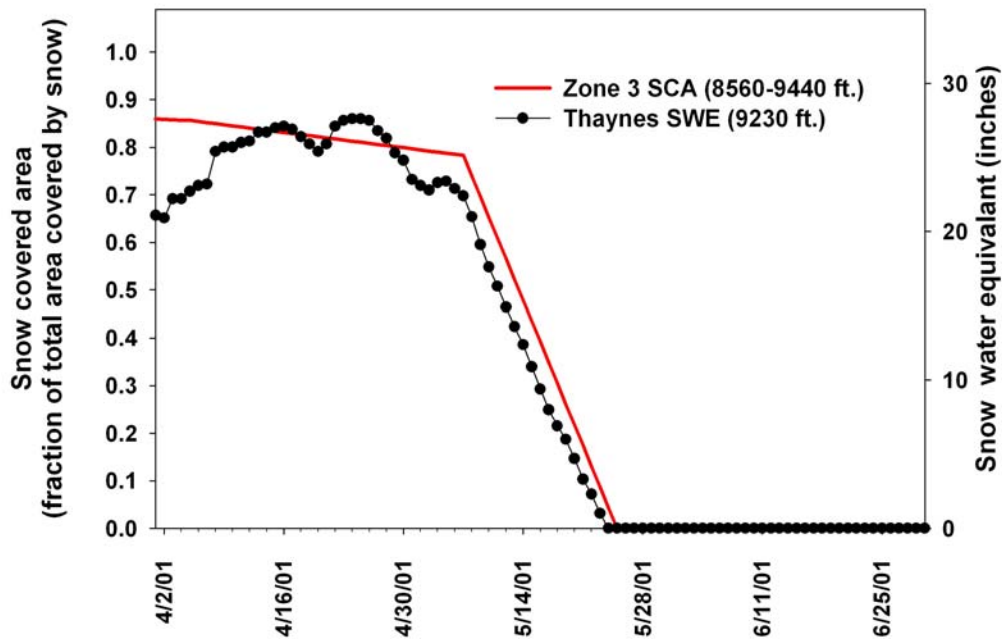
Figure 3.5. Modeled SCA depletion in Zone 3 on PCMR and actual data on SWE depletion at the Thaynes Canyon SNOTEL site for the spring of 2001.
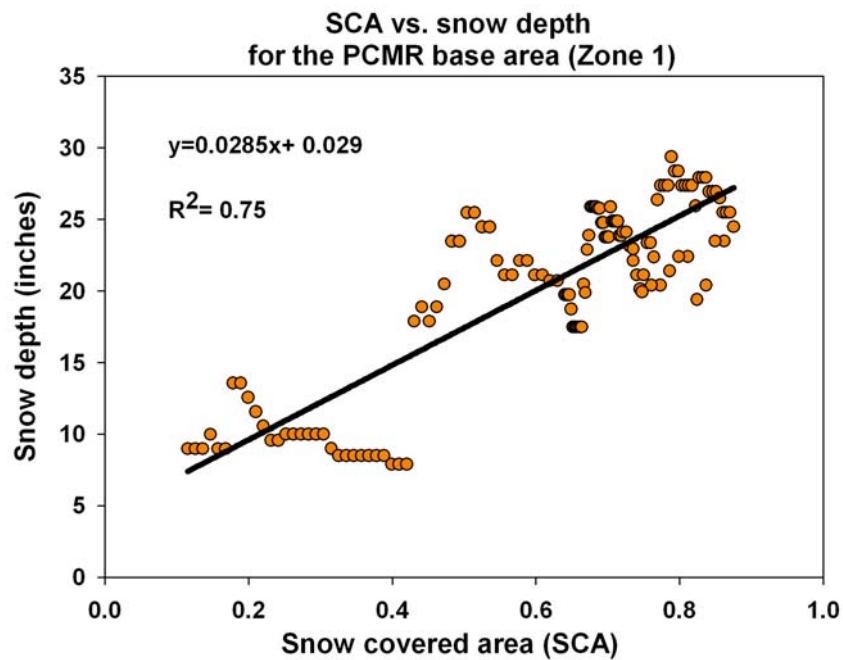
Figure 3.6. Example of SCA vs. snow depth relationship from the base area of PCMR for the 2000–2001 season for Zone 1 (elevation 6,889 to 7,680 ft).

We modeled future climate change scenarios by scaling observed temperature and precipitation records by the predicted monthly changes from the climate models (Chapter 2).For example, if a model projected November to be 2°C warmer than observed temperature for a future scenario, we would add 2°C to the daily observed temperatures for all the days in November. The SRM generated estimated SCA depletion curves from the winter end date (defined as March 1) to the end of the water year (September 30).

We applied the predicted monthly changes in Park City area temperature from the climate models to average weekly observed historical records (1988–present) from the Thaynes Canyon SNOTEL station to estimate the change in timing and rate of snowpack buildup in the future. For example, if the historical record shows that a temperature increase of a given amount delays the start of snow accumulation by five days, then we applied a five-day delay to the snowpack accumulation observed in 2001(our representative year). SCA rates of change were then scaled by the projected monthly changes in precipitation.

In order to predict snow depth for future scenarios, we developed a relationship between snow depth and SCA by plotting SCA and measured snow depth in 2000–2001 for each elevation zone. As an example, Figure 3.6 illustrates this relationship for the base area (Zone 1) [snow depth = $(0.0285 \times SCA) + 0.029$]. Actual measured snow depth data were available from the Jupiter station at the top of the PCMR, the Summit mid-mountain station, and at the golf course near the base area elevation (Figure 3.7). These locations lie in elevation Zones 4, 3, and 1, respectively. To generate a snow depth time series to correlate to daily SCA for the mean of each elevation zone, we interpolated linearly between the three measured datasets (Figure 3.8). Since the relationship between the three measured datasets varied with date, a separate linear interpolation by elevation was conducted for each week throughout the 2000–2001 winter. We used this information to estimate future snow depths given the modeled SCA. Snow depths at the golf course, and Summit and Jupiter stations are not enhanced by snowmaking, and are therefore likely to underestimate observed depths at the base area where snowmaking occurs. Thus, our approach predicts natural snowpack characteristics only. We did not evaluate the effects of augmentation with man-made snow.

3.4   SRM Modeling Results

In the following sections, we describe the results of the models that predict how the start date of snowpack buildup, the start date of snow melt, SCA, and snow depth will respond to climate change in the years 2030, 2050, and 2075.
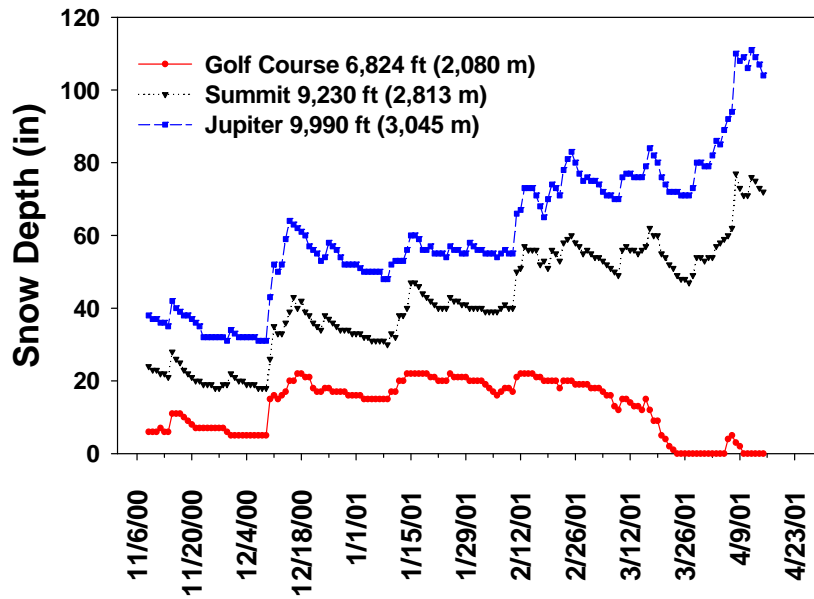
Figure 3.7. Measured snow depths at the golf course, mid (Summit), and top (Jupiter) of Park City Mountain.
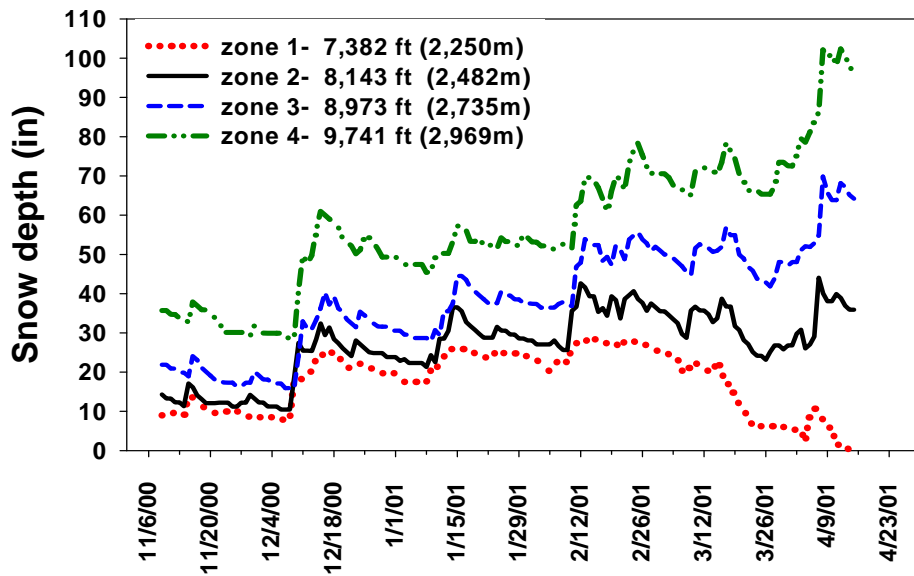
Figure 3.8. Interpolated snow depths for elevations representing each defined elevation zone in the SRM model for the 2000–2001 ski season.

3.4.1   2030

As mentioned earlier, the start of snowpack buildup is defined as the date when precipitation falls as snow rather than as rain and remains as snow on the ground. Historically, the average start date of snowpack buildup at the PCMR has been November 11, based on observed historical records from the Park City golf course weather station (daily average 1988–present) lapsed to the PCMR base area elevation. Our modeling result is that the start of snowpack buildup at the PCMR base area is predicted to begin about one week later in 2030. Recall from Chapter 2 that the only GCM scenario run for 2030 was A1B since the different emissions scenarios do not diverge by 2030. We also ran the SDSM and PCM-RCM scenarios for 2030. Predicted temperatures will still allow some snowpack buildup to occur before Thanksgiving, and approximately two weeks of conditions suitable for snowmaking prior to Thanksgiving. In 2030, snow melt at the base area is predicted to begin about one week earlier than the historical melt initiation date of March 16 under the A1B and PCM-RCM scenarios,[1] and only one day earlier under the A2 and B2 scenarios.

The predicted SCA at PCMR's base area in 2030 is shown in Figure 3.9, and predicted snow depth is shown in Figure 3.10. Snow depth is predicted to be slightly below historically observed depths throughout the ski season (Figure 3.10). For all scenarios in 2030, melt begins earlier than historically, as determined by predicted temperatures. The result is more reduced snow depth by spring break (March 25) due to earlier melt initiation. The earlier snowmelt date causes less than a 50% reduction is snow depth by March 25 for all but the PCM-RCM scenario, which predicts that skiable snow will remain at the base area throughout the spring break season in 2030. Skiable snow is unlikely to exist at the base area during spring break under the PCM-RCM scenario in 2030.

The impact of climate change at the top of mountain will be less pronounced than at the base area in 2030 (Figure 3.11). The start of snowpack buildup at the top of the PCMR will begin about one week later than the average historical start date of October 23. All scenarios, except PCM-RCM, come close to the average historical maximum snow coverage and depth because of minimal (0.6–1.2°C) predicted winter warming. In the PCM-RCM scenario, winter precipitation at the top of the mountain will decrease approximately 18%. This causes predicted maximum snow depths to be 45% below average historical maximums at spring break (Figure 3.12). Although melt initiation is predicted to occur about 10 days earlier than the historical melt initiation date of April 14 for all scenarios, the melt effects will not be apparent by the end of March (i.e., end of spring break).

---

1. PCM-RCM is both a model and emission scenario. The emission scenario is a 1% increase in CO_2 concentrations per year. This scenario is very similar to the A1 scenario.
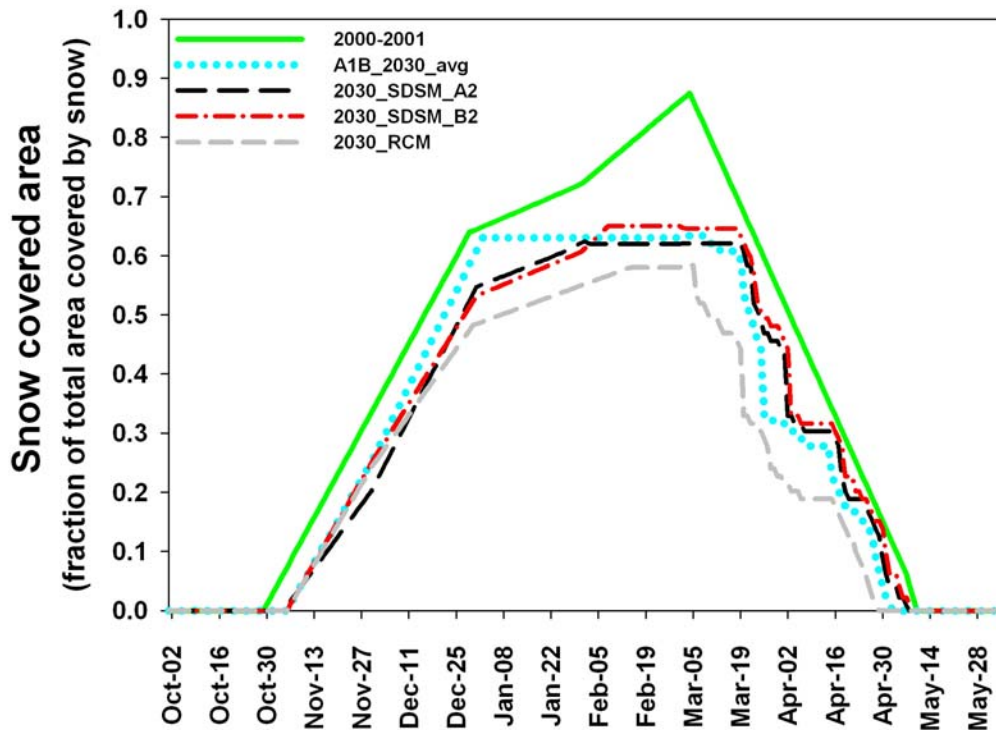
Figure 3.9. Modeled SCA time series at PCMR's base area in 2030 under different climate scenarios. 2000–2001 represents the historically observed SCA for an average ski season.

3.4.2 2050

By 2050, climate change is predicted to have a substantial impact on snow coverage and snow depth at PCMR's base area, although results vary by CO_2 emissions scenario. Snowpack buildup will be delayed by 1.5 weeks under all scenarios but the high emissions A1FI. Under the A1FI scenario, snowpack buildup is delayed by a little over two weeks. The predicted SCAs at PCMR's base area for 2050 are shown in Figure 3.13.
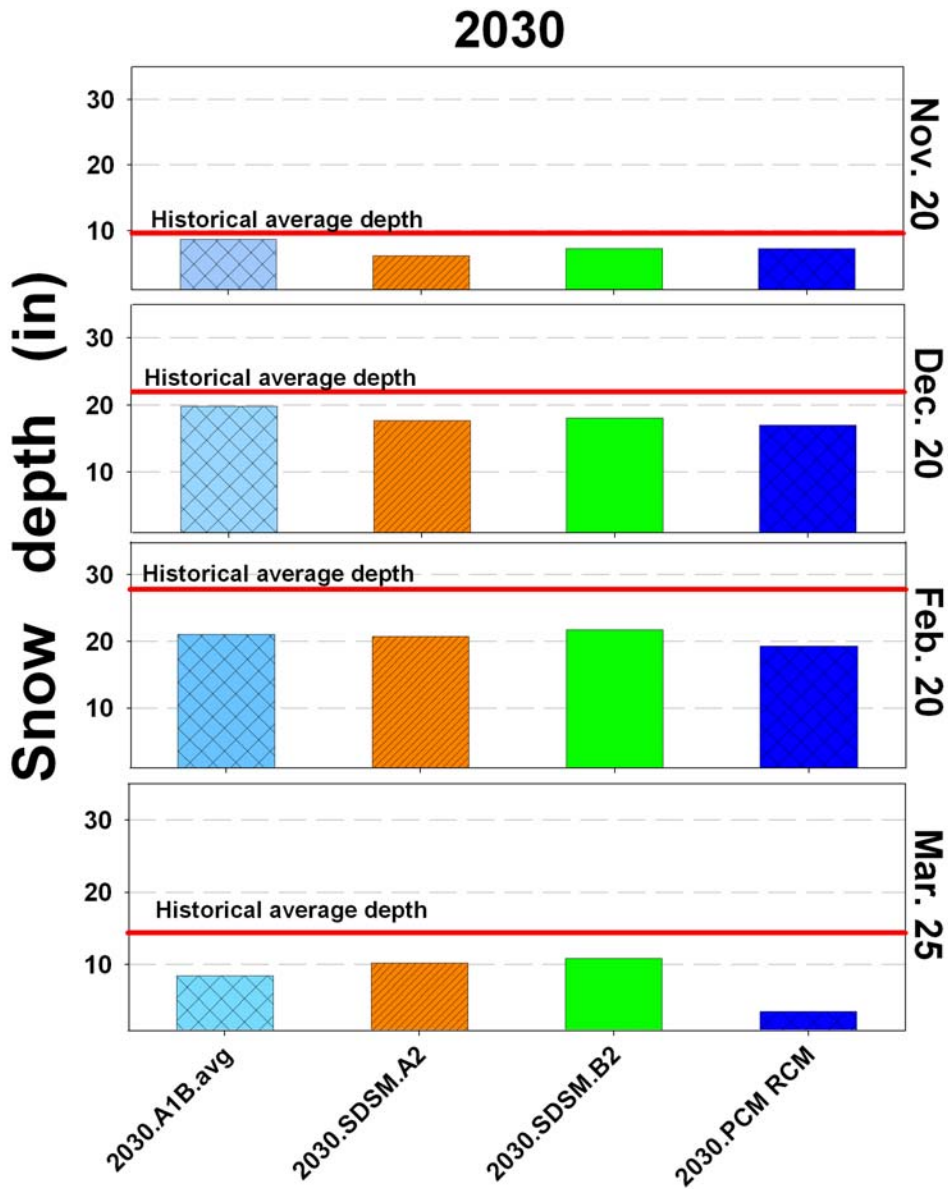
Figure 3.10. Estimated snow depths at PCMR's base area for 2030.
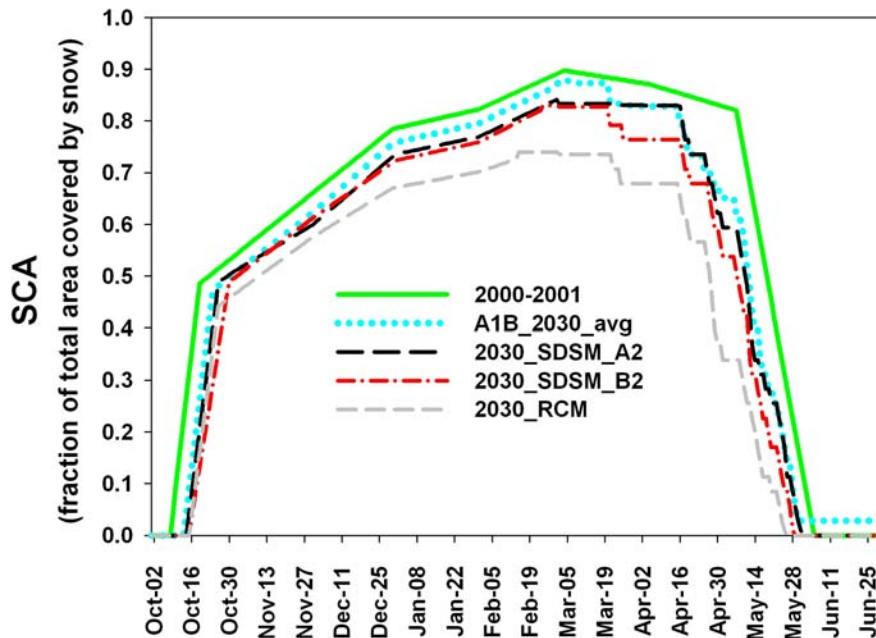
Figure 3.11. Modeled SCA time series at the top of PCMR in 2030 under different climate scenarios.

Snow melt at the base area is predicted to begin one week to 12 days earlier under the low and middle emissions scenarios, and two weeks earlier under the high emissions scenarios. The resulting impacts on estimated snow depths are shown in Figure 3.14. For all scenarios, there will be either very little or no snow at the base area by Thanksgiving, and mid-winter snow depths will be 20% to 40% less than historically observed values. By the spring break season, snow depths are predicted to be less than 10 inches under all scenarios except SDSM B2 due to an earlier onset of melt. This suggests that skiable snow is unlikely during spring break under all but the SDSM B2 scenario.
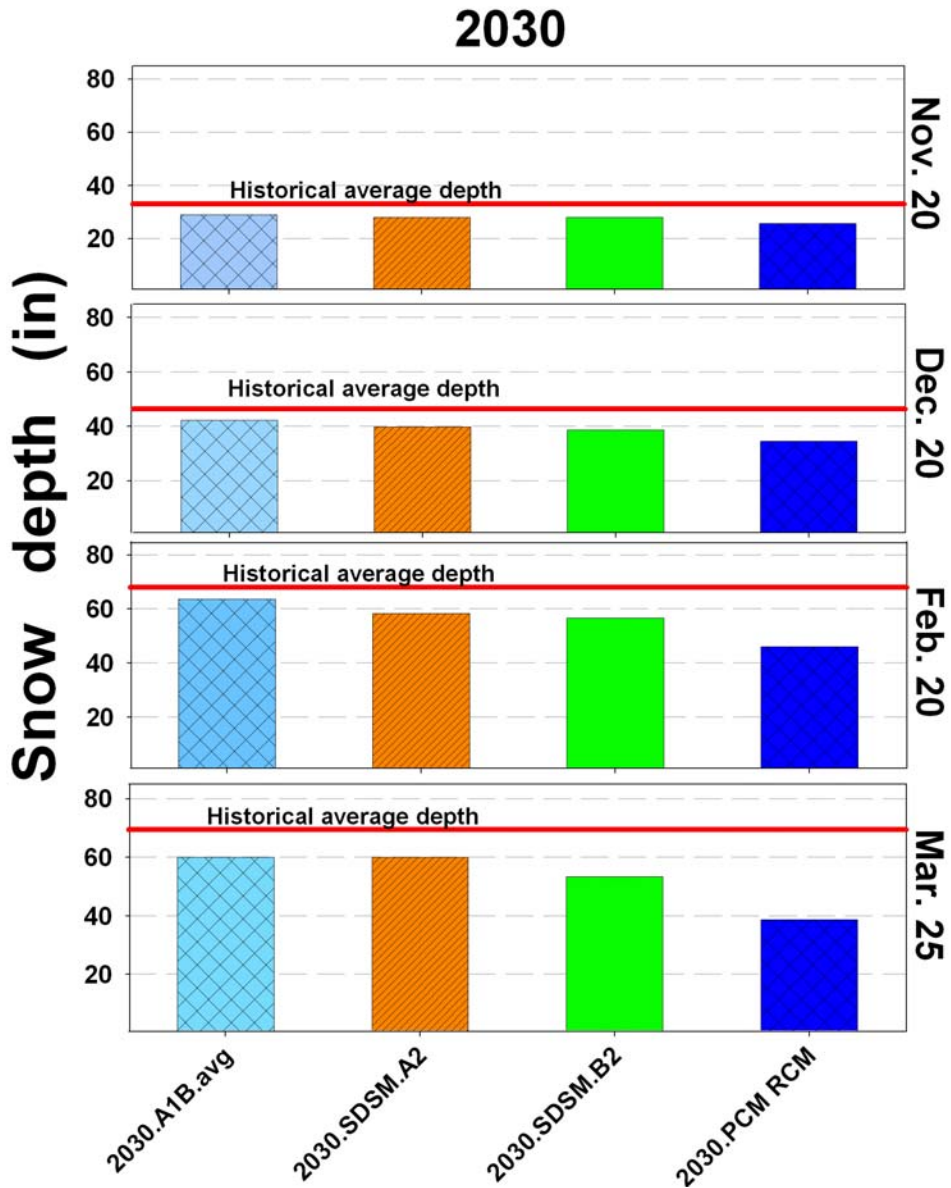
Figure 3.12. Snow depths at the top of PCMR for 2030.
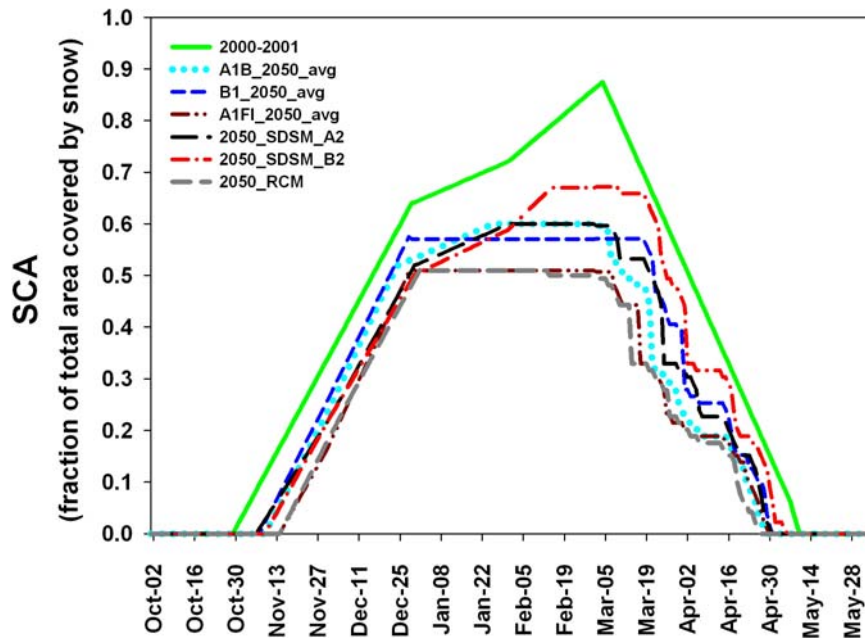
Figure 3.13. Modeled SCA at PCMR's base area in 2050 under different climate scenarios.

The impact at the top of PCMR will not be not as dramatic as that predicted for the base area, although changes in snow coverage and depths are predicted to be substantial. Initiation of snow accumulation will be delayed by about one week under all but the A1FI scenario. Under the A1FI scenario, snow accumulation is delayed by two weeks. Figure 3.15 shows estimated SCA for all scenarios at the top of PCMR in 2050. Melt initiation at the top of the ski area will occur one to two weeks earlier under the low and middle emissions scenarios, and four weeks earlier under the high emissions scenarios. The estimated snow depths are shown in Figure 3.16. The delay in snow accumulation will result in reduced (61% to 94% of historical average) snow depths at the top of the mountain. In 2050, the top of PCMR is predicted to have a persistent (albeit reduced) snowpack for the entire ski season.
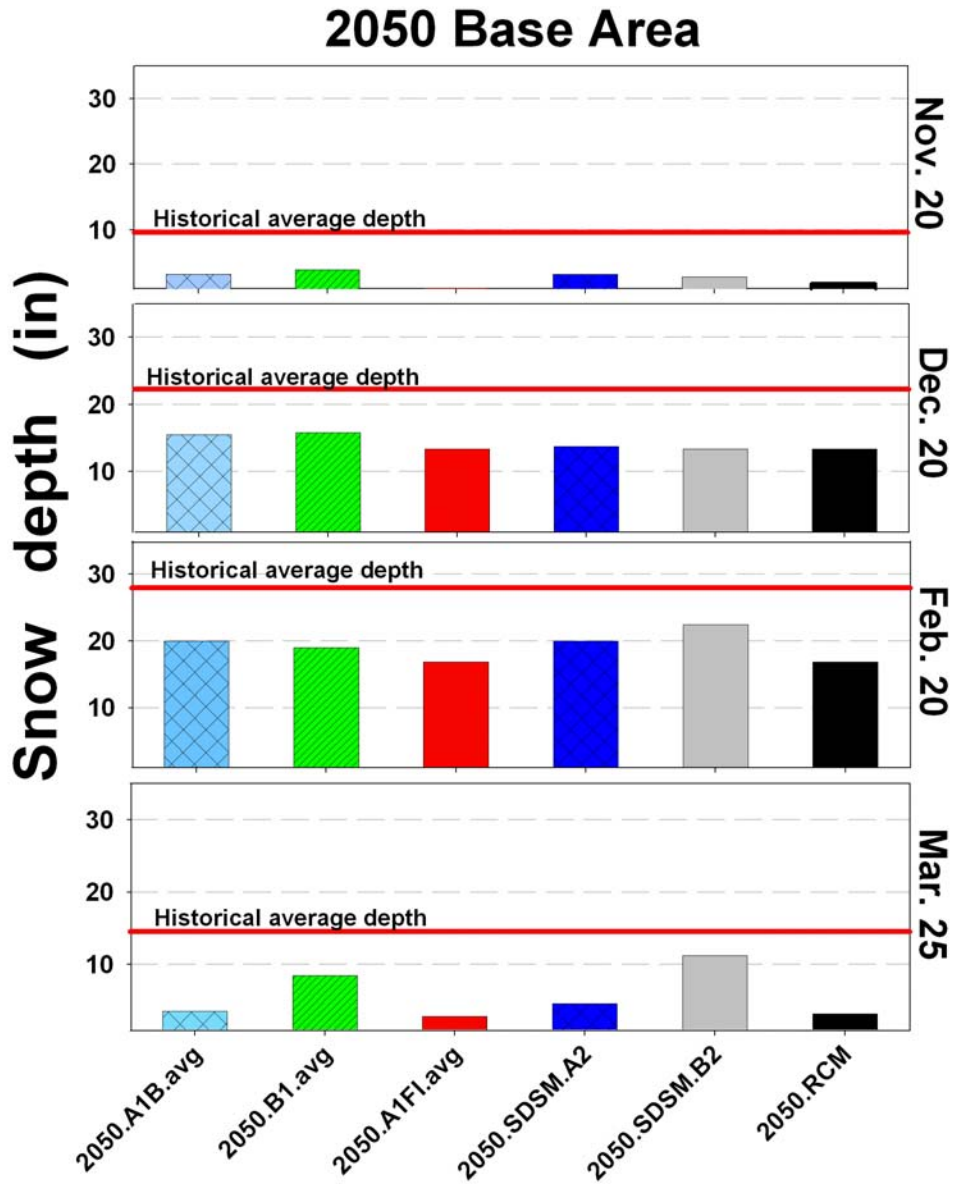
Figure 3.14. Base area snow depths at PCMR for 2050.
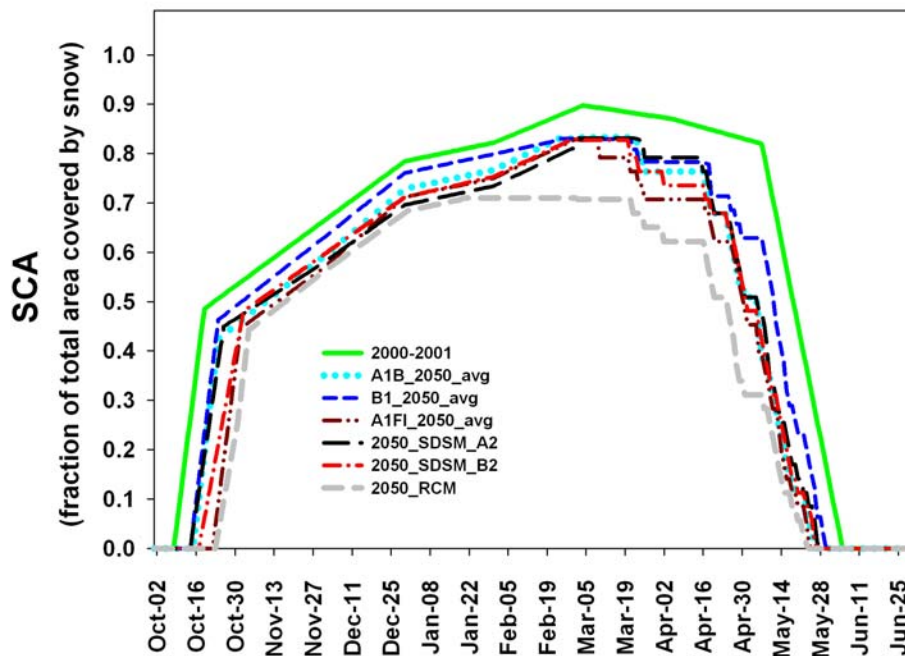
Figure 3.15. Modeled SCA time series at the top of PCMR in 2050 under different climate scenarios.

3.4.3   2075

By 2075, snow conditions are predicted to be worse than in 2050, and vary more strongly with emissions scenario than in 2050. Snowpack buildup will be delayed by 10 days to five and a half weeks, with the shortest delay predicted for the low emissions scenario, and the longest delay predicted under the high emission scenario. The predicted SCA at PCMR's base area for 2075 is shown in Figure 3.17. Under all emission scenarios, by 2075 the base area of PCMR will not have a skiable snowpack for Thanksgiving and spring break.[2]

---

2. The PCM-RCM results are for 2070.
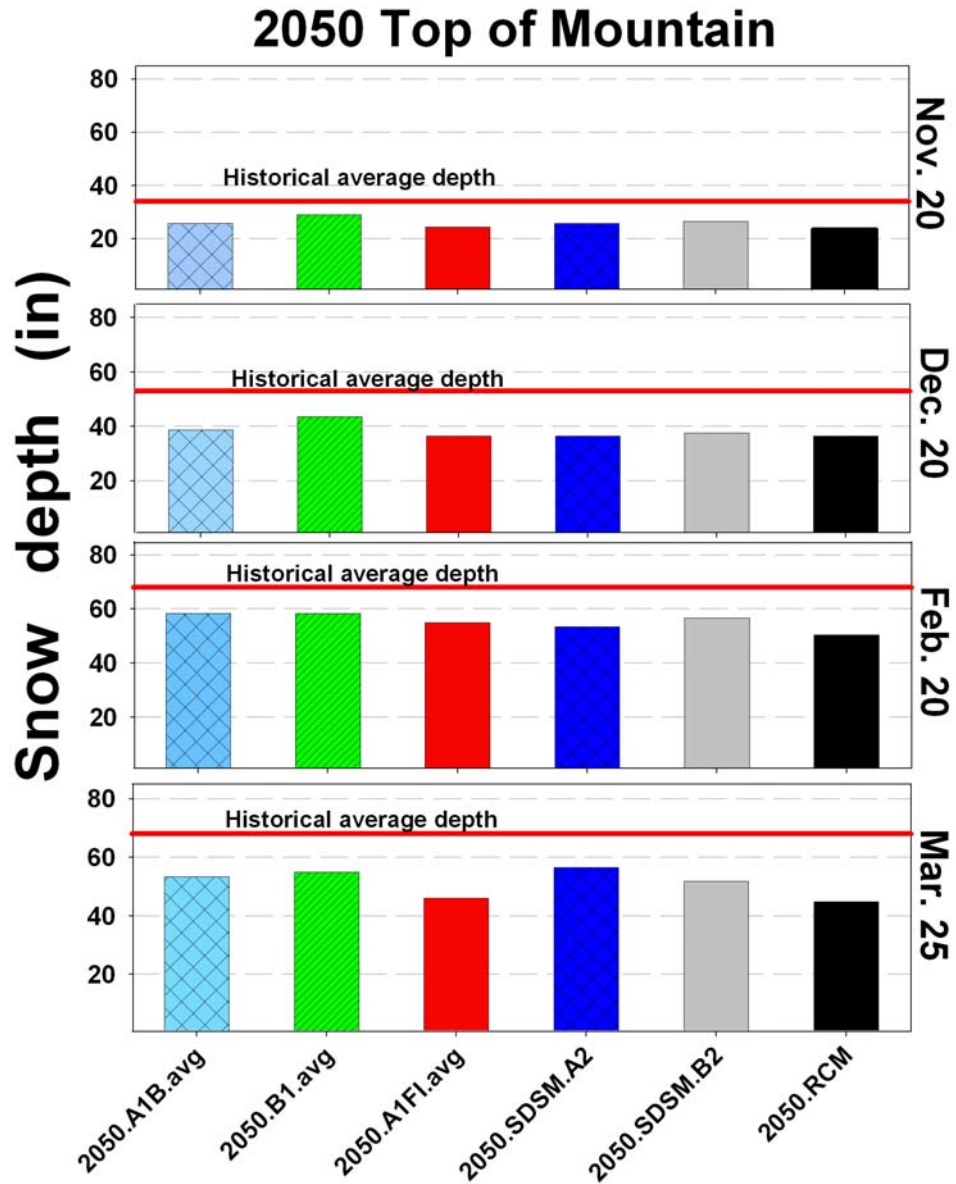
Figure 3.16. Snow depths at the top of PCMR in 2050.
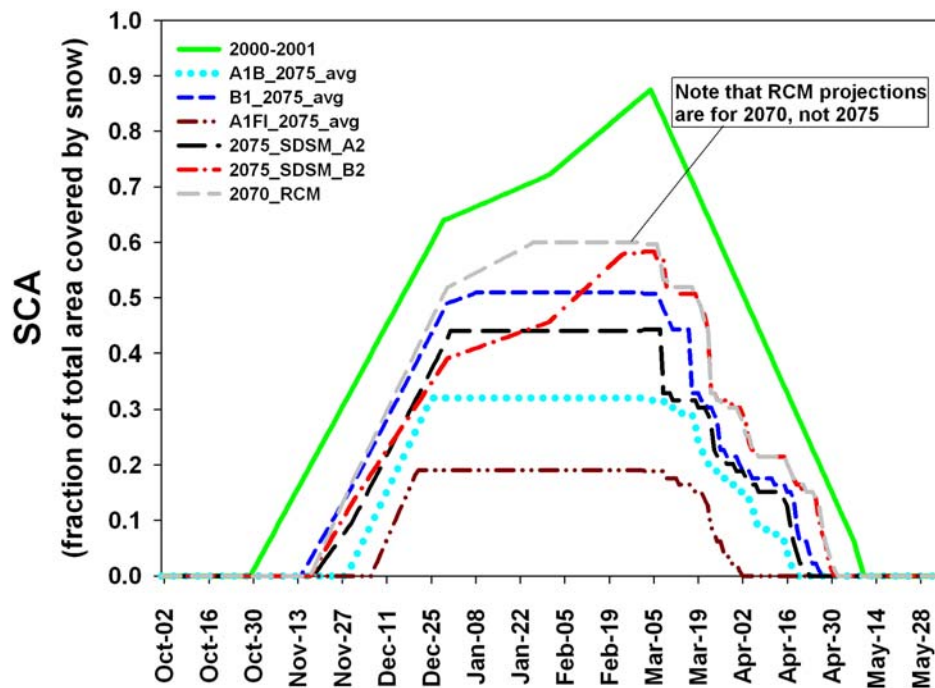
Figure 3.17. Modeled SCA time series at PCMR's base area in 2075 under different climate scenarios.

The snow line will move up to approximately 2,450 m (8,000 ft) under the A1FI (high emissions) scenario, and skiable snow at the base area is unlikely for the entire ski season. Under all other scenarios, a snowpack will eventually develop at the base area by mid-winter. Under these scenarios, snow coverage and depths at the base area will be substantially reduced (20% to 72% of historical average), but snow will not disappear completely.

Snow melt at the base area will occur periodically throughout the winter under the middle and high emissions (A1B and A1FI) scenarios. For all other scenarios, melt will occur one to two weeks earlier than the historical melt initiation date of March 16. Figure 3.18 shows that by 2075, skiable snow may only exist at the base area during mid-winter (December through February). Snow depth seasonal maximums for the A1B and A1FI scenarios occur by February 20, and only reach 20% to 37% of the average historical maximum. By 2075, snow depths during March are substantially reduced for all scenarios to the point where skiing may no longer be possible during the spring break season.
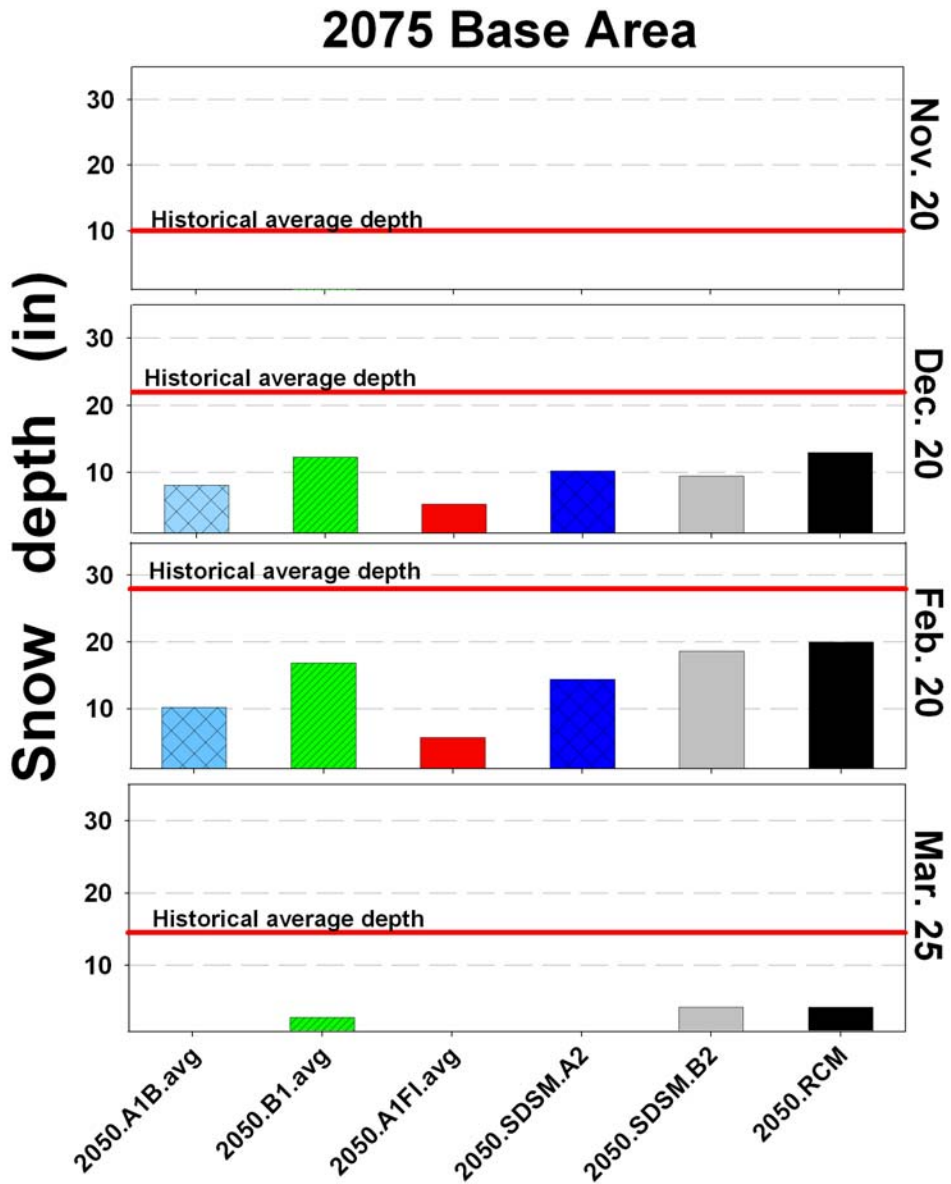
Figure 3.18. Base area snow depths at PCMR for 2075.

By 2075 at the top of the mountain, snow depth is also substantially decreased, although the cooler temperatures at this higher elevation insulate the snowpack from potential warming enough to maintain a seasonal snowpack (Figure 3.19). The snow deficit caused by October precipitation coming as rain is never regained, as indicated by maximum SCA values below the historical average values. Melt initiation occurs between three and five and a half weeks earlier under the GCM scenarios, with melt initiating earliest under the high emissions scenario, and latest under the low emissions scenario. Melt is predicted to begin one to two weeks earlier for the PCM-RCM and statistical downscaling scenarios. Skiable snow would probably exist at the top of the mountain under all scenarios, although snow depths would be significantly reduced (26% to 89% of historical average depths) (Figure 3.20).
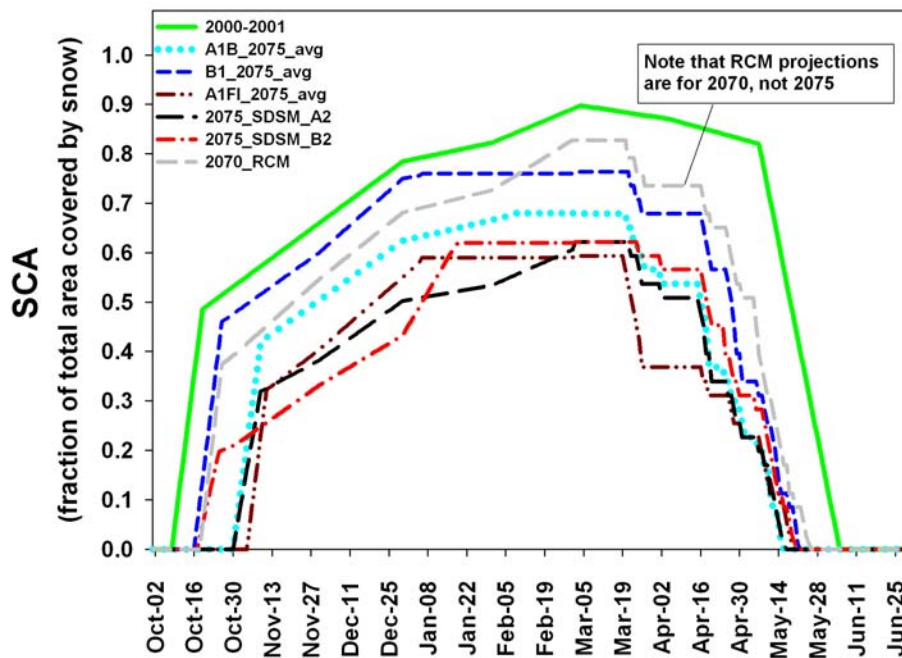
Figure 3.19. Modeled SCA for the top of PCMR in 2075.
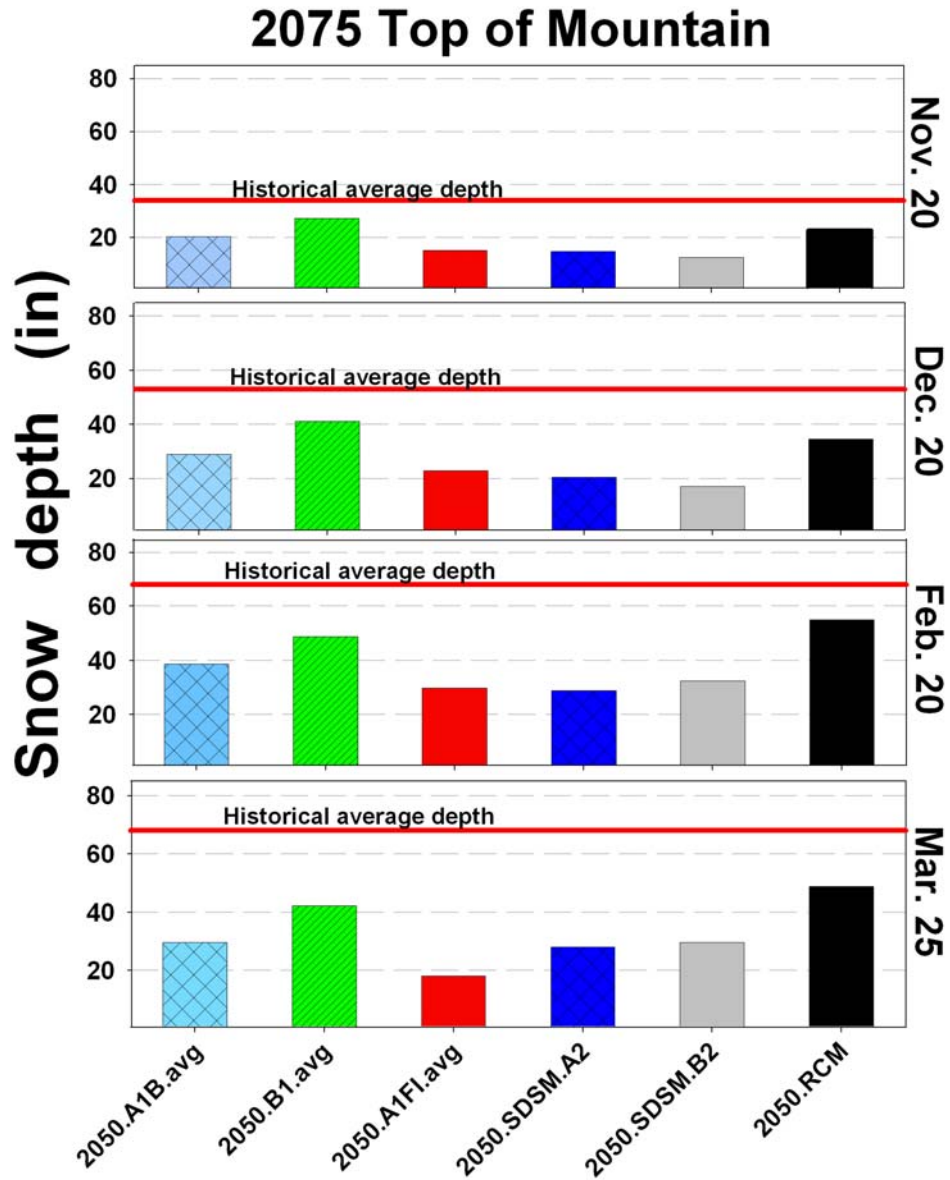
Figure 3.20. Snow depths at the top of Park City Mountain in 2075.

3.5 Snowpack Summary

The predicted rising temperatures will delay the date that snow starts to accumulate at the Park City base area by one week by 2030, one and a half to two weeks by 2050, and from two to five and a half weeks by 2075. In all scenarios for all years, the delayed accumulation causes the maximum snow depths to fall short of the average historical maximum. Predicted snow depth in 2030 during spring break is about 29% to 76% lower at the base area than in 2000–2001, with a small decrease in depth near the top of the mountain. The onset of snowmelt is predicted to start earlier by a week or less in all model scenarios. All model predictions, with the exception of the PCM-RCM scenario, show skiable snow for all elevations and dates on Park City in 2030, but not in 2050 and 2075.

Thanksgiving snow depths are predicted to be at or near zero under all scenarios in 2050 at the base area. Similarly, skiable snow during spring break is unlikely under all but the SDSM B2 scenario. The top of the ski area will maintain skiable snow throughout the ski season in 2050 under all scenarios, although snow depths will be reduced by 6% to 36% compared to historical depths.

By 2075, skiable snow at the base area is unlikely for Thanksgiving and spring break, as predicted under all scenarios. The snowline will move to approximately 2,450 m (8,000 ft) under the high emissions (A1FI) scenario, and skiable snow is unlikely at the base area for the entire ski season. By 2075 all other emission scenarios predict that a persistent snowpack will exist at the base area during mid-winter. Skiable snow is predicted to exist at the top of the mountain in 2075 under all scenarios, but snow depths are predicted to only reach 26% to 89% of historical average depths.

4.   Economic Impacts

The ski industry is a significant component of Park City's regional economy. For example, in a study by the University of Utah, researchers estimated that Utah's nonresident skiers and snowboarders generated 19,323 jobs and increased the total earnings of Utah's workers by $416,936,054 in the 2005–2006 ski season (Isaacson, 2006).

Changes in snowpack can affect local economies. A study for the Aspen Global Change Institute estimated that a 10% to 20% decrease in snow at Aspen could lead to between $7,969,000 and $55,967,000 in lost personal income in 2030 because of a reduction in skier visits as a response to the decrease in snow (Gosnell et al., 2006). In this chapter we use the predicted changes in snowpack estimated in Chapter 3 to predict the resulting changes in skier days and economic productivity of the Park City region.

4.1   Introduction

The more snow a region has, the more likely it is to attract visiting skiers. For Park City, as for most ski resort communities, visiting skiers are an important part of the local economy. The opposite is also true: the less snow a region has, relative to other ski areas, the less attractive it is to skiers, which will reduce skiing-related economic activity within the region. In this chapter, we estimate the potential skiing-related economic loss to the Park City regional economy resulting from reduced skier visits in response to climate change. We estimated the magnitude of this loss in two steps:

1.   We developed a statistical relationship between snowpack and skier days to predict changes in skier days resulting from snowpack changes

2.   We estimated the changes in total economic output, earnings, and jobs in the Park City region that result from the predicted changes in skier days.[1]

The remainder of this chapter describes these steps in detail and presents the results. In Section 4.2, we present the statistical relationship between snowpack and skier days for PCMR. In Section 4.3, we estimate economic impacts of a skier day on the Park City regional economy, then present the quantitative results in Section 4.4. Finally, in Section 4.5, we conclude with a qualitative discussion of PCMR specific vulnerabilities and potential adaptation strategies.

---

1. All reported dollar estimates are in 2009 dollars.

4.2   Impacts of Projected Snowpack Changes on Skier Days: Predicting Changes in Skier Days

To estimate the economic impacts of climate change on skier days, we first develop a statistical relationship between the level of snowpack and number of skier days at PCMR. As reported in Chapter 3, snowpack at PCMR is projected to decrease in both 2030 and 2050 because of climate change.[2] Snowpack and skier days have been shown to be positively related (Gosnell et al., 2006) – that is, a reduction in snowpack will lead to fewer people skiing. In order to predict the number of skier days lost due to decreased snowpack resulting from climate change, we developed a linear regression model of skier days and snowpack using historical data. We then used this model to predict the number of skier days in each month under the snow conditions predicted in 2030 and 2050. We do not project economic impacts for 2075 due to high uncertainty in projecting other economic variables this far into the future.

4.2.1   Developing a baseline statistical relationship between snowpack and skier days

We used monthly data on skier days and snowpack at PCMR from the 1998–1999 season to the 2006–2007 season. Monthly snowpack measurements for this time period are available at the Summit station and at the Jupiter station on PCMR. These are at elevations of 2,813 m (9,229 ft) and 3,045 m (9,990 ft), respectively. Since future changes in snowpack are projected at the area weighted elevations of the mountain zones (see Chapter 3), we combined the two station snowpack measurements to develop an overall snowpack measurement. This measurement accounts for the size of the relative areas that Summit and Jupiter stations represent within these zones (Zones 3 and 4, respectively).

In addition to snowpack, there are other factors that influence the number of skier visitor days in a season. To predict future changes in skier days, we developed a monthly model of skiing which includes several factors to help predict the seasonality of skier days. These factors include:

▸   A monthly indicator variable, which we include to account for the fact that there are more skier days in some months than in others. For example, there are more skier days in December than February due to holiday ski vacations (even when snowpack amounts are the same).

---

2. We used snowpack as our proxy for climate change because it accounts for changes in both precipitation and temperature (both of which affect snow conditions) and because snowpack is likely the climate variable most highly related to skier days.

▸   An interaction variable between snowpack and the monthly indicator variable. Specifically, this controls for the fact that an additional inch of snow in one month may have a different effect on skier days than an additional inch of snow in another month.

▸   Snowpack in previous months of the same season. This variable accounts for the time lags involved in booking ski vacations. For example, if a resort is having a bad snow month in November, this could influence skiers' decisions to book trips for Christmas, despite potentially better snowfall in December.

▸   Year indicator variables. These variables are included to account for differences in the number of skier days over time. There are several factors that influence skier days over time, including lift capacity, ticket price, and the proportion of the population who ski. Both lift capacity and ticket price have grown rather consistently over time, thus the season indicator variables account for the influences of these factors.

Including these factors in our model makes it a better predictor of the overall relationship between snowpack and skier days.

4.2.2   Model results and verification

Details of the model and results are presented in Appendix F. Using standard measures to evaluate the quality of the developed statistical relationships (e.g., significance of variables, R^2) the developed model fits the data quite well.

One evaluation of how well the model fits the data is to evaluate predicted vs. actual seasonal skier days from 1997 to 2007. In Figure 4.1, we graphically present predicted vs. actual annual skier days, finding that the model predicts actual season numbers with a high accuracy rate. As an illustrative example, we compared the model predicted results for the 2006–2007 season with the actual number of skier days. There were 1,746,333 skier days recorded in the 2006–2007 season and our model predicted 1,661,530 skier days. This is less than a 5% difference.

The model predicts accurately across years, but also within years. Using the 2004–2005 season as an example, we evaluated predicted versus actual monthly skier days. Figure 4.2 illustrates the strong relationship between predicted and actual seasonality of skier days by month. While there is some expected variability, the predicted skier days from the model accurately replicate the monthly percentages and seasonal pattern.
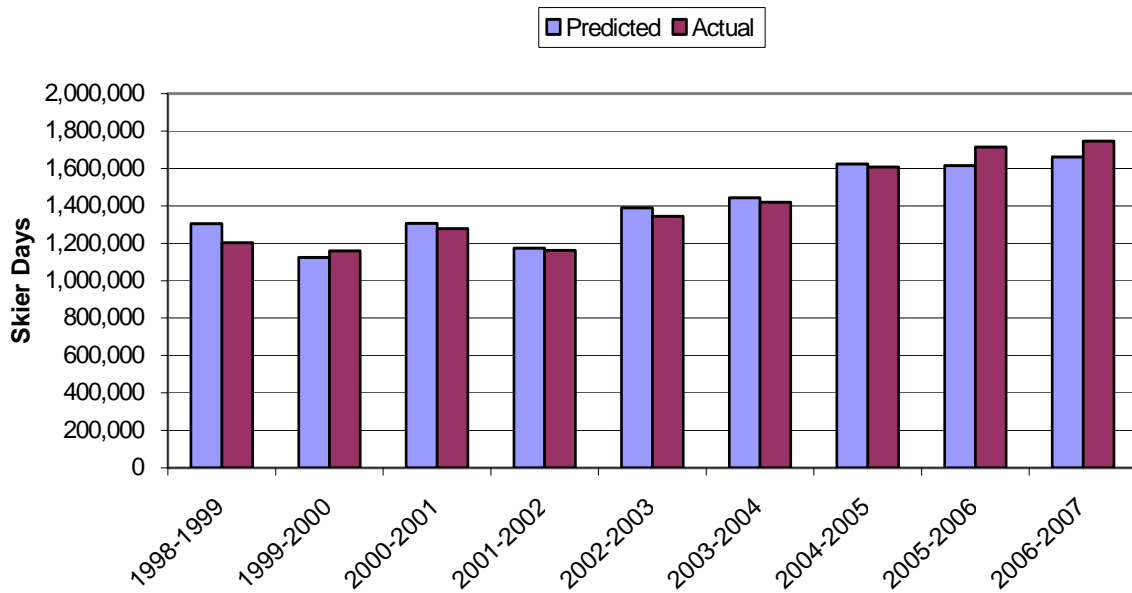
Figure 4.1. Predicted versus actual skier days, 1998–2007.
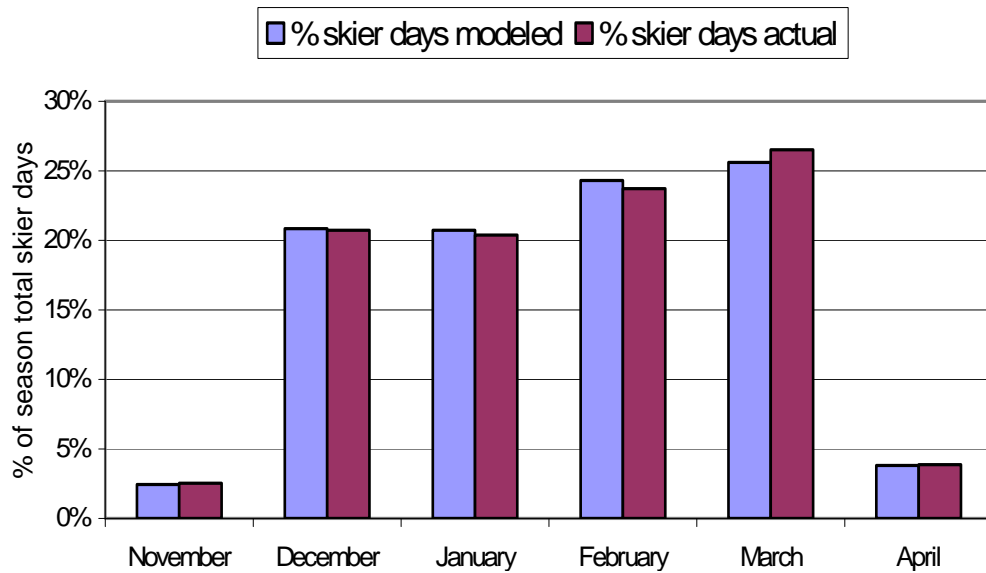
Figure 4.2. Modeled versus actual monthly skier days for the period 2004–2005.

4.2.3   Predicting future skier days with and without climate change

To predict future losses in skier days associated with reduced future snowpack, we first predict the baseline number of skier days in 2030 and 2050. These amounts represent the number of skier days in 2030 and 2050 that would occur without climate change but including other potential factors such as population growth and ski industry growth. We then predict the number of skier days in 2030 and 2050 under the emissions scenarios and snowpack reductions described in Chapter 2.

Skier days without climate change

Baseline skier days are a function of anticipated ski industry growth under a "no climate change" scenario. Because of limiting factors (e.g., physical mountain area, maximum lift capacity, lodging capacity), growth at ski areas is not unbounded. Working with PCMR, we developed a reasonable estimate of growth from now until 2030 and from 2030 until 2050 under the "no climate change" scenario. Estimated future growth is based on past year growth in skier days, accounting for capacity constraints at the resorts and anticipated changes in the proportion of the population who ski. In this analysis, we have adjusted for the exceptionally good ski season of 2007–2008 and assume PCMR will maintain its historical average share of the regional ski market in the future. That is, we assume PCMR, Deer Valley, and the Canyons will grow at the same rate.

Without climate change, skier days are expected to grow, on average, at a rate of 1% from now until 2030 and, on average, at a rate of 0.5% from 2030 to 2050. Based on this growth pattern, without climate change, projected total annual skier days for the three Park City resorts total 1,869,630 in 2030 and 2,065,746 in 2050.

Figure 4.3 shows the historic growth pattern of skier days in the Park City area with the assumed growth trends to 2030 and 2050, absent climate change.

Skier days with climate change

We used the developed statistical relationship between snowpack and skier days at PCMR to predict skier days at all three Park City resorts in 2030 and 2050, given the snowpack projections presented in Chapter 3. PCMR provides a reasonable indicator of potential changes at the other two resorts since they are so close in proximity and border PCMR on two sides.
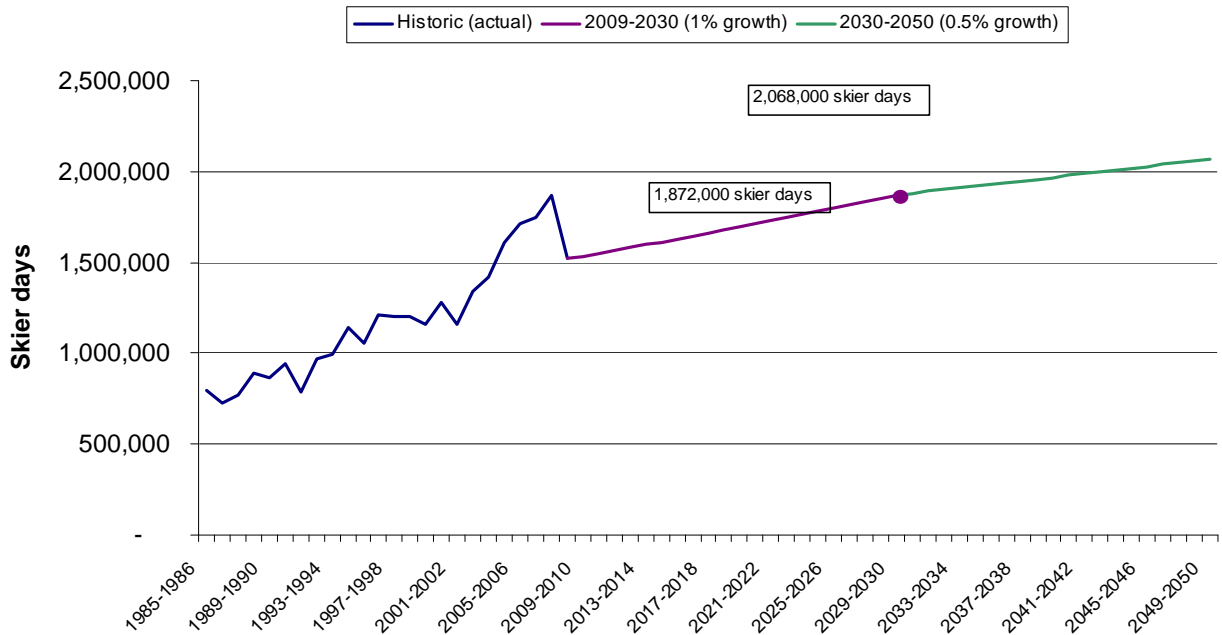
Figure 4.3. Historic growth pattern of skier days in the Park City area with the assumed growth trends to 2030 and 2050.

Differential effect of snow loss at base of mountain

PCMR, the Canyons, and Deer Valley do not have the ability to download skiers from mid-mountain and are thus especially vulnerable to decreased snowpack at the base. Even if the middle and top of the mountain are skiable, if there is not skiable snow at the base of the mountain, the resorts will not be operational. We identified the periods in which the base of the mountain would not have skiable snow by comparing the snowpack projections to critical snowpack thresholds (see Chapter 3). To account for these periods, we identified the proportion of skier days that historically occurred during those time periods. We then applied this proportion to our estimate of skier days in 2030 and 2050 with no climate change. This provided an estimate of skier days lost due to insufficient snow at the base. Since some of the skier days lost due to insufficient snow at the base overlap with losses predicted by the model (losses due to overall decreases in snow across the entire mountain), we subtract this overlap to avoid double-counting. Below we present an example calculation.

Skier days lost due to insufficient snow at the base: An example calculation

Early and late season reductions in skier days will occur for two reasons. First, opening day of the ski season will be pushed back and closing day will be pushed forward due to lack of snow at the mountain base; and second, decreased levels of snowpack after opening day and before closing day will reduce the number of skiers. The statistical relationship developed between snowpack and skier days can predict the second loss. However, to account for the later opening day losses and earlier closing day losses, we need to adjust the predicted losses. Using the middle emissions scenario in 2050 as an example, the snowpack model predicts that critical snow depth will not meet threshold levels at the mountain base until approximately November 20. Therefore, skiing will start later in 2050 than it does currently. Historically, 6% of annual skier days occur in November, and of all November skier days, 19% occur before November 20. Therefore, due to the later ski season start we expect an initial loss of 19% of November skier days by 2050.[3] In 2050, we predict 2,065,746 annual skier days *without* climate change, and estimate the lost skier days resulting from insufficient snow at the base to be approximately 23,550 (19% × 6% × 2,065,746) in November 2050 under the middle emissions scenario. To calculate total November losses, this estimate of lost skier days is combined with the lost skier days predicted by the snowpack-skier day model, adjusted for the shortened November ski season.

4.2.4   Lost skier days

Figure 4.4 shows the total projected lost annual skier days for the Park City-area attributed to decreased snowpack under the alternative emissions scenarios. The numbers are presented in Table 4.1.

Overall, predicted reductions in snowpack are significant and lead to significant reductions in skier days. By 2030, snowpack is predicted to decrease by 15%, leading to 203,270 lost skier days. In 2050, predicted snowpack reductions range from 27% (low emissions scenario) to 43% (high emissions scenario), leading to losses in skier days between 271,733 and 664,471. April skiing is severely affected in this analysis as all of April skier days are lost by 2030. The economic impacts associated with these lost skier days are discussed in the next section.

---

3. We assume average baseline seasonality in 2030 and 2050 to be the same as the historic average.
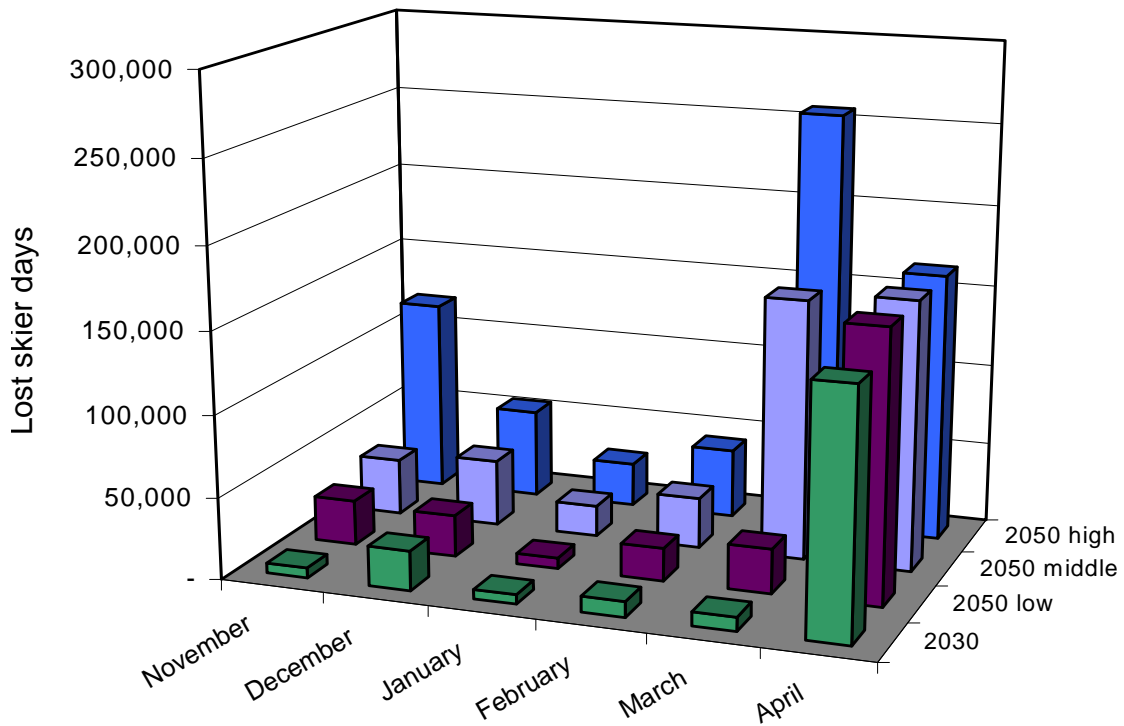
Figure 4.4. Total projected lost annual skier days attributed to decreased snowpack under the alternative emissions scenarios for 2030 and 2050.

Table 4.1. Projected skier days with and without climate change

Year and scenario	% change in snowpack[a]	Skier days without climate change (1,000s)	Skier days with climate change (1,000s)	Lost skier days from climate change (1,000s)
2030 (A1B)	-15%	1,870	1,667	203
2050 Low (B1)	-27%	2,066	1,794	272
2050 Middle (A1B)	-34%	2,066	1,617	449
2050 High (A1FI)	-43%	2,066	1,402	664

a. Approximate % change in snowpack is calculated as the average annual snowpack; averaged over all elevation zones.

4.3   Economic Impacts of a Skier Day

The next step in estimating the potential consequences of climate change on Park City's economy is to estimate the economic contribution of skier expenditures to Park City's economy so that the predicted losses in skier days can be translated into Park City economic losses. The skiing industry contributes to the local economy by bringing outside money into the economy in the form of visitor spending. Visiting skiers spend money on a number of goods and services (e.g., lift tickets, food, retail) which affect several local industries, including the three main resorts, restaurants, hotels, retail shops, and other tourist-related enterprises. These industries directly affect the economy by purchasing intermediary goods (e.g., restaurant supplies, wholesale goods for retail sales) and by providing jobs. The industries that provide intermediary goods and services to the ski industry purchase their own intermediary goods and services from other local industries, and the pattern repeats itself. Thus, the original money from visitor spending creates a multiplier effect on the local economy.

Economists have developed a way to estimate this multiplier effect, known as input-output (I/O) analysis. I/O analysis entails calculating the extent to which direct activities (e.g., skier spending) stimulate further economic effects, spreading employment and income, thus accounting for linkages among industries (University of South Carolina, 2009). That is, I/O analysis accounts for the production linkages between different industries of the local economy, and in turn, calculates the economic multiplier associated with various industry activities. These impacts are calculated using a multiplier effect. Multipliers are often used in recreation studies to estimate the impacts of tourism on the local economy, as they account for how visitor spending is amplified. The spending and hiring in a tourism industry, such as the ski industry, creates multiple layers of income for other industries (University of South Carolina, 2009).

The economic impacts of a visitor skier day are quantified using three metrics: economic output, earnings (also referred to as labor income), and employment. In simple terms these metrics are defined as (University of South Carolina, 2009):

▸   *Output* (or total impact). This is the contribution to overall economic activity. It measures the annual value of goods and services associated with skiing related business activities.[4]

▸   *Earnings* (or labor income). This is the contribution of output to wages and salaries.

▸   *Employment*. This is the total number of jobs associated with the measured economic activities tied to skiing.

---

4. For the technical definitions reported by the Bureau of Economic Analysis (BEA), see Appendix G.

Economic multipliers are developed by the federal government and incorporated into both federal and private industry I/O models. We used multipliers from the BEA's Regional Input-Output Modeling system (RIMS II) (U.S. Department of Commerce, 2009).

The multipliers specify regions at the county scale, and we used the multipliers for Summit County, Utah, where all three resorts are located. The multipliers are provided by industry type and are specific to Summit County. Since the multipliers estimate the economic impact of *outside* money coming into a region, the economic impact of a skier day is estimated for visiting skiers only (i.e., skiers who live outside Summit County).

Ski Utah's 2007−2008 Skier and Snowboarder survey (Ski Utah, 2009) reports spending per skier day in Summit County for skiers from out-of-state and from in-state but out of Summit County. This spending is broken out by type of expenditure. On average, an out-of state skier visiting Summit County spent $437 per skier per day and an in-state non-local visitor spent $212. From data reported in Ski Utah's 2007−2008 Skier and Snowboarder survey, we calculated that 96% of non-local skiers are out-of-state, while 4% are in-state.[5] Thus the weighted average per day visitor spending is $428.

Different sectors of the economy (e.g., lodging, food service) contribute to the regional economy to different degrees. We matched skier expenditures to the specific industry for which RIMS II provides multipliers and calculates the economic impact. Each visitor skier day brings in $428 on average from outside the county. This spending results in $590.39 in annual output, of which $133.56 is seen through increased labor earnings. In addition, every 1,000 skier days provides 7.46 jobs to Summit county. In Appendix G, we present expenditures and multipliers by industry type along with detailed calculations.

4.4   Results: Potential Economic Impacts of Climate Change on Park City's Economy

The projected climate change related changes in skiing-related output, earnings, and jobs is calculated as the output, earnings, and jobs per skier day times the predicted change in skier days. Since the I/O multipliers are based on spending by skiers from outside Summit County, we scale the number of lost skier days to reflect out-of-area skiers only. Working with PCMR, we estimated that 75% of the total skier days in Summit County are from outside the area (Krista

---

5. The visitor type table (Table 22, p. 17) reports that 53% of Utah's skiers are out-of-state and 2% are local overnight. We assume local overnight visitors are not local to the region they are staying overnight. Thus 55% of Utah's skiers are "visitors," of which 53% are out-of-state and 2% are in-state. We assume this proportion of visitors to Utah holds for Park City.

Perry, PCMR, personal communication, August 20, 2009), and thus we assume that 75% of the predicted changes in skier days in the future are for skiers from outside Summit County. Estimated changes in output, earnings, and jobs reflect the annual impact for only the single years of 2030 and 2050, and do not reflect the cumulative potential lost earnings and jobs that would occur in other years (i.e., they do not account for lost skier days and the associated economic impacts in 2029, 2028, and so on).

In 2030, the predicted 15% decrease in snowpack is estimated to result in $120.0 million in lost output. This output includes the direct effects or impacts of visitors spending money (e.g., buying dinner), indirect effects such as the restaurant buying food from a distributor, and the induced effects caused by changes in the household income and spending of the restaurant workers. This lost output is estimated to result in an estimated 1,137 lost jobs and $20.4 million in the form of lost earnings (or labor income).

In 2050, the potential impacts range from $160.4 million in lost output, $27.2 million in lost earnings, and 1,520 lost jobs (low emissions scenarios) to $392.3 million in lost output, $66.6 million in lost earnings, and 3,717 lost jobs (high emissions scenario). Table 4.2 presents the estimated potential economic impacts of climate change on Park City's economy, in terms of lost output, earnings, and jobs by year and scenario.

Table 4.2. Potential economic impacts of climate change on Park City's economy in 2030 and 2050

Year and scenario	% change in snowpack[a]	Estimated lost visitor skier days	Lost output[b]	Lost earnings[b]	Lost jobs[b]
2030	-15%	152,453	$120,008,684	$20,361,574	1,137
2050 Low (B1)	-27%	203,800	$160,428,276	$27,219,466	1,520
2050 Middle (A1B)	-34%	336,665	$265,017,949	$44,964,935	2,511
2050 High (A1FI)	-43%	498,353	$392,296,985	$66,560,052	3,717

a. Approximate % change in snowpack is calculated as the average annual snowpack; averaged over all elevation zones.
b. All dollars are 2009.

4.5   Resort Specific Vulnerabilities and Potential Adaptation Strategies

Changes to snowpack are expected to change not only skier behavior, but also resort operations. To gather information on resort-specific impacts of climate change on operations, we

interviewed PCMR managers about resort-specific vulnerabilities and potential adaptation strategies. This section summarizes the findings of these interviews, and presents the potential impacts of climate change on resort operations and potential strategies for adaptation.

Three major resort-specific vulnerabilities to climate change were identified: the lack of downloading capabilities, reliance on snowmaking, and the inability to accommodate shifts in the seasonality of the ski season. Downloading could reduce the number of skier days lost because it would allow the resort to operate when there is skiable snow up the mountain but not at the base. The lack of downloading capabilities is estimated to result in the loss of an additional 149,081 skier days in 2030, and depending on the emissions scenario, between 185,886 and 488,183 skier days in 2050. Thus the addition of mid-mountain downloading capabilities could potentially reduce the economic impacts of climate change. Table 4.3 shows the economic losses associated with the lack of downloading capabilities. These are the potential benefits of investing in mid-mountain downloading capabilities as an adaptation strategy, assuming that the need to download would not in itself affect skier days.

Table 4.3. Impacts associated with lack of downloading capabilities

Period	Lost skier days associated with lack of downloading capabilities	Lost output associated with lack of downloading capabilities	Lost earnings associated with lack of downloading capabilities	Lost jobs associated with lack of downloading capabilities
2030	107,342	$84,498,205	$14,336,600	801
2050-B1	130,517	$102,741,177	$17,431,839	974
2050-A1B	219,306	$172,634,540	$29,290,472	1,636
2050-A1FI	331,974	$261,325,847	$44,338,505	2,476

The second major resort-specific vulnerability to climate change is PCMR's reliance on snowmaking. Currently, PCMR relies on snowmaking to open in mid-November and makes snow on around 35% of its runs. Snowmaking requires *consecutive* nights with temperatures below 28°F. Higher temperatures in just one night can be detrimental to the snowmaking process. Since the climate models used in the snowpack analysis provide monthly average temperatures, there is no way to effectively estimate this potential harm. Moreover, additional snowmaking would require additional water rights, which are expensive, are sometimes hard to secure, and are dependent on flows. As nightly temperatures increase, the costs of making snow rise. More snowmaking guns are required to run longer on more parts of the mountain.

PCMR is exceptionally dependent on early season skier days due to their inability to accommodate shifts in the seasonality of the ski season. Specifically, PCMR is often close to capacity during the Christmas holiday and cannot accommodate more skiers. Thus, there is no

ability for the loss of early season skier days to be recovered during the holiday season by accommodating more skiers. Furthermore, PCMR is very reliant on the Christmas holiday. Thus, PCMR is vulnerable to warmer nightly temperatures pushing the opening date beyond the Christmas holiday.

As temperatures warm, a natural adaptation strategy is to create runs at higher elevations where temperatures are often lower. The limited areas in which upward retreat is possible (Jupiter and McConkey bowls) are mostly expert terrain, which will not effectively offset the loss of the majority of PCMR's skiers who are at the intermediate/advanced level.

4.6   Economic Impacts Summary

In summary, snowpack is highly correlated with the number of skier days. As snowpack is reduced, the associated lost skier days could have non-trivial economic consequences. In 2030, the estimated decrease in snowpack is estimated to result in $120.0 million in lost output. This output includes direct effects or impacts of visitors spending money (e.g., buying dinner), indirect effects such as the restaurant buying food from a distributor, and induced effects caused by changes in household income and restaurant worker spending. This lost output is estimated to result in an estimated 1,137 lost jobs and $20.4 million in the form of lost earnings (or labor income). In 2050, the potential impacts range from $160.4 million in lost output, $27.2 million in lost earnings, and 1,520 lost jobs (low emissions scenarios) to $392.3 million in lost output, $66.6 million in lost earnings, and 3,717 lost jobs (high emissions scenario). PCMR is especially vulnerable to reduced snowpack at the base, warm nightly temperatures (which interfere with snowmaking), and the inability to accommodate shifts in seasonality.

5. Uncertainty

As noted in Chapter 2, there is uncertainty from the climate models about the magnitude of warming at Park City and whether precipitation in the Park City region will increase or decrease. The predicted change in precipitation as a result of GHG emissions is more uncertain than the predicted temperature change. In addition to uncertainty about how the climate in Park City will respond to GHG emissions, and exactly what those emission levels will be in the future, there is uncertainty inherent in the snow modeling.

We are reporting results for specific years (2030, 2050, and 2075) to illustrate changes from average conditions. The results should not be interpreted as an accurate prediction of precise snow depths or coverage on a particular date, but rather as representative conditions around a particular time period.

Snow coverage and depths were determined based on changes from observed coverage and depth for a single representative ski season in 2000–2001. However, individual years will exhibit variability with greater or smaller snow coverage and depth values than those observed in 2000–2001. This year-to-year variability is not accounted for in the snowpack modeling. The measured snow depths at the study plots are not enhanced by snowmaking, and are therefore likely to underestimate observed depths on the slopes where snow making activities take place. Our approach projects natural snowpack characteristics only. We did not evaluate the effects of augmentation with man-made snow.

Additionally, economic variables are very difficult to predict. The economic impacts of a skier day are estimated in 2009, using current economic information. While, multipliers have been found to be relatively stable over time (Conway, 1977), clearly, economies change over time. It should be understood that this analysis estimates the changes in economic activity (as measured by output, earnings, and jobs) related to a change in skier days, *holding all else constant*. Furthermore, as with all economic variables, there will likely be reactions to these changes in the economy that will further change the economic makeup of the area.

6. Summary and Conclusions

GHG concentrations are expected to continue to rise, causing a change in global climate. In Park City, temperatures will probably increase substantially over the coming century. The amount of warming depends on future GHG emissions and how they affect climate in the Rockies. Different assumptions about emissions result in projected warming ranging from 2.1 to 5.0°C (3.8 to 9.0°F) by 2075 relative to temperatures in Park City in the 1990s. By the century's end, Park City's temperatures may resemble the current temperatures of Salt Lake City. Warming is predicted to be more pronounced during the summer months than the winter months.

On average, the climate models project a small decrease in annual precipitation, a small increase in winter precipitation, and a substantial decrease in summer precipitation by 2075, regardless of the emissions scenario or modeling approach. However, because of the variability between models, we cannot be sure whether precipitation over the central Rockies will decrease or increase during the 21st century.

Using six climate change scenarios and the SRM, we estimate that the average date when snow starts to accumulate at the Park City base area will be delayed by approximately one week by 2030, one and a half to two weeks by 2050, and from two to five and a half weeks by 2075. In 2030, all modeled scenarios, with the exception of the regional climate model during spring break, predict skiable snow for all elevations and dates throughout the average ski season. By 2050, however, Thanksgiving snow depths at the base area are predicted to be at or near zero for all scenarios, and skiable snow is unlikely in all but one scenario (SDSM B2) for spring break. The top of the ski area is predicted to maintain skiable snow throughout the ski season in 2050, but snow depths will be reduced by 6% to 36%, compared to historical averages. By 2075, skiable snow at the base area is unlikely for Thanksgiving and spring break for the average season under all emission scenarios. Under the high emissions scenario, by 2075 a persistent snowpack will exist only for the upper third of the mountain.

Snowpack begins to be substantially impacted when winter temperatures warm more than approximately 2 to 3°C (4 to 5°F). Climate model results suggest that winter warming in the central Rocky Mountains is approximately one-third greater than the GMT. This implies that Park City might experience a 2 to 3°C (4 to 5°F) warming when the GMT warming is only 1.5 to 2.3°C (3 to 4°F). The climate models and observed trends at weather stations indicate that such an increase in temperature could be realized by mid-century.

It is unlikely that early season reductions in snowpack can be offset with snowmaking by 2075, since temperatures will not become cold enough until late November to early December. Additional snowmaking later in the winter months, however, could bolster the snowpack enough to maintain skiable snow into the spring break season. The economic implications of additional

snowmaking, and other potential adaptation strategies such as downloading skiers in the spring, may need to be considered by PCMR owners and operators in the face of a changing climate.

These modeling results are intended to provide a range of possible and plausible future scenarios to assist ski area managers in assessing the consequences of climate change. The results should be interpreted with the realization that there is uncertainty in predicting future GHG emissions, the effect of emissions on climate, and the effect of climate changes on snowpack characteristics.

Economic models indicate that snowpack is highly correlated with the number of skier days. As snowpack is reduced, the associated lost skier days could have non-trivial economic consequences on the Park City region. By 2030, the estimated decrease in snowpack is estimated to result in $120.0 million in lost output. This output includes direct effects or impacts of visitors spending money (e.g., buying dinner), indirect effects such as the restaurant buying food from a distributor, and induced effects caused by changes in household income and restaurant worker spending. This lost output is estimated to result in an estimated 1,137 lost jobs and $20.4 million in the form of lost earnings (or labor income). By 2050, the potential impacts range from $160.4 million in lost output, $27.2 million in lost earnings, and 1,520 lost jobs (low emissions scenario) to $392.3 million in lost output, $66.6 million in lost earnings, and 3,717 lost jobs (high emissions scenario).

References

AGCI. 2006. *Climate Change and Aspen: An Assessment of Impacts and Potential Responses*. ISBN 0-9741467-3-0. Prepared for the City of Aspen by the Aspen Global Change Institute, Center of the American West, Rural Planning Institute, Stratus Consulting Inc., and Wildlife & Wetland Solutions, LLC. Aspen Global Change Institute, Aspen. July.

Agrawala, S. (ed.). 2007. *Climate Change in the European Alps: Adapting Winter Tourism and Natural Hazards Management*. Organisation for Economic Co-operation and Development, Paris.

Armstrong, R.L. and E. Brun (eds.). 2008. *Snow and Climate: Physical Processes, Surface Energy Exchange and Modeling*. ISBN-978-0-521-85454-2. Cambridge University Press, Cambridge, UK and New York.

Barry, R.G., R. Armstrong, T. Callaghan, J. Cherry, S. Gearheard, A. Nolin, D. Russel, and C. Zöckler. 2007. Snow. In *Global Outlook for Ice and Snow,* J. Eamer (ed.). ISBN: 978-92-807-2799-9. United Nations Environment Programme.

Christensen, J.H., B. Hewitson, A. Busuioc, A. Chen, X. Gao, I. Held, R. Jones, R.K. Kolli, W.-T. Kwon, R. Laprise, V. Magaña Rueda, L. Mearns, C.G. Menéndez, J. Räisänen, A. Rinke, A. Sarr, and P. Whetton. 2007. Regional climate projections. In *Climate Change 2007: The Physical Science Basis*. Contribution of Working Group I to the Fourth Assessment Report of the Intergovernmental Panel on Climate Change, S. Solomon, D. Qin, M. Manning, Z. Chen, M. Marquis, K.B. Averyt, M. Tignor and H.L. Miller (eds.). Cambridge University Press, Cambridge, UK and New York.

Climate Impacts Group. 2006. Hydrology and Water Resources, Key Findings. Available: http://www.cses.washington.edu/cig/res/hwr/hwrkeyfindings.shtml. Accessed 5/31/2006.

Conway, R.S. 1977. The stability of regional input-output multipliers. *Environment and Planning* A(9):197-214.

Dai, A., W.M. Washington, G.A. Meehl, T.W. Bettge, and W.G. Strand. 2004. The ACPI climate change simulations. *Climatic Change* 62(1-3):29-43.

Dozier, J. and T. Painter. 2004. Multispectral and hyperspectral remote sensing of alpine snow properties. *Annual Review of Earth Planet Science* 32:465-494.

Galloway, R.W. 1988. The potential impact of climate changes on Australian ski fields. In *Greenhouse: Planning for Climatic Change*, G.I. Pearman (ed.). CSIRO, Melbourne, pp. 428-437.

GLCF. 2004. Institute for Advanced Computer Studies, University of MD. Global Land Cover Facility. Available: ftp://ftp.glcf.umiacs.umd.edu/glcf/Landsat/WRS2/p038/r032/p038r032_7x19990814.ETM-EarthSat-Orthorectified/. Accessed 5/30/2006.

Gosnell, H., G. Preston, and B. Travis. 2006. Socioeconomics: Impacts and adaptations. Appendix D in *Climate Change and Aspen: An Assessment of Impacts and Potential Responses,* J. Katzenberger and K. Crandall (eds.). Aspen Global Change Institute, CO, pp. 57–80.

Hennessy, K., P. Whetton, I. Smith, J. Bathols, M. Hutchinson, and J. Sharples. 2003. *The Impact of Climate Change on Snow Conditions in Mainland Australia*. CSIRO Atmospheric Research, Aspendale, Victoria, Australia.

Houghton, J.T., Y. Ding, D.J. Griggs, M. Noguer, P.J. van der Linden, D. Xiaosu, and K. Maskell (eds.). 2001. *Climate Change 2001: The Scientific Basis*. Cambridge University Press, New York.

Isaacson, A.E. 2006. Economic Impact of the Utah Alpine Ski Industry. Policy Perspectives. Bureau of Economic and Business Research, University of Utah. Vol. 2, Issue 7. Available: http://www.imakenews.com/cppa/e_article000623459.cfm?x = b11,0. Accessed 9/19/2009.

Klein, A.G., D.K. Hall, and K. Siedel. 1998. Algorithm intercomparison for accuracy assessment of the MODIS snow – mapping algorithm. Proceedings of the 55th Annual Eastern Snow Conference, Jackson, NH, June 2-3, 1998, pp. 37-45.

König, U. 1998. *Tourism in a Warmer World: Implications of Climate Change due to Enhanced Greenhouse Effect for the Ski Industry in the Australian Alps.* Wirtschaftsgeographie und Raumplanung, Vol. 28. University of Zurich.

Leggett, J., W.J. Pepper, and R.J. Swart. 1992. Emissions scenarios for IPCC: An update. In *Climate Change 1992-The Supplementary Report to the IPCC Scientific Assessment,* J.T. Houghton, B.A. Callander, and S.K. Varney (eds.). WMO/UNEP Intergovernmental Panel on Climate Change. Cambridge University Press, Cambridge, UK. pp. 69-95.

Lemke, P., J. Ren, R.B. Alley, I. Allison, J. Carrasco, G. Flato, Y. Fujii, G. Kaser, P. Mote, R.H. Thomas, and T. Zhang. 2007. Observations: Changes in snow, ice and frozen ground. In *Climate Change 2007: The Physical Science Basis. Contribution of Working Group I to the Fourth Assessment Report of the Intergovernmental Panel on Climate Change,* S. Solomon, D. Qin, M.

Manning, Z. Chen, M. Marquis, K.B. Averyt, M. Tignor, and H.L. Miller (eds.). Cambridge University Press, Cambridge, UK and New York.

Leung, L.R. and Y. Qian. 2005. Hydrologic response to climate variability, climate change, and climate extreme in the U.S.: Climate model evaluation and projections. In *Regional Hydrological Impacts of Climatic Change – Impact Assessment and Decision Making*, Wagener, T., S. Franks, V. Gupta Hoshin, E. Bogh, L. Bastidas, C. Nobre, and C. de Oliveira Galvao (eds.). IAHS Publication 295, pp. 37-44.

Leung, L.R., Y. Qian, and X. Bian. 2003a. Hydroclimate of the western United States based on observations and regional climate simulation of 1981-2000. Part I: Seasonal statistics. *Journal of Climate* 16(12):1892-1911.

Leung, L.R., Y. Qian, X. Bian, and A. Hunt. 2003b. Hydroclimate of the western United States based on observations and regional climate simulation of 1981-2000. Part II: Mesoscale ENSO anomalies. *Journal of Climate* 16(12):1912-1928.

Leung, L.R., Y. Qian, X. Bian, W.M. Washington, J. Han, and J.O. Roads. 2004. Mid-century ensemble regional climate change scenarios for the western United States. *Climatic Change*, 62(1-3):75-113.

Martinec, J. 1975. Snowmelt-runoff model for stream flow forecasts. *Nordic Hydrology* 6(3):145-154.

Martinec, J., A. Rango, and R. Roberts. 1994. *The Snowmelt Runoff Model (SRM) User's Manual,* M.F. Baumgartner (ed.). Geographica Bernensia, Department of Geography, University of Berne, Switzerland.

McCarthy, J., O. Canziani, N. Leary, D. Dokken, and K. White (eds.). 2001. *Climate Change 2001: Impacts, Adaptation, and Vulnerability.* Cambridge University Press, New York.

Meehl, G.A., T.F. Stocker, W.D. Collins, P. Friedlingstein, A.T. Gaye, J.M. Gregory, A. Kitoh, R. Knutti, J.M. Murphy, A. Noda, S.C.B. Raper, I.G. Watterson, A.J. Weaver, and Z.-C. Zhao. 2007. Global climate projections. In *Climate Change 2007: The Physical Science Basis. Contribution of Working Group I to the Fourth Assessment Report of the Intergovernmental Panel on Climate Change*, S. Solomon, D. Qin, M. Manning, Z. Chen, M. Marquis, K.B. Averyt, M. Tignor and H.L. Miller (eds.). Cambridge University Press, Cambridge, UK and New York.

Nakićenović, N. and R. Swart (eds.). 2000. *Special Report on Emissions Scenarios.* Cambridge University Press, Cambridge, UK.

National Assessment Synthesis Team. 2000. *Climate Change Impacts on the United States: The Potential Consequences of Climate Variability and Change.* US Global Change Research Program, Washington, DC.

Nolin, A.W. and C. Daly. 2006. Mapping "at-risk" snow in the Pacific Northwest. *J. Hydrometeor* 7:1164-1171.

NRCS. 2009. Site Information and Reports for Thaynes Canyon. Natural Resources Conservation Service. Available: http://www.wcc.nrcs.usda.gov/snotel/snotel.pl?sitenum = 814&state = ut. Accessed 8/15/2009.

PCMDI. 2008. Program for Climate Model Diagnosis and Intercomparison. Lawrence Livermore National Laboratory, San Francisco CA. Available: http://wwwpcmdi.llnl.gov/ipcc/model_documentation/ipcc_model_documentation.php. Accessed 9/21/2009.

Schröter, D. 2005. Vulnerability to Changes in Ecosystem Services. CID Graduate Student and Postdoctoral Fellow. Working Paper No. 10. July. Available: www.cid.harvard.edu/cidwp/pdf/grad_student/010.pdf. Accessed 11/2/2005.

Scott, D. and B. Jones. 2005. Climate Change & Banff National Park: Implications for Tourism and Recreation. Report prepared for the Town of Banff. University of Waterloo, Waterloo, ON.

Scott, D., J. Dawson, and B. Jones. 2008. Climate change vulnerability of the US Northeast winter recreation-tourism sector. *Mitig Adapt Strat Glob Change* 13:577-596.

Scott, D., G. McBoyle, and B. Mills. 2003. Climate change and the skiing industry in southern Ontario (Canada): Exploring the importance of snowmaking as a technical adaptation. *Climate Res.* 23:171-181.

Scott, D., G. McBoyle, and A. Minogue. 2007. Climate change and Quebec's ski industry. In *Global Environmental Change: Human Policy and Dimensions*. Manuscript No. doi:10.1016/j.gloenvcha.2006.05.004. pp. 181-190.

Ski Utah. 2009. Utah Skier/Snowboarder Survey 2007–2008. Prepared by Wikstrom Economics and Planning Consultants, Inc.

Solomon, S., D. Qin, M. Manning, R.B. Alley, T. Berntsen, N.L. Bindoff, Z. Chen, A. Chidthaisong, J.M. Gregory, G.C. Hegerl, M. Heimann, B. Hewitson, B.J. Hoskins, F. Joos, J. Jouzel, V. Kattsov, U. Lohmann, T. Matsuno, M. Molina, N. Nicholls, J. Overpeck, G. Raga, V. Ramaswamy, J. Ren, M. Rusticucci, R. Somerville, T.F. Stocker, P. Whetton, R.A. Wood, and D. Wratt. 2007. Technical summary. In *Climate Change 2007: The Physical Science Basis.*

Contribution of Working Group I to the Fourth Assessment Report of the Intergovernmental Panel on Climate Change, S. Solomon, D. Qin, M. Manning, Z. Chen, M. Marquis, K.B. Averyt, M. Tignor and H.L. Miller (eds.). Cambridge University Press, Cambridge, UK and New York.

SRM. 2002. Snowmelt Runoff Model. Available: http://hydrolab.arsusda.gov/cgi-bin/srmhome. Accessed 1/15/2008.

Tegart, W.J. McG., G.W. Sheldon, and D.C. Griffiths. 1990. *Climate Change-The IPCC Impacts Assessment*. WMO/UNEP Intergovernmental Panel on Climate Change. Australian Government Publishing Service, Canberra.

University of South Carolina. 2009. Underappreciated Assets: The Economic Impact of South Carolina's Natural Resources. Moore School of Business. April.

U.S. Department of Commerce. 2007. RIMS II Workshop. Presented by Zoe Ambargis and Rebecca Bess. Bureau of Economic Analysis. Presented at the Annual AUBER Conference, Pensecola, FL. October 13, 1997. Available: http://uwf.edu/auber/conf/Pensacola07/presentations/AUBER%20RIMS%20Presentation.ppt. Accessed 9/28/2009.

U.S. Department of Commerce. 2009. RIMS II Multipliers. Total Multipliers for Output, Earnings, Employment, and Value Added by Industry Aggregation for Summit County, UT (Type II). Ordered 7/13/2009.

USGS EROS Data Center. 1999. USGS 10 Meter Resolution, One-Sixtieth Degree National Elevation Dataset for CONUS, Alaska, Hawaii, Puerto Rico, and the U.S. Virgin Islands. Edition 1. Raster digital data. U.S. Geological Survey Earth Resources Observation and Science, Sioux Falls, SD. Available: http://gisdata.usgs.net/ned/. Accessed 7/26/2005.

USGS EROS Data Center. 2001. Landsat ETM+ level-1G SLC-Off Gap-Filled Remote Sensing Image. U.S. Geological Survey Earth Resources Observation and Science, Sioux Falls, SD.

Watson, R.T., M.C. Zinyowera, and R.H. Moss (eds.). 1996. *Climate Change 1995: The IPCC Second Assessment Report, Volume 2: Scientific-Technical Analyses of Impacts, Adaptations, and Mitigation of Climate Change*. Cambridge University Press, Cambridge, UK.

Wigley, T.M.L. 2008. MAGICC/SCENGEN version 5.3 User's Manual. Available: http://www.cgd.ucar.edu/cas/wigley/magicc/UserMan5.3.v2.pdf. Accessed 4/15/2008.

WRCC. 2008a. Alta, Utah (420072). Period of Record Monthly Climate Summary. Available: http://www.wrcc.dri.edu/cgi-bin/cliMAIN.pl?ut0072. Accessed 12/28/2006.

WRCC. 2008b. Logan Utah State Univ., Utah (425186). Period of Record Monthly Climate Summary. Available: http://www.wrcc.dri.edu/cgi-bin/cliMAIN.pl?ut5186. Accessed 12/28/2006.

WRCC. 2008c. Mountain Dell Dam, Utah (425892). Period of Record Monthly Climate Summary. Available: http://www.wrcc.dri.edu/cgi-bin/cliMAIN.pl?ut5892. Accessed 12/28/2006.

WRCC. 2008d. Salt Lake City NWSFO, Utah (427598). Period of Record Monthly Climate Summary. Available: http://www.wrcc.dri.edu/cgi-bin/cliMAIN.pl?ut7598. Accessed 12/28/2006.

WRCC. 2008e. Silver Lake Brighton, Utah (427846). Period of Record Monthly Climate Summary. Available: http://www.wrcc.dri.edu/cgi-bin/cliMAIN.pl?ut7846. Accessed 12/28/2006.

A. Brief Description of SRES Storylines and Associated Scenarios

The Intergovernmental Panel on Climate Change (IPCC) developed a Special Report on Emission Scenarios (SRES) to provide more consistent projections of greenhouse gas (GHG) emissions – projections that considered the complex social, economic, and technological relationships that underlie energy use and resulting emissions. The SRES approach aimed for an underlying consistency of these complex relationships. The result was a set of logical storylines that encompass the social and physical relationships driving GHG emissions (Nakićenović and Swart, 2000). For more details on these storylines and scenarios, please refer to the IPCC report at http://www.grida.no/climate/ipcc/emission/.

At the core of the SRES approach are four poles along two major axes:

▶ Economic vs. environmental
▶ Global vs. regional.

As shown in Figure A.1, combinations of these four poles give rise to four primary storylines:

▶ A1 – Economic growth and liberal globalization
▶ A2 – Economic growth with a greater regional focus
▶ B1 – Environmentally sensitive with strong global relationships
▶ B2 – Environmentally sensitive with a highly regional focus.

Each storyline describes a global paradigm based on prevalent social characteristics, values, and attitudes that determine, for example, the extent of globalization, economic development patterns, and environmental resource quality. The storylines are by their nature highly speculative. Nonetheless, they provide identifiable starting points that are defined and consistent with available datasets for projecting some variables (most notably population, income, land use, and emissions). They have been used in previous and ongoing assessments and provide a basis for intercountry comparisons.
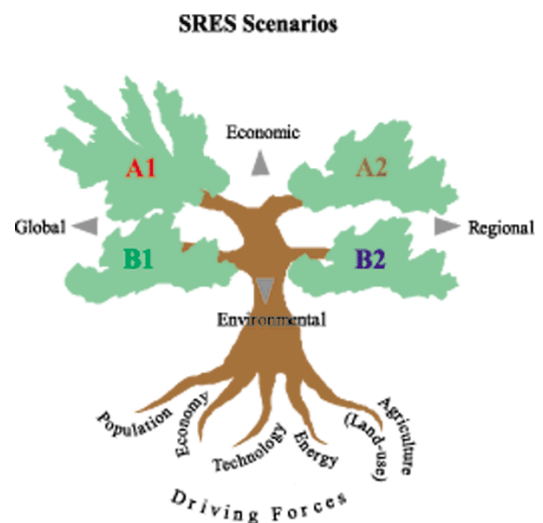

Figure A.1. Conceptual relationships underlying the SRES scenarios.

Source: Nakićenović and Swart, 2000.

The A1 and B1 storylines focus on global solutions to economic, social, and environmental sustainability, with A1 focusing on economic growth and B1 focusing on environmental sensitivity. The A2 and B2 storylines focus on regional solutions with a strong emphasis on self-reliance. They differ in that A2 focuses on strong economic growth and B2 focuses on environmental sensitivity. The IPCC describes their differences as follows: "While the A1 and B1 storylines, to different degrees, emphasize successful economic global convergence and social and cultural interactions, A2 and B2 focus on a blossoming of diverse regional development pathways."

The A1 storyline, in general, assumes strong economic growth and liberal globalization characterized by low population growth, very high gross domestic product (GDP) growth, high-to-very high energy use, low-to-medium changes in land use, medium-to-high resource availability (of conventional and unconventional oil and gas), and rapid technological advancement. The A1 scenario assumes convergence among regions, including a substantial reduction in regional differences in per capita income in which the current distinctions between "poor" and "rich" countries eventually dissolves; increased capacity building; and increased social and cultural interactions. A1 emphasizes market-based solutions, high savings, and investment, especially in education and technology, and international mobility of people, ideas, and technology.

The A1 storyline is broken up into scenarios that characterize alternative developments of energy technologies. A1FI represents the "fossil intensive" scenario and results in the highest emissions and the highest atmospheric concentrations of carbon dioxide (Schröter, 2005). The A1B scenario represents a "balanced" development of energy technologies. It assumes that no one energy source is relied on too heavily and that similar improvement rates apply to all energy supply and end-use technologies (Nakićenović and Swart, 2000).

The A2 storyline describes a world with regional economic growth characterized by high population growth, medium GDP growth, high energy use, medium-to-high changes in land use, low resource availability of conventional and unconventional oil and gas, and slow technological advancement. This storyline assumes a very heterogeneous world that focuses on self-reliance and the preservation of local identities, and assumes that per capita economic growth and technological change are more fragmented and slower than in other scenarios. The A2 storyline only has one scenario, so the terms A2 storyline and A2 scenario are used synonymously.

The B1 storyline describes a convergent world that emphasizes global solutions to economic, social, and environmental sustainability. Focusing on environmental sensitivity and strong global relationships, B1 is characterized by low population growth, high GDP growth, low energy use, high changes in land use, low resource availability of conventional and unconventional oil and gas, and medium technological advancement. The B1 storyline assumes rapid adjustments in the economy to the service and information sectors, decreases in material intensity, and the

introduction of clean and resource-efficient technologies. A major theme in the B1 storyline is a high level of environmental and social consciousness combined with a global approach to sustainable development. The B1 storyline only has one scenario, so the terms B1 storyline and B1 scenario are used synonymously.

The B2 storyline, like the A2 storyline, focuses on regional solutions to economic, social, and environmental sustainability. The storyline focuses on environmental protection and social equality and is characterized by medium population and GDP growth, medium energy use, medium changes in land use, medium resource availability, and medium technological advancement. Similar to the A2 and B1 storylines, the B2 storyline has only has one scenario, so the terms B2 storyline and B2 scenario are used synonymously.

B. Area Averaging in SCENGEN for Spatially Averaged Climate Changes

(Adapted from Tom M.L. Wigley, National Center for Atmospheric Research, personal communication, November 11, 2007)

A new feature in SCENGEN (Global and Regional Climate SCENario GENerator) is the option to replace individual grid box (cell) values by the area average of 9 cells centered on the individual cell. This is referred to as "smoothing" below.

Smoothing is useful for estimating climate changes at a specific latitude/longitude location. Results for the individual $2.5° \times 2.5°$ cell in which the site is located are subject to more noise than a larger area surrounding the site, so a 9-cell ($7.5° \times 7.5°$) area average is generally considered a more stable estimate of site changes than an individual cell. A key point here is that, although there will be small-scale site-specific changes, the current resolution of Atmosphere/Ocean General Circulation Models (AOGCMs) is not able to capture such high-resolution information – so individual grid box values cannot be expected to be fully representative of the site-specific changes. The smoothing feature is also useful in producing less spatially noisy output maps.

The smoothing function in the current version of SCENGEN replaces all the output grid box values by the 9-cell area average. The average is defined by:

$$\langle X_{ij} \rangle = \Sigma \left(X_{ij} \cos(\phi_{ij}) \right) / \Sigma \left(\cos(\phi_{ij}) \right)$$

where i is latitude, j is longitude, and the summation is over i-1, i, i+1, j-1, j, and j+1. ϕ_{ij} is the latitude of the ij-th cell. Currently, area averaging is not applied to the variability variables.

Smoothing is only applied to variables that are used for mapped outputs. Raw, unsmoothed data should be used for tabulated results. The results of smoothing are shown in the following example, using annual precipitation as the variable, A1B as the emissions scenario, a climate sensitivity of 3.0°C, output year 2050 global-mean temperature change from 1990 of 1.63°C, and average over all 20 AOGCMs (see Figures B.1 and B.2).
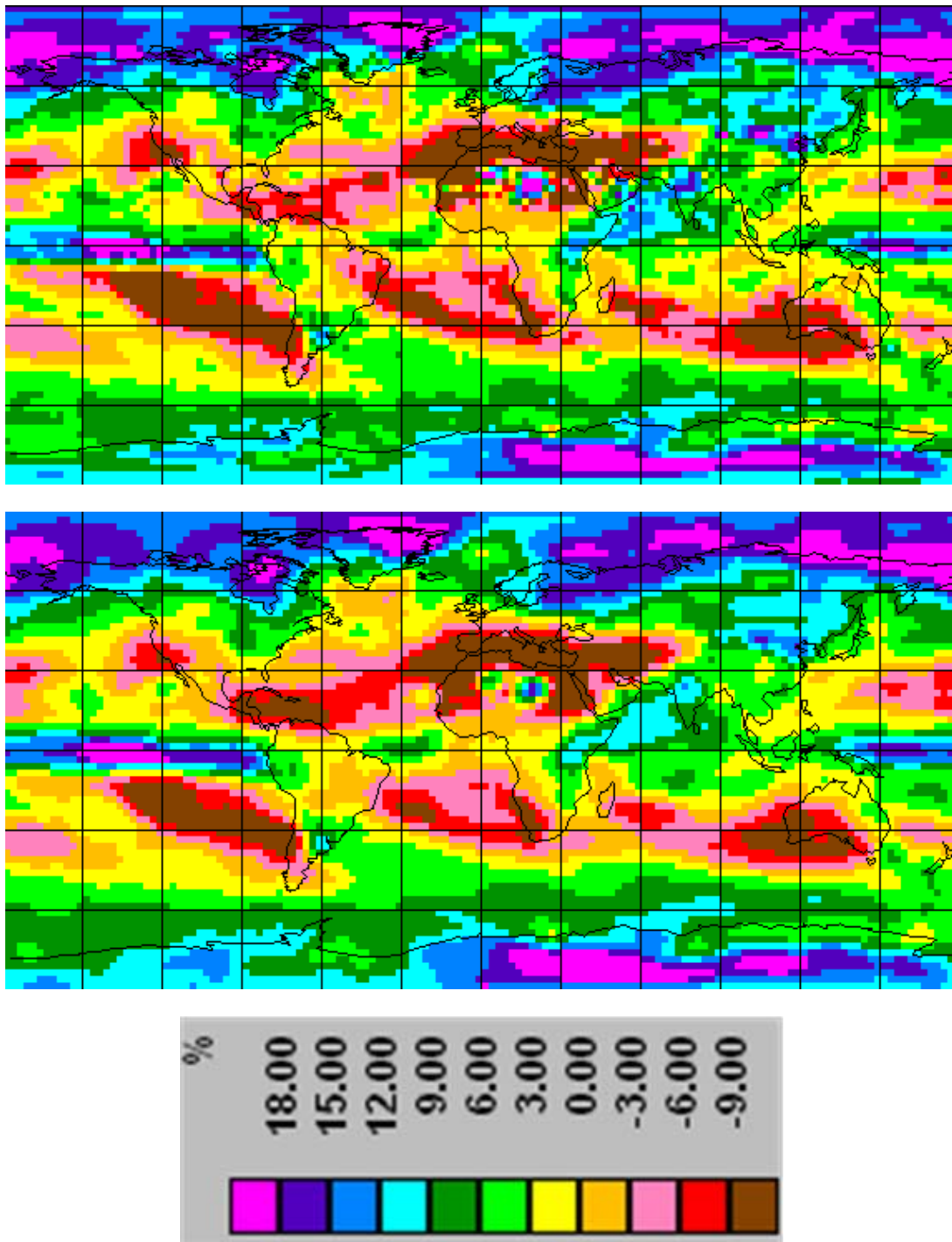
Figure B.1. Raw vs. smoothed global annual precipitation change patterns. Top panel shows raw data, and the lower panel shows smoothed data.
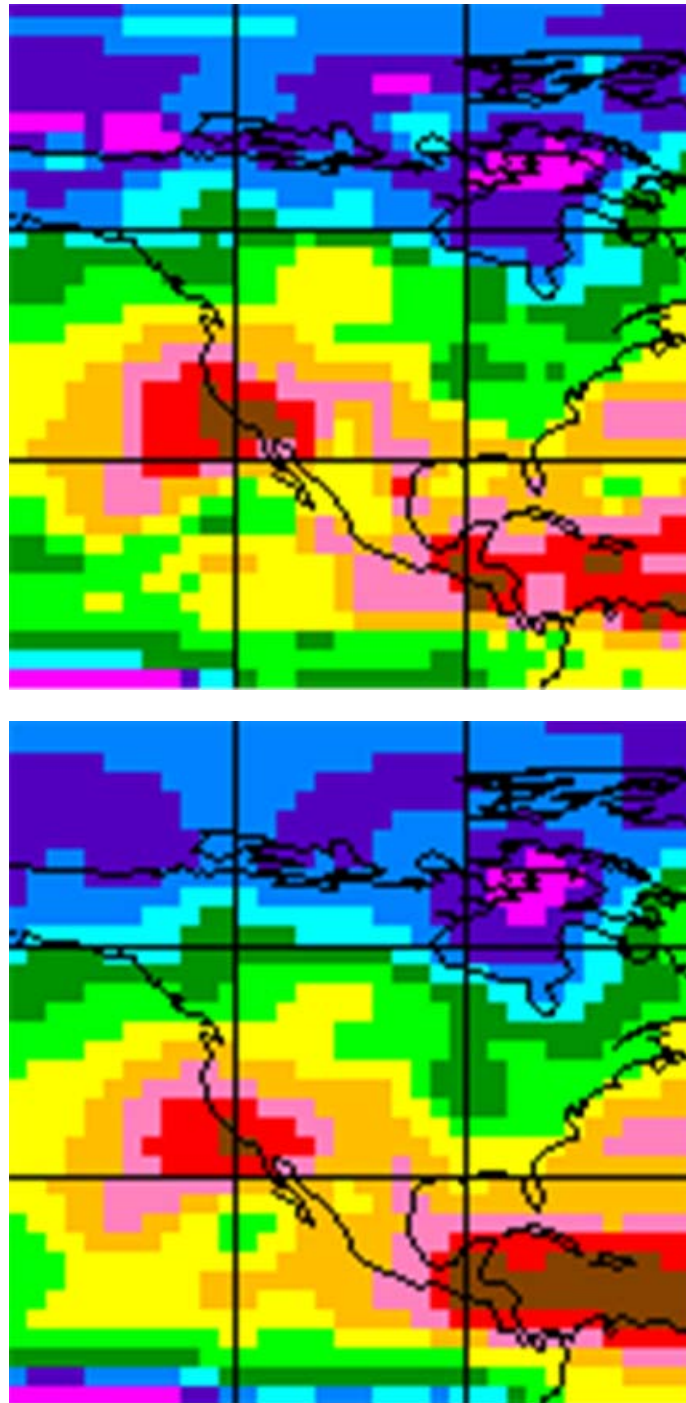
Figure B.2. Blow-up of the North America region from Figure B.1. Top panel shows raw data, and bottom panel shows smoothed data. Scale same as in Figure B.1.

C. Seven Selected Global Climate Model Simulations of Current Climate and Observed Climate

Figures C.1 and C.2 display observed (in 2000) temperature and precipitation for the nine grid boxes centered on Park City, and the simulations of current climate for the seven models. All data are from MAGICC/SCENGEN (Model for the Assessment of Greenhouse-gas Induced Climate Change/Global and Regional Climate SCENario GENerator). All seven models closely simulate the observed seasonality of observed temperatures, and model errors (compared to actual) range from 0.0 to 8.6°C (0.0 to 15.5°F) in individual months.

For precipitation, the models' performance is more mixed. All seven models overstate precipitation in 2000. Nevertheless, the magnitude and patterns of the observed precipitation is reasonably simulated, with errors ranging from 0.001 millimeters (mm) to 3.87 mm.

Figure C.1. Modeled vs. observed current (2000) temperature for the central Cascades.

Figure C.2. Modeled vs. observed current (2000) precipitation for the central Cascades.

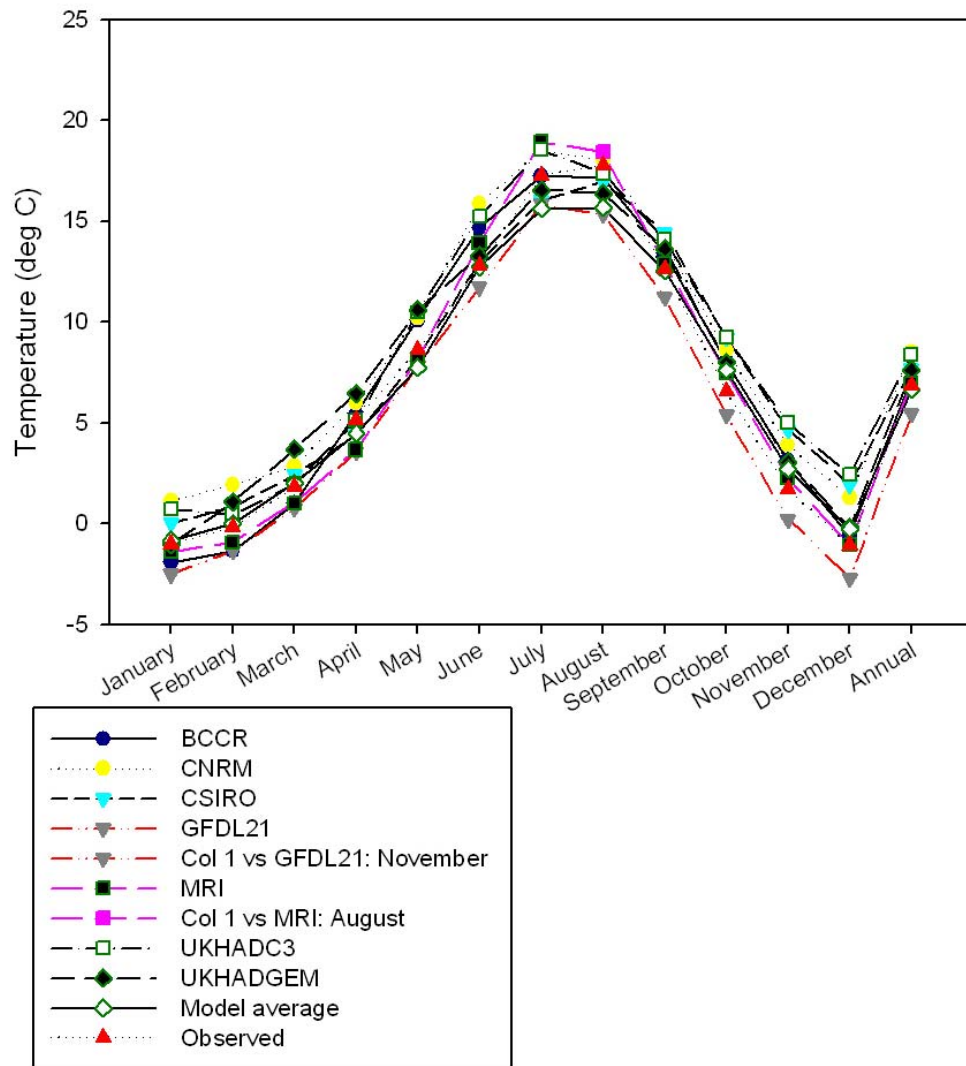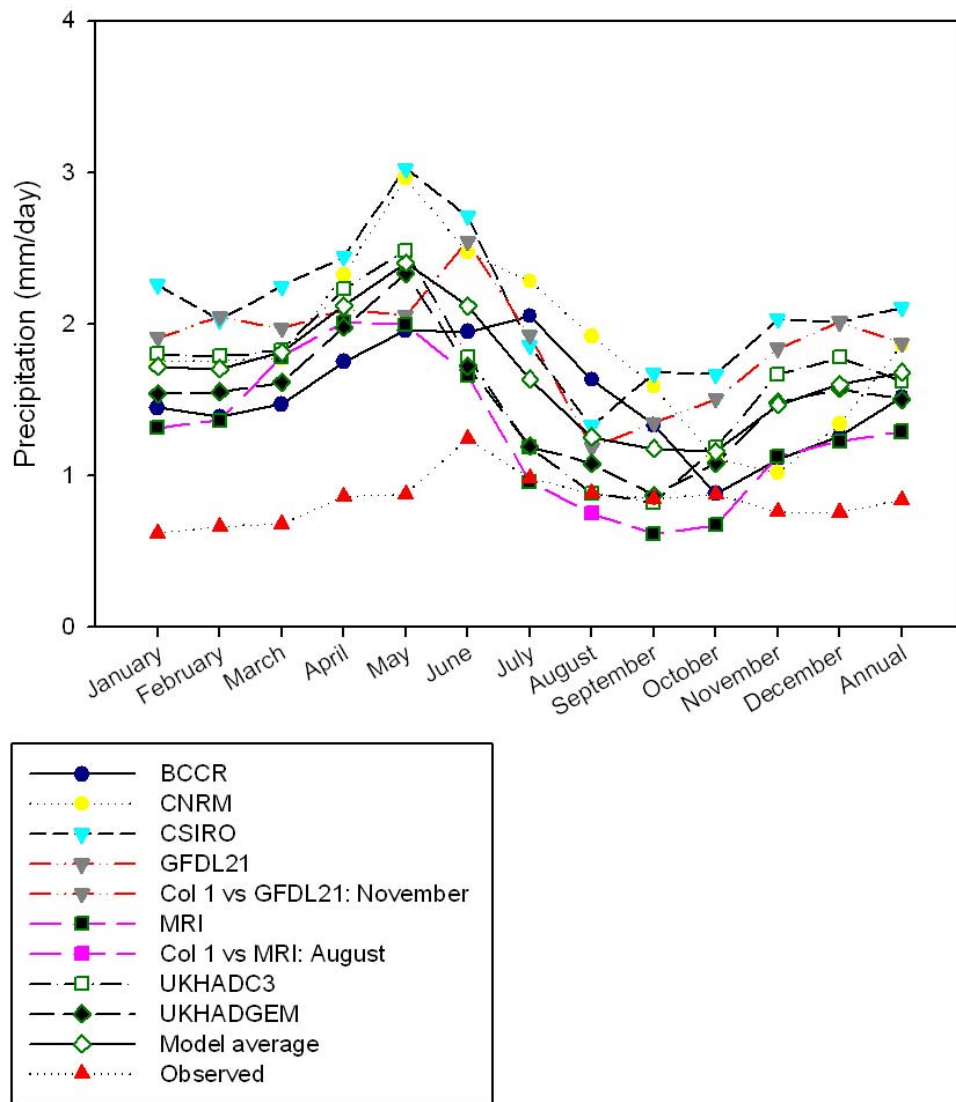# D. SDSM Calibration for Thaynes Canyon, 1988–2000

Authored by Dr. Robert Wilby

D.1 Comment on Data Quality

Observed daily TAVG and PRCP series were taken from the SNOTEL station at Thaynes Canyon, Utah (40.6236ºN, 111.53ºW, 9,230 feet). The data begin on June 24, 1988, and are available until September 30, 2008.

The records were screened for outliers, data entry errors, and internal consistency. This led to the removal of suspect high TAVG values (> 40ºC) between June 1, 1993 and July 16, 1993. One suspect low TAVG (-51.4ºC) on October 29, 1993 was removed.

The Statistical Downscaling Model (SDSM) was calibrated against the remaining data for the period 1988–2000. Data are available for the year 2001 onwards, but were not used on the assumption that climate change(s) could be present in the record. Table D.1 shows the NCEP re-analysis predictors selected for model calibration, and the partial correlations of each variable with daily TAVG and PRCP.

Table D.1. NCEP predictor variables for the grid-box centered on 40°N, 112.5°W

Predictand	Predictors (NCEP re-analysis)	Partial *r*
TAVG	Mean sea level pressure (MSLP)	-0.82
	Near surface divergence (DSUR)	0.41
	Meridianal wind component at 500 hPa level (V500)	0.29
	500 hPa geopotential height (H500)	0.96
PRCP[a]	Relative humidity at 500 hPa level (R500)	0.25
	Vorticity at 500 hPa level (Z500)	0.09
	Zonal wind component at 850 hPa level (U850)	0.26
	500 hPa geopotential height (H500)	-0.16

a. Fourth root transformation for rainfall amount process.

D.2   Biases in Summer TAVG Downscaling Predictor Variables
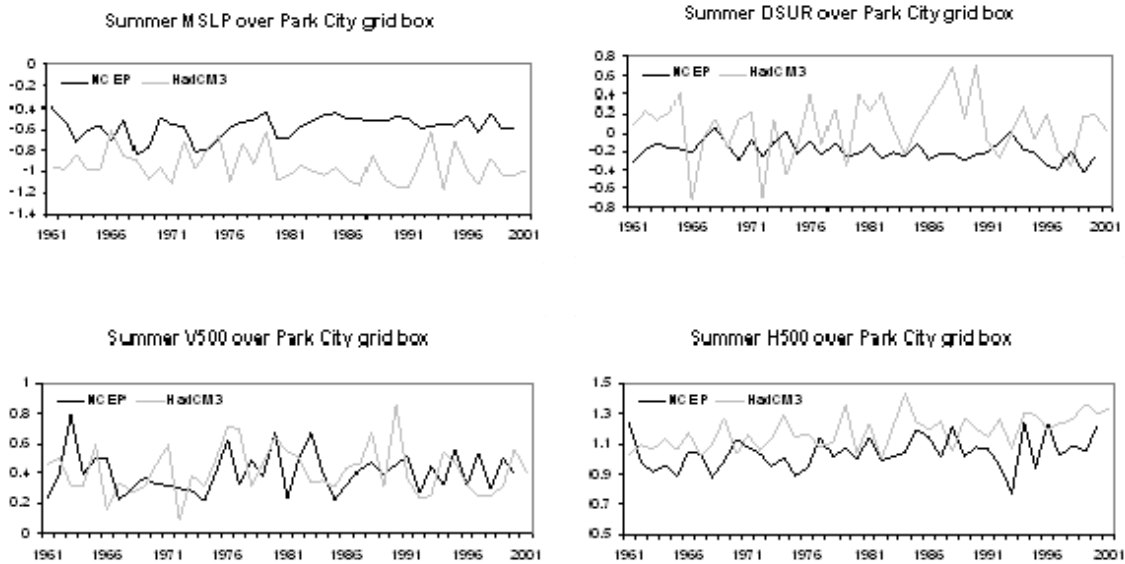
Figure D.1. Comparison of summer mean NCEP and HadCM3 A2 run predictor variables for the grid-box centered on 40°N, 112.5°W. The most significant biases in HadCM3 summer predictors are in MSLP (negative) and DSUR (positive).
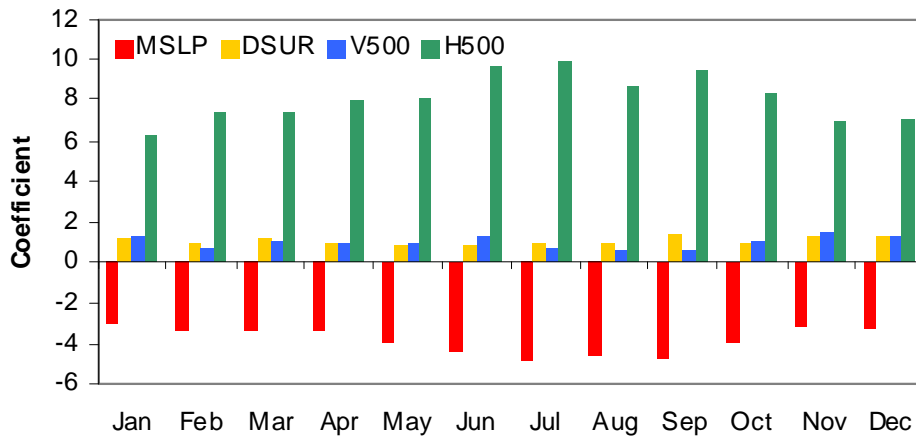
Figure D.2. Predictor variable weights for TAVG calibrated against NCEP.

D.3   Thaynes Canyon Daily Average Temperature (TAVG)

Thaynes Canyon TAVG 1993 (r=0.96)
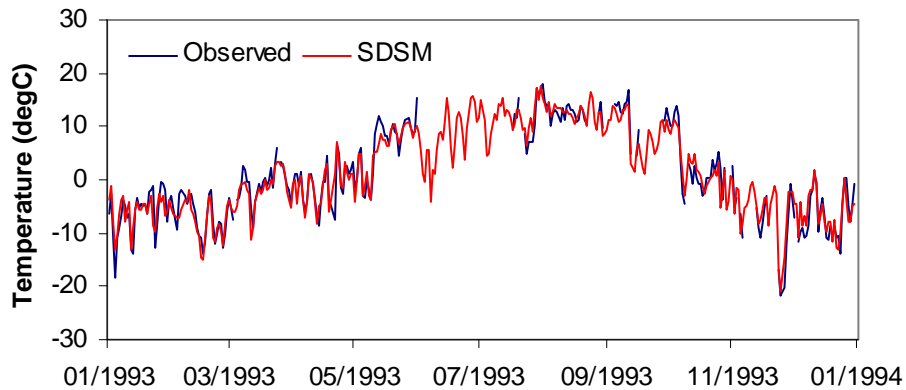
Thaynes Canyon TAVG 1999 (r=0.97)
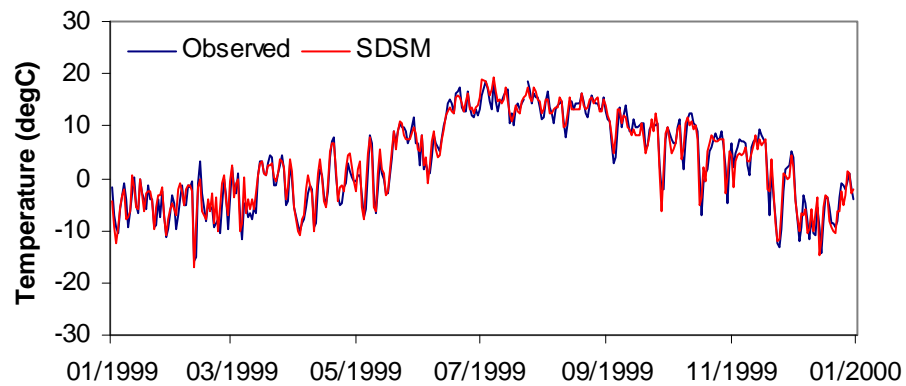
Figure D.3. Illustration of daily time-series behavior: Comparison of downscaled and observed TAVG for 1993 and 1999. Note the missing data in the summer of 1993.

Thaynes Canyon TAVG 2000

Figure D.4. Illustration of cumulative distribution function (CDF): Comparison of downscaled and observed daily TAVG for 2000 (the warmest year in the training set).

Thaynes Canyon annual mean TAVG (r=0.71)

Figure D.5. Observed and downscaled annual mean TAVG. Note that the hindcast downscaling was performed using large-scale NCEP predictor variables for 1961−2000.

Thaynes Canyon winter mean TAVG (r=0.70)

Thaynes Canyon spring mean TAVG (r=0.93)

Thaynes Canyon summer mean TAVG (r=0.92)

Thaynes Canyon fall mean TAVG (r=0.85)

Figure D.6. Observed and downscaled seasonal mean TAVG. Note that the downscaling was performed using large-scale NCEP predictor variables for 1961−2000.

Thaynes Canyon winter mean TAVG

Thaynes Canyon spring mean TAVG

Thaynes Canyon summer mean TAVG

Thaynes Canyon fall mean TAVG

Figure D.7. Seasonal mean TAVG for 1961−2099 downscaled from HadCM3 output under SRES A2 and B2 emissions.

Table D.2. Changes in seasonal mean TAVG (°C) for HadCM3, A2, and B2 emissions

	DJF		MAM		JJA		SON	
	A2	**B2**	**A2**	**B2**	**A2**	**B2**	**A2**	**B2**
2020s	1.5	1.0	0.9	1.3	2.3	3.0	2.0	2.1
2050s	2.9	1.3	2.3	2.2	4.8	4.5	3.1	3.7
2080s	5.0	2.0	4.0	2.6	7.6	5.4	5.6	4.5
Bias[a]	*-0.9*	*-0.9*	*-0.4*	*-0.4*	*3.1*	*3.0*	*-0.6*	*-0.6*

a. Estimated with respect to TAVG downscaled from NCEP re-analysis 1961–1990.

D.4   Thaynes Canyon Daily Precipitation (PRCP)
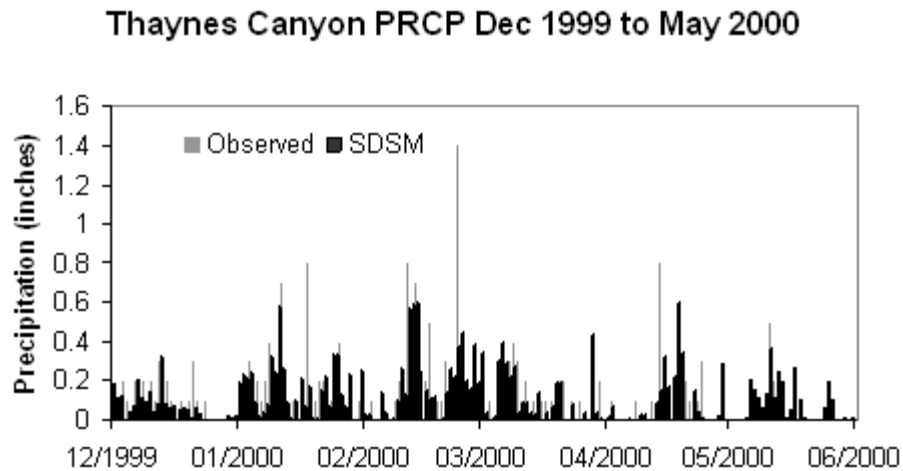
Figure D.8. Illustration of daily time-series behavior: Comparison of downscaled and observed PRCP for the winter/spring of 1999–2000.
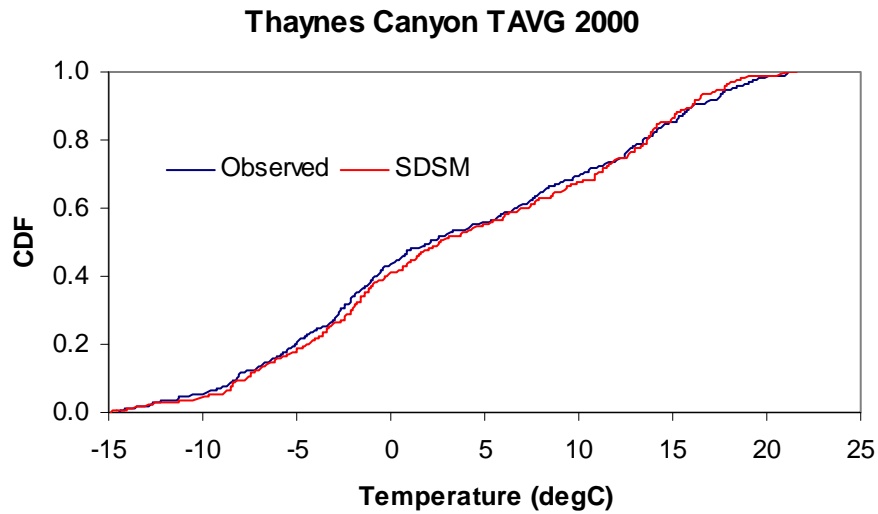
Thaynes Canyon PRCP 1991-2000
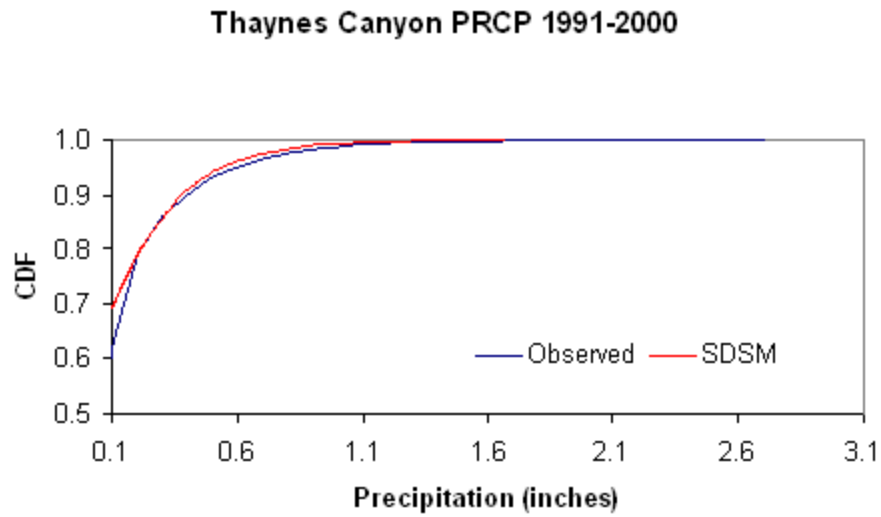
Figure D.9. Illustration of cumulative distribution function (CDF): Comparison of downscaled and observed daily PRCP for 1991–2000. Note that SDSM gives the fraction of days with nonzero precipitation (~37%) compared with observed (~38%).

Thaynes Canyon annual total PRCP (r=0.54)
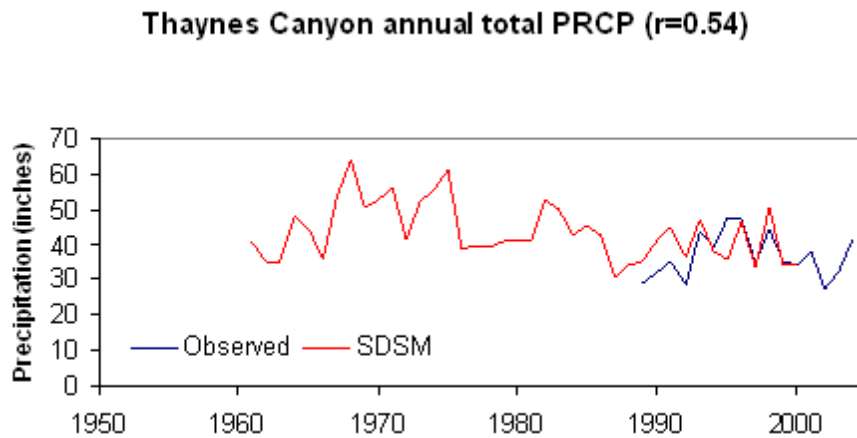
Figure D.10. Observed and downscaled annual PRCP. Note that the downscaling was performed using large-scale NCEP predictor variables for 1961–2000.

Thaynes Canyon winter total PRCP (r=0.55)

Thaynes Canyon spring total PRCP (r=0.61)

Thaynes Canyon summer total PRCP (r=0.70)
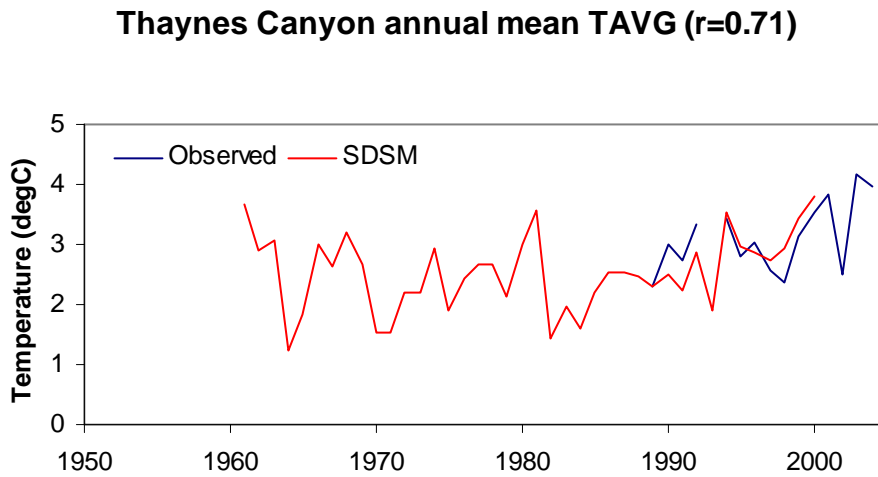
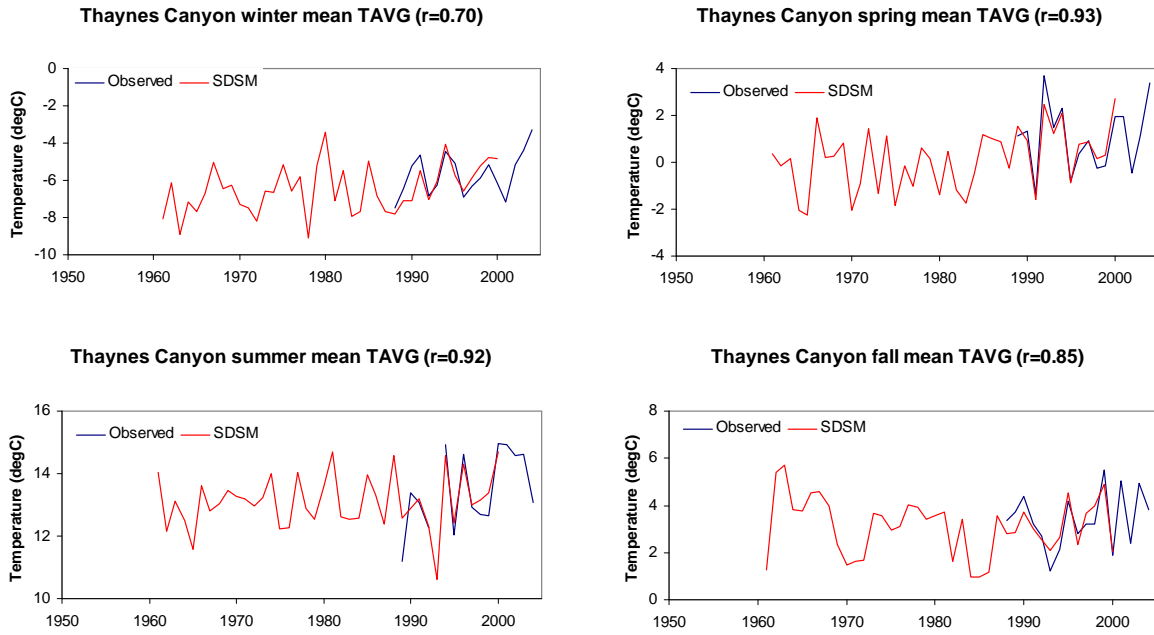Thaynes Canyon fall mean PRCP (r=0.84)

Figure D.11. Observed and downscaled seasonal total PRCP. Note that the downscaling was performed using large-scale NCEP predictor variables for 1961−2000.
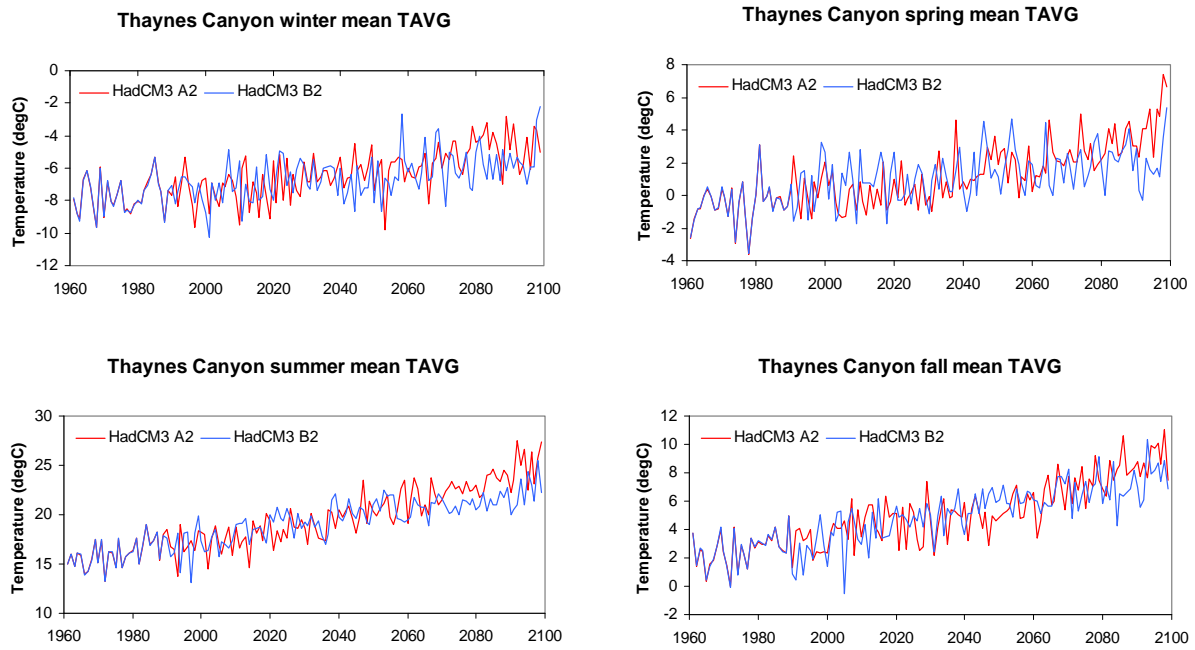
Thaynes Canyon winter total PRCP

Thaynes Canyon spring total PRCP

Thaynes Canyon summer total PRCP

Thaynes Canyon fall total PRCP
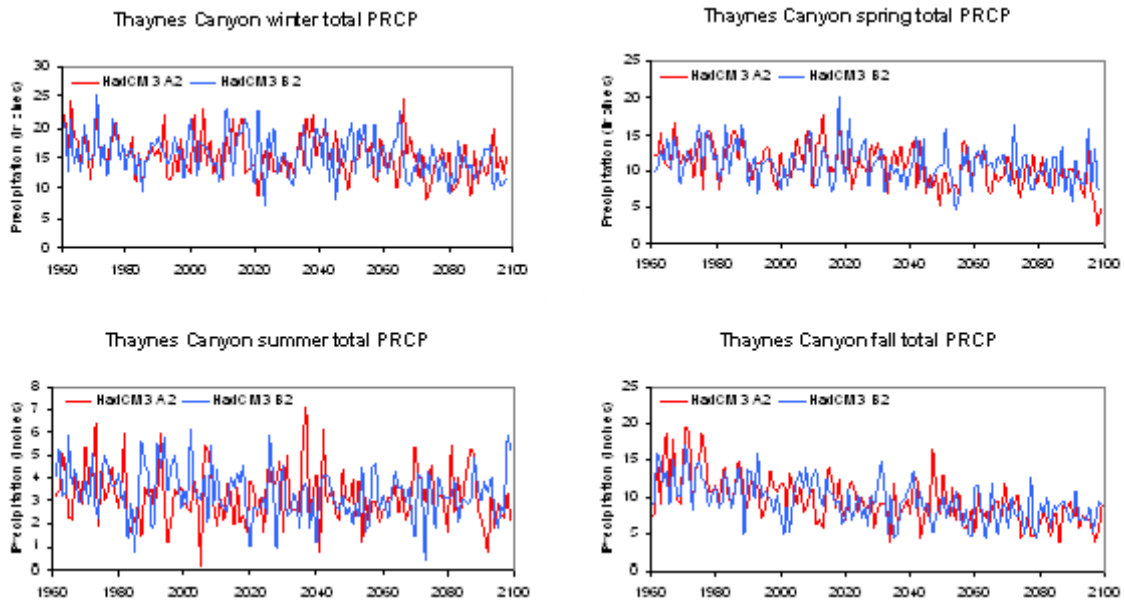
Figure D.12. Seasonal total PRCP for 1961−2099 downscaled from HadCM3 output under SRES A2 and B2 emissions.

Table D.3. Changes in seasonal total PRCP (%) for HadCM3, A2, and B2 emissions

	DJF		MAM		JJA		SON	
	A2	**B2**	**A2**	**B2**	**A2**	**B2**	**A2**	**B2**
2020s	-4	0	-6	-12	-7	-16	-30	-19
2050s	-7	-3	-21	-13	-13	-14	-31	-30
2080s	-20	-18	-29	-19	-9	-9	-47	-32
Bias[a]	*7*	*5*	*-10*	*-11*	*-28*	*-24*	*17*	*7*

a. Estimated with respect to PRCP downscaled from NCEP re-analysis for 1961–1990.

D.5 Summary

D.5.1 Temperature scenarios

▸ Overall, SDSM reproduces > 80% of the daily variation in TAVG at Thaynes Canyon for the period 1988–2000 given only information from atmospheric predictor variables overlying the target region.

▸ Relatively poor skill for individual seasons (e.g., summer 1989) is linked, in part, to missing observed data.

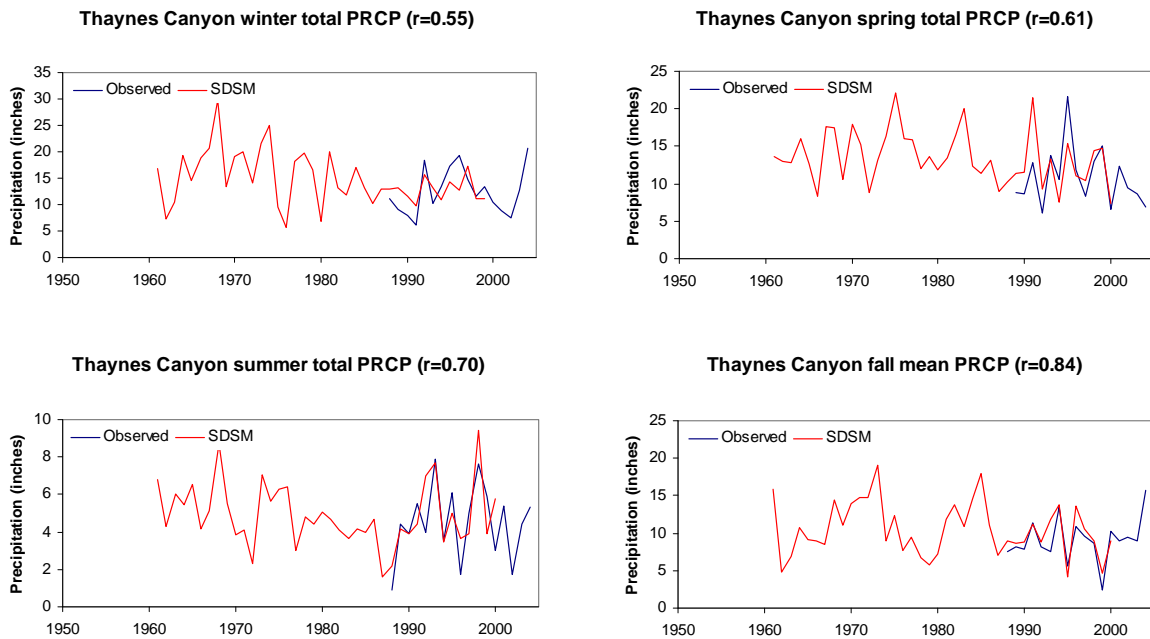▸ Hindcast TAVG series downscaled by SDSM from NCEP predictors suggest rapid warming in winter and spring between 1961 and 2000. Over this period the seasonal temperature change was +0.4°C/decade (winter and spring), +0.1°C/decade (summer), and -0.2°C/decade (autumn).

▸ Warming is expected in all seasons for the 2020s, 2050s, and 2080s under both emissions scenarios. The warming is most rapid in summer, but projected rates of warming in winter and spring are comparable to historic rates (see above).

▸ The projected temperature changes are relatively high compared with other high elevation stations in the western United States (e.g., Niwot Ridge, Independence Pass), but the pattern of most rapid warming in summer is consistent between sites.

▶ The high rates of warming at Thaynes Canyon could be an artifact of the large bias (+3ºC) in the scenarios downscaled from HadCM3 predictors when compared with NCEP predictors for 1961–1990. The difference in downscaled TAVG was attributed to a significant negative bias in HadCM3 MSLP, and positive bias in DSUR compared with NCEP.

▶ The bias due to downscaling predictors is less than 1ºC in other seasons.

D.5.2 Precipitation scenarios

▶ Predictability of daily and seasonal PRCP totals at Thaynes Canyon using regional NCEP variables is less than TAVG.

▶ Assessment of model skill for interannual and interdecadal totals was not possible due to the short observation record.

▶ Despite the brevity of the calibration set, SDSM produces realistic daily time-series of precipitation occurrence and wet-day totals. Overall, the model tends to underestimate the frequency of heavy precipitation events (> 1 inch/day).

▶ Biases in PRCP totals due to downscaling predictor variables (i.e., NCEP compared with HadCM3) were greatest in summer, and least in winter/ spring.

▶ With the above in mind, future projections based on HadCM3 output suggest less precipitation in all seasons. However, the largest reductions are expected in fall and spring and to a less extent in winter and summer.

E. Geographic Information Systems/Remote Sensing Methods

Methods used to generate digital elevation model and elevation classes

Here we describe the methods used to generate the elevation zones and snow-covered area estimates required for the snowpack modeling. The characterized elevation zones and snow coverage values are input parameters used in the Snowpack Runoff Model (SRM). For the elevation input parameter, 10-meter (m) resolution digital elevation model (DEM) data from the U.S. Geological Survey's (USGS's) National Elevation Dataset (NED) were downloaded from http://gisdata.usgs.net/ned/ for the area that includes Mt. Bachelor (USGS EROS Data Center, 1999).The DEM was then subset to the boundary of the ski area, which was derived from heads-up digitizing from digital raster graphics provided by the ski area. We then classified the elevation data into the following three elevation zones:

1. 1,670–2,036 m [5,480–6,680 feet (ft)]
2. 2,036–2,401 m (6,680–7,880 ft)
3. 2,401–2,761 m (7,880–9,059 ft).

Total area and minimum, maximum, and mean elevation statistics were then generated for each elevation zone for use in the SRM model.

We also used the DEM data in the orthorectification of imagery to generate the snow cover estimates mentioned below.

Methods used to generate snow cover data

We estimated snow cover using satellite data. We acquired seven Landsat 7 Enhanced Thematic Mapper (ETM+) level 1G SLC-off gap filled scenes and one Landsat 5 Thematic Mapper (TM) scene from the USGS EROS Data Center (2001). The scenes covered the dates of October 2, November 3, and December 21, 1999 for the early season, and March 19, April 11, May 21 (TM), June 14, and August 17, 2000 for the late season.

Six Landsat bands (1–5, 7), covering the visible to short wave infrared (SWIR) portion of the electromagnetic spectrum, were imported into the ERDAS Imagine software (v. 9.1), and combined into six respective multispectral images. Each image was then orthorectified. Locations on the imagery were co-located with locations on an existing orthorectified (October 2, 1999) Landsat 7 ETM+ image (band 8, 14.25-m cell size; GLCF, 2004) and used as ground control points to georeference the unreferenced imagery to real-world locations. To

correct for terrain displacement, the DEM was used as input into the orthorectification process. In processing the data, the nearest-neighbor method was used during resampling.

The orthorectified imagery was then used as input to derive the snow-covered area. The Normalized Difference Snow Index (NDSI), which exploits the high reflectance in wavelengths where snow is bright [green, 0.525−0.605 micrometer (μm) Landsat] vs. wavelengths where snow is dark (SWIR, 1.55−1.75 μm Landsat), was used to identify snow cover and was calculated as follows:

$$NDSI = (TM\ band2 - TM\ band\ 5) / (TM\ band2 + TM\ band5) \tag{1}$$

As the NDSI ratio tends to falsely classify dark areas in the imagery as snow, densely forested areas were classified separately from non-forested areas (Klein et al., 1998; Dozier and Painter, 2004). We generated a forest/non-forest dataset using the Normalized Difference Vegetation Index (NDVI) from the November 3, 1999 Landsat image as follows:

$$NDVI = (TM\ band4 - TM\ band3) / (TM\ band4 + TM\ band3) \tag{2}$$

Forest areas were identified for cells with an NDVI ratio greater than 0.06, and ratios less than 0.06 were classified as non-forest. Using the forest/non-forest NDVI layer as a mask, we classified snow cover in forested areas for NDSI values greater than 0.4, while in non-forested areas we used an NDSI value of greater than 0.48. These values were determined through visual comparison with the raw imagery.

Lastly, the snow-covered area was overlaid with the four-classed elevation layer to calculate the percent snow cover by elevation class.

F.   Skier Days Model: Regression Results

We modeled monthly skier days as a linear function of area-weighted monthly snowpack, controlling for the following variables:

▸ A monthly indicator variable (referred to as "<month> month indicator"), which we included to account for the fact that there are naturally more skier days in some months than in others (i.e., it allows for changes in the intercept based on month and snowpack). November is excluded as the reference month. Therefore, the estimated coefficients for non-November months are relative to the November intercept.

▸ An interaction variable between snowpack and the monthly indicator variable (referred to as "<month> snowpack interaction"). This is included to control for the interaction effect between snowpack and the individual month. Specifically, it controls for the fact that an additional inch of snow in one month may have a different effect on skier days than an additional inch of snow in another month (i.e., it allows for shifts in the slope based on month and snowpack).

▸ Snowpack in the early season as measured by the effects of November snowpack on skier days in December and January (referred to as "Nov snow impacts on Dec" and "Nov snow impacts on Jan," respectively). This variable accounts for the time lags involved in booking ski vacations. For example, if a resort is having a bad snow year at the beginning of the season, this could influence skiers' decisions to book trips during the Christmas holiday, regardless of what the snow conditions actually are at that time.

▸ Time trend (referred to as "<season> season indicator"). This variable is included to account for differences in the number of skier days over time.

We had 54 observations with an overall fit of $R^2 = 99.2$. Table F.1 presents the coefficients and their p-values. Significant levels are identified with "*"s: *** indicates that the estimated coefficient is significant at the 99% level, and * indicates that the estimated coefficient is significant at the 90% level. Variables that are not significant at the * level remain in the model due to expectations on their relationship with skier days.

Table F.1. Skier day regression results: Estimated coefficients and p-values

Variable	Coefficient	P-value
Dec month indicator	70,069.6	0.006***
Jan month indicator	100,103.0	0.000***
Feb month indicator	58,922.3	0.052*
Mar month indicator	87,037.6	0.003***
Apr month indicator	14,520.7	0.547
Snowpack	850.9	0.174
Nov snow impacts on Dec	1,159.5	0.351
Nov snow impacts on Jan	697.3	0.392
Dec snowpack interaction	7.5	0.995
Jan snowpack interaction	-393.7	0.571
Feb snowpack interaction	527.9	0.383
Mar snowpack interaction	171.7	0.767
Apr snowpack interaction	-539.6	0.358
1999–00 season indicator	-278.8	0.977
2000–01 season indicator	-1,699.4	0.848
2001–02 season indicator	-16,306.3	0.080*
2002–03 season indicator	15,329.0	0.098*
2003–04 season indicator	1,962.4	0.831
2004–05 season indicator	-15,108.9	0.284
2005–06 season indicator	7,428.5	0.473
2006–07 season indicator	28,754.1	0.003***
Constant	-8,242.2	0.669

G. Input-output Multipliers

G.1 Technical Definitions of Input-output Metrics

The metrics used to measure economic impacts are formally defined as follows:

‣ **Output –** Intermediate purchases plus the sum of earnings (includes proprietors' earnings), taxes on production and imports less subsidies, and non-proprietors' portion of gross operating surplus. Multipliers measure the total industry output per $1 change in final demand.

‣ **Earnings –** Sum of wages and salaries, proprietors' income, and employer contributions for health insurance excluding contributions for social insurance. Multipliers measure the total household earnings per $1 change in final demand.

‣ **Employment –** Number of jobs. Full- and part-time (includes proprietors' jobs). Multipliers measure the total number of jobs per $1 million change in final demand (U.S. Department of Commerce, 2007).

G.2 Converting Visitor Spending into Producer Value

We used type II final demand multipliers from the Bureau of Economic Analysis' (BEA's) Regional Input-Output Modeling system (RIMS II). Type II multipliers are used to measure the economic impact of industries and household expenditures. These multipliers estimate the economic input using the *producer's value,* which excludes distribution costs such as transportation costs and wholesale and retail trade margins, but includes excise taxes collected and paid by producers (U.S. Department of Commerce, 2007). Producer values are calculated from expenditures using ratios from the RIMS II national distribution cost tables (Rebecca Bess, BEA, personal communication, August 20, 2009). We additionally scaled the retail and gas and transportation sectors to better reflect the makeup of the local economy. For the retail sector, we used the ratios of consumer to producer value reported in Isaacson (2006; which reports ratios developed for the State of Utah instead of the nation as a whole). That is, we assume retail expenditure net distribution costs are 32% of consumer expenditures. We also used the ratio reported in Isaacson (2006) for the gas and transportation sector, with a modification to reflect the fact that there are no refineries in Park City. Specifically, we assumed that gas spending is 50% of the spending reported as "'gas and transportation" and that gas makes up 60% of the transit and ground transportation sector in RIMS II. Therefore, we take 60% of the 50% on gas

(= 30%) (and leave the other 50% for transportation as is), which yields a consumer to producer ratio of 80%.

G.3 Expenditure and Multiplier Tables

Table G.1 reports the weighted average visitor skier expenditures by expenditure category and associated producer value. Table G.2 reports the multipliers by economic sector, and Table G.3 reports the output, earnings, and jobs per skier day by expenditure category.

Table G.1. Producer values by expenditure category

Expenditure category	Visitor spending per day	Economic sector	Consumer to producer ratio	Producer value
On-mountain expenditures				
Lift passes	$57.74	Amusements, gambling, and recreation	1	$57.74
Equipment rentals	$17.99	Amusements, gambling, and recreation	1	$17.99
Lessons	$20.66	Amusements, gambling, and recreation	1	$20.66
Other on-mountain	$22.15	Amusements, gambling, and recreation	1	$22.15
Food and beverage	$33.44	Food services and drinking places	1	$33.44
Base/in-town expenditures				
Food and beverage	$91.17	Food services and drinking places	1	$91.17
Retail purchases	$38.41	Retail trade	0.32	$12.29
Entertainment	$8.11	Amusements, gambling, and recreation	1	$8.11
Gas and other transportation	$14.54	Transit and ground passenger transportation	0.8	$11.63
Other services	$15.41	Other services	1	$15.41
Lodging	$109.18	Accommodation	1	$109.18
Total	**$428.80**			**$399.78**

Note: Since the multipliers are specific to Summit County (i.e., are based on industries within Summit County), only industries that are within Summit County are included in the industry multipliers, even through the industry titles are general for the United States. For example, while the ""Amusements, gambling, and recreation"" industry may include gambling in some locations, the multipliers for Summit County reflect the fact that gambling is not a component in this industry in this region.

Table G.2. RIMS II final demand multipliers for Summit County

Economic sector	Output multiplier	Earnings multiplier	Jobs multiplier (per $1 change in final demand)
Accommodation	1.4492	0.2973	0.0000134088
Food services and drinking places	1.4809	0.3300	0.0000223675
Retail trade	1.4759	0.3509	0.0000147371
Other services	1.621	0.3403	0.0000135355
Transit and ground passenger transportation	1.4771	0.4347	0.0000201307
Amusements, gambling, and recreation	1.4791	0.3581	0.0000204042

Table G.3. Economic impacts per skier day by expenditure category

Expenditure category	Visitor spending per day	Output per visitor skier day	Earnings per visitor skier day	1,000 jobs per visitor skier day
On-mountain expenditures				
Lift passes	$57.74	$85.41	$20.68	1.178
Equipment rentals	$17.99	$26.62	$6.44	0.367
Lessons	$20.66	$30.56	$7.40	0.422
Other on-mountain	$22.15	$32.76	$7.94	0.452
Food and beverage	$33.44	$49.52	$11.04	0.748
Base/in-town expenditures				
Food and beverage	$91.17	$135.02	$30.09	2.039
Retail purchases	$38.41	$18.14	$4.31	0.181
Entertainment	$8.11	$11.99	$2.90	0.165
Gas and other transportation	$14.54	$17.18	$5.06	0.234
Other services	$15.41	$24.97	$5.24	0.209
Lodging	$109.18	$158.22	$32.46	1.464
Total	**$428.80**	**$590.39**	**$133.55**	**7.459**